The influence of geological data on the reservoir modelling and history matching process

G. de Jager

The influence of geological data on the reservoir modelling and history matching process

Proefschrift

ter verkrijging van de graad van doctor

aan de Technische Universiteit Delft,

op gezag van de Rector Magnificus prof.ir. K.C.A.M. Luyben,

voorzitter van het College voor Promoties,

in het openbaar te verdedigen op woensdag 11 april 2012 om 10:00 uur

door Gerben DE JAGER

doctorandus in de Geologie

geboren te Nijmegen

Dit proefschrift is goedgekeurd door de promotor:
Prof. dr. S.M. Luthi

Samenstelling promotiecommissie:

Rector Magnificus,	voorzitter
Prof. Dr. S.M. Luthi,	Technische Universiteit Delft, promotor
Prof. Dr. Ir. J.D. Jansen,	Technische Universiteit Delft
Prof. Dr.Ir. M.F.P. Bierkens,	Universiteit Utrecht
Prof. Ir. C.P.J.W. van Kruisdijk,	Royal Dutch Shell
Prof. W.R. Rossen,	Technische Universiteit Delft
Dr. J.E.A. Storms,	Technische Universiteit Delft
Dr. Ir. E. Peters,	TNO
Prof. Dr. J. Bruining	Technische Universiteit Delft, reservelid

Copyright © by G. de Jager, Section of Applied Geology, Faculty of Civil Engineering and Geotechnology, Delft University of Technology. All rights reserved, no parts of this thesis may be reproduced, stored in any retrieval system or transmitted, in any forms ro by any means, electronic, mechanical, photocopying, recording or otherwise without the prior written permission of the author.

Voor Iris, Roan en Timo

Contents

1. Introduction

A long-term increasing demand in hydrocarbons, with a short-term uncertain market means that oil companies are intent on obtaining as tight a grasp on the complex workflow from discovery to production of an oil reservoir as possible. Unfortunately data is scarce, computing power expensive and communication between various disciplines limited. This chapter will shed light on various difficulties in the process from exploration to production, and show where this thesis can contribute.

1.1 Hydrocarbons and their production

1.1.1 Energy consumption

Worldwide energy consumption has been increasing, and according to the International Energy Outlook 2010 (**Fig. 1.1**) will continue for the foreseeable future. In this figure the unit used (quadrillion British thermal unit, or BTU) is often referred to as a quad. As a reference, the energy consumption of the USA is currently estimated at just under 100 quads. The largest part of the projected increase will be occur in countries not part of the Organisation for Economic Co-operation and Development (OECD), which for a large part consist of developing countries. For these countries, renewable energy sources will only be a limited option because currently these are still less economical than conventional sources. For energy consumption in the form of hydrocarbons, an increase is therefore predicted, albeit in a decreasing proportion of total energy consumption (**Fig. 1.2**). The relative decrease of hydrocarbons is caused mainly by a predicted increase in the use of coal and renewable energy sources. While renewable energy sources usage will increase due to increased economical competitiveness, coal usage will increase in part due to the predicted future scarcity of hydrocarbons. To sustain energy consumption until 2035, production needs to be increased by 50 quads (1.5 billion m3) of liquids and 50 quads (1.3 trillion m3) of gas.

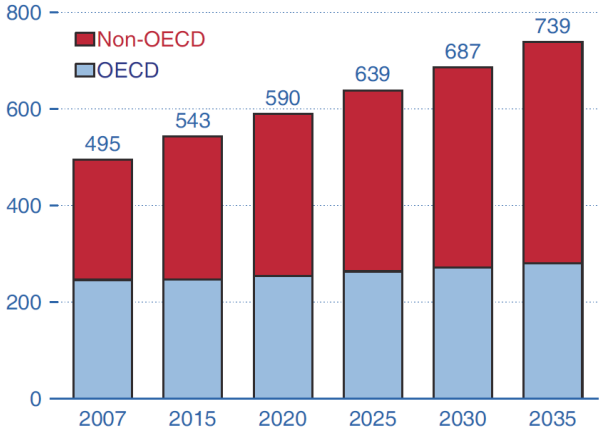

Figure 1.1. Total predicted World energy consumption, 2007-2035 (quadrillion Btu). OECD countries as of March 2010 (EIA 2010).

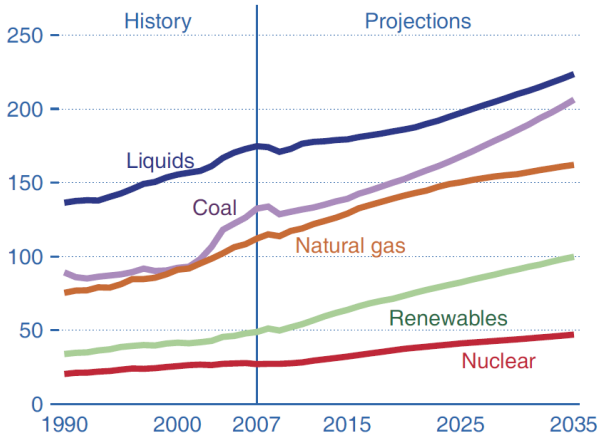

Figure 1.2. World marketed energy use by fuel type, 1990-2035 (quadrillion Btu) (EIA 2010).

1.1.2 Oil price change & future outlook

Associated with increases in demand are increases in price (**Fig. 1.3**). However, because oil prices are not solely based on supply and demand due to large amounts of oil trading, a large uncertainty exists in projected oil prices. The E&P industry is struggling to forecast its future activities in a time with large uncertainties on future pricing.

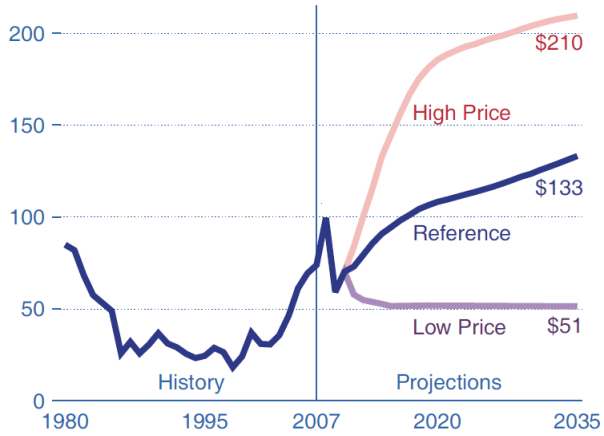

Figure 1.3. World oil prices for three predicted scenarios, 1980-2035 (2008 dollars per barrel) (EIA 2010)

1.2 The Exploration and Production (E&P) Process

1.2.1 Origins of oil and gas

Oil and gas are formed when organic material in a source rock is heated (matured), and over time chemically transformed to a complex mixture of hydrocarbons, together with several other chemical components. The source rocks can be deposits from anoxic lakes, planktonic remains from oceans or coal beds. Due to their relatively light mass hydrocarbons tend to travel upwards. A large proportion of hydrocarbons will escape to the surface in a process called migration, but a proportion will be captured in *traps*. A trap is formed when a porous rock is overlain by an impermeable *seal* in a structure which allows the hydrocarbons to stay in place. This system, often referred to as a *petroleum system*, can be reduced to having three essential components: a source rock, maturation, and a trap. A simple illustration of

this system is shown in **Fig. 1.4**. For this thesis we are mainly interested in the properties of the reservoir rocks, which determine to a large extent whether and to what extent the hydrocarbons can be produced.

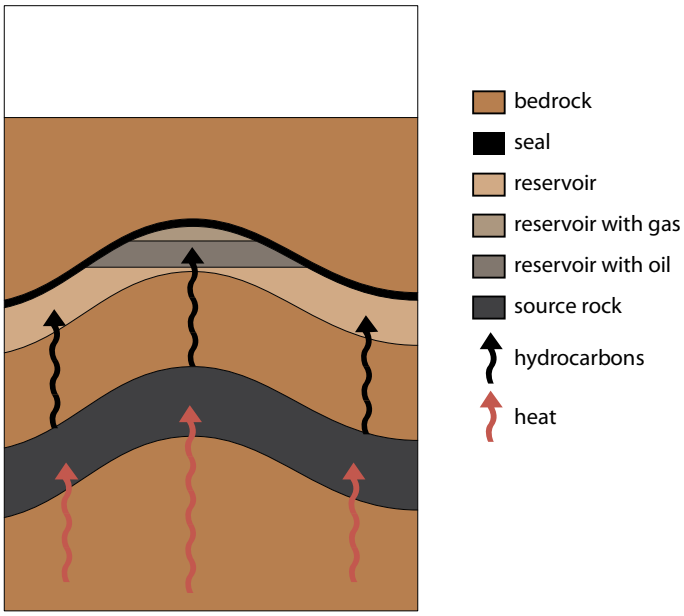

Figure 1.4. Petroleum system, consisting of a source-rock contributing hydrocarbons after maturation, that migrates to the reservoir-rock where it is trapped by the seal.

1.2.2 Exploration

Before hydrocarbons can be produced, they need to be located. This can be difficult, as there are generally no indications at the surface if hydrocarbons are present in the subsurface. Often hydrocarbon reservoirs are located at great depths below the surface. An extra difficulty is added when they are located in areas which are difficult to reach, for instance offshore, below jungles or in the Arctic.

A tool often used to find hydrocarbon reservoirs is seismic imaging. This is a process where acoustic waves are reflected by layers below the surface and the returning waves recorded. The time at which the waves return is an indication of the depth of

the layers. This can be used to form an image of the earth's subsurface. This image is then examined to find potential locations where hydrocarbons might be found.

When a location with reservoir potential has been found, wells will be drilled into this reservoir to ascertain actual hydrocarbon presence, as well as to gather information of the geological properties of the reservoir and surrounding area. The latter can be done by taking samples from the well, either as a core or as small samples (sidewall samples) at regular spacing along the well. Measuring tools can also be lowered in the well to gather data on the rock properties in the form of logs.

Using all the data gathered so far, a geologist will then create a reservoir model. This contains information on how the rock properties might vary throughout the reservoir. A large variety of techniques can be used to create a reservoir model, which will be discussed in detail in chapter 2. These models all have in common that they allow the geologist to combine a wide variety of data, together with a general geological knowledge on the characteristics of geological features, to generate one or more models. These models represent the best guess as to what the reservoir looks like, in terms of its geometry, its intrinsic properties and its fluid content.

Using the reservoir model, as well as data on the physical and chemical properties of the fluids, gasses and rocks, a reservoir engineer can then perform a flow simulation. This is a computer simulation of how the fluids and gasses will behave in the reservoir once the reservoir is taken into production. The results are then used to determine whether a reservoir is economical (if enough hydrocarbons can be produced economically), as well as indicating the optimal number and locations of wells to be drilled. If the economics of the reservoir are predicted to be profitable, the reservoir can be developed further.

1.2.3 Development

The development phase consists of drilling wells, placing production facilities and attaching these to pipelines or other methods that can transport the hydrocarbons to facilities where they can be refined. This phase is associated with high costs, as each well can cost up to 100 million dollars and little or no income is being generated from production yet.

1.2.4 Production

The production phase of a reservoir is when the hydrocarbons are being produced. Within the producing lifetime of a reservoir of 10 years to several decades, three production stages can be encountered. The first is *primary production*, which is when little effort is required to extract the hydrocarbons. The hydrocarbons will flow freely due to the high pressure in the reservoir, called *natural drive*. After some time, reservoir pressure will drop and extra measures are required to maintain production. This stage is called *secondary production*, and is associated with injecting water or gasses through injector wells to maintain pressure and essentially push the hydrocarbons out of the reservoir (*artificial drive*). *Tertiary production* or *enhanced oil recovery* (EOR) refers to the technique of injecting chemicals that allow the last producible remains to be removed. These chemicals can be steam, CO_2 or surfactants. Generally speaking, not all hydrocarbons from the reservoir will be produced. After primary production 5%-15%% is produced, which is increased to 30%-50% after secondary production and tertiary production can add another 5%-15% (Gluyas and Swarbrick 2005).

1.2.5 FDP

The goal of any reservoir development is to maximize economic returns. This is achieved by designing a field development plan (FDP). The economics of a reservoir depend on the placement of wells, the rate and timing at which wells will produce or inject, as well as the surface facilities. The way the development is maximized is by performing numerical fluid flow simulations (flow simulation in short) on the reservoir model with several proposed development plans. This allows an optimal configuration to be determined.

The outcome of the FDP depends strongly on the reservoir model used to create the plan. Especially in highly heterogeneous reservoir types where a low permeability background is crossed by high permeability features such as channels or fractures. In these types of reservoirs the correct properties and placement of the geological features is essential. However, almost always not enough data is available to identify the correct properties and locations. Furthermore, it is not properly understood how errors in the reservoir model relate to errors in the “optimal” FDP. To correctly deal with uncertainties within the geological model, a large number of possible reservoir

models should be used when planning the FDP. This is unfortunately computationally not viable and is in practice almost never performed.

1.2.6 History matching

After the reservoir has been in production for some time, a wealth of data will have been gathered, for instance how the seismic image changes over time (4D seismic), how production rates and pressures in the reservoir change over time, as well as changes in chemistry of the produced liquids and gasses. This data can then be used to update or improve the reservoir models, a process called history matching (**Fig. 1.5**). In this procedure, there is the reservoir which has been constructed based on data available at the start of the lifetime of the field (well, seismic, general geology) is used in a flow simulator, which gives a set of simulated flow data. Also, the actual reservoir is providing data. Most likely a difference will be found between the two, and this can be used to improve the reservoir model. This new reservoir model can subsequently be used to provide better control strategies, mainly in the form of production or injection rates at the wells. This process can be performed as often as new data becomes available, however in practice this is time consuming and happens much less regularly.

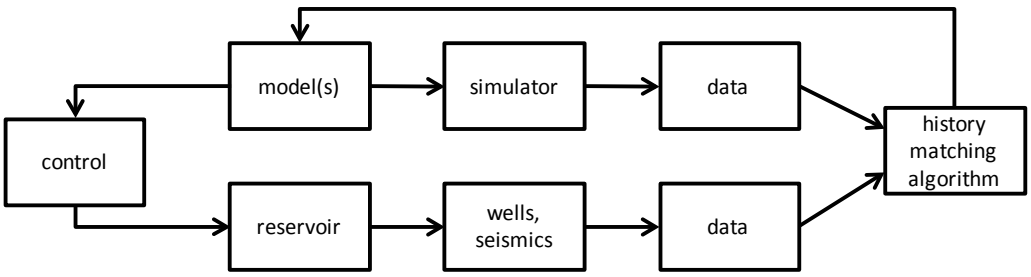

Figure 1.5. Flowchart showing history matching and feedback into reservoir control (closed-loop reservoir management).

1.3 Objectives

Data of the relationship between geological information and quality of predictions of reservoir flow are rare, and quantifications of this relationship are rarely performed. The goal of this thesis is to examine various aspects of geological data which can be used in the reservoir modeling process, and how they relate to flow predictions. This is subdivided into three distinct sections:

- Quantify the effect of changing the model input parameters on flow behavior (metrics) for both pixel-based and object-based modeling techniques.
- Quantify how the accuracy of analogue model choice relates to the accuracy of flow prediction.
- Find a metric to characterize reservoir models which strongly relates to flow behavior, and examine how this can be used in history matching.

1.4 Thesis Outline

The outline of this thesis is as follows:

Chapter 2 consists of a literature review on geological modeling techniques. The techniques are subdivided into four separate sections. The first focuses on *pixel-based* techniques, where a reservoir model is generated by assigning a value to locations within the reservoir sequentially. The second part is on *object-based* techniques. Here the reservoir model is populated by specific geological bodies of user-defined shape, size and property values. The third type of modeling technique is the set composed of various *process-based* or *process-imitating* techniques. These techniques recreate geological systems over time by reproducing the processes which formed the reservoirs. Lastly *model combinations* of different techniques will be shown.

Chapter 3 describes an analysis on how several geological parameters of a variogram-based reservoir model influence the flow behavior of a reservoir model. Numerous models are created with different properties and subsequently a flow simulation is performed on each of them. The flow data is analyzed to find relationships between altering input parameters and flow response. Additionally, parameter interactions are examined. The parameter values for the reservoir models

are determined by using *Design of Experiments*, and the data is analyzed using various statistical techniques such as ANOVA and response surface modeling.

Chapter 4 also uses an experimental design / response surface methodology explained in detail in chapter 3, but applied to a channelized reservoir. The highly permeable channels form a heterogeneous reservoir with a significant influence of the parameter values on production behavior.

Chapter 5 is based on de Jager and Luthi (2011). Here a technique is described to find a relationship between reservoir properties and flow behavior. Instead of looking at model parameters as in the previous chapters, here the term *accessibility* is introduced. Accessibility is a value that is calculated for each cell in the reservoir and describes how accessible the cell is from the wells in the reservoir. Accessibility is shown to relate to production behavior, and can therefore be used as a quick technique to differentiate between reservoir models.

Chapter 6 describes how the data used in generating the reservoir model influences the predicted flow response of a set of reservoir models. A complex and relatively realistic truth case is developed, from which well data is obtained. A number of analogue models are chosen from which data on geological properties is derived. These analogue models are correct in varying degrees, and the assumption is tested whether an accurate analogue model will also create an accurate prediction of flow behavior, and if increasing the error in analogue automatically causes a larger error in the prediction of flow behavior.

2. Literature review

A large variety of geological modeling techniques have been created over the years, with a variety of goals in mind. Initial focus was on mapping ore deposits, but in recent decades the focus in research has been dominated by reproducing complex geology for flow transport, both for hydrological as well as petroleum settings. Two main issues make the correct reproduction of complex geology difficult.

The first is the sparseness of data. Generally only data from a limited number of wells is available, in some cases augmented by seismic information. This causes the modeling process to be ill-posed or, in other words, multiple models can be generated based on the data, but only a subset will approximate reality.

The second is the difference in scale between the data types themselves, as well as between the data and the model. From wells we can get very local and very precise data from cores. Formation imaging tools can give a lot of information, but are convert to information which can be used in the modeling process. These can be combined with a suite of other tools, for instance gamma ray, neutron density, conductivity, resistivity and pressure data. Often seismic data is also available, which is on a very large scale, but often of a resolution below that of the required model. Most of these data are static, i.e. do not change over time, and is useful for a static geological model. But dynamic data, such as flow rates, can be very valuable in generating a correct model. Both data types should be used when available, but combining them in a single model is difficult. Below an overview is given for a wide variety of modeling techniques. The focus is on automatic reproduction techniques of fluvial reservoirs for hydrocarbon exploration, but various related techniques will also be covered. Fluvial reservoirs are chosen because of their high heterogeneity, and therefore difficulty to model as well as importance to model correctly.

2.1 Modeling

The first geological model can be said to have been created implicitly by Darcy (1856). Although his experiments described flow in a homogeneous layer, he produced cross-sections of an aquifer tapped by an artesian well, therefore implicitly differentiating between an aquifer and an impervious layer. Other early work was done by Dupuit (1857), who extended Darcy's law to homogeneous natural aquifers,

and Theis (1935), who used well data to obtain average rock properties. One of the first true heterogeneous geological models was produced by Whitehurst (1778), when he published simple layer cake models to assist in the discovery of valuable minerals. With Muskat (1949) the first understanding of true geological models was born, when he states "It appears extremely unlikely that actual underground strata will be of strictly uniform permeability over distances or areas associated with oil-producing reservoirs". The ability to handle these heterogeneities did not exist until much later, an overview of the different techniques below shows.

Although there are a variety of techniques available to create models by hand (e.g. (Johnson and Krol 1984)), here the focus will be on automated modeling techniques. These modeling techniques can be subdivided into four types:

3. Pixel-based modeling, where modeling of reservoir properties proceeds by assigning a value to each location in the reservoir, or pixel, separately

4. Object-based modeling, where the model is generated by placing geological bodies, or objects, within the reservoir framework

5. Process-based modeling, where the geological processes which form the reservoir are reproduced numerically

6. Process-imitating, where due to computer processing limitations the geological processes are simplified

These distinctions are not clear-cut, and often hybrid techniques are used, or combinations of methods within the same reservoir are used to replicate different aspects. Below is a description of a representative selection of such modeling techniques.

2.2 Pixel-based modeling

2.2.1 Two-point modeling

Two-point stochastic modeling techniques are a group of geostatistical methods that can be used to interpolate data between two or more measurement points. Kriging is the earliest technique, developed by Matheron (1963) based on the work of Krige (1951). The data used in kriging can be represented as the variogram (**Fig. 2.1**), which

is a plot of how the semivariance (Y) changes over distance (h), where the semivariance is:

$$\gamma_h = \sum_{i=1}^{m} \frac{(z_{x_i} - z_{(x+h)_i})^2}{2m}$$

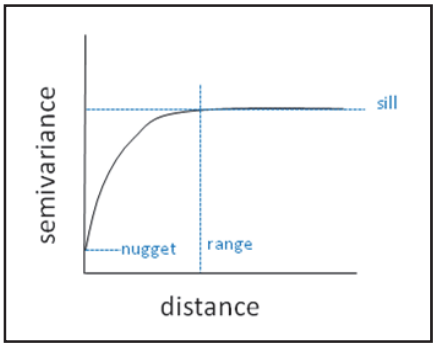

Figure 2.1. An example of a variogram which characterizes how the variance changes over distance.

The semivariance is thus proportional to the root mean square error of the difference in property z over distance h. Calculating Y as a function of h generates the variogram shown in figure Fig. 1. The variogram can be described in terms of the following parameters:

- Range: the distance beyond which no relation between the properties is found
- Sill: the semivariance value at the range
- Nugget: the value of Y at h=0; often interpreted as noise, measurement error or small scale variations in the property being examined

To create a model based on the variogram can be done by *punctual kriging*, a geostatistical technique to interpolate property z around measurement points. To intuitively describe the process of kriging, a simple example will be used where 3 measurements of z are available. To estimate z at location p, we could use a weighted average:

$$\hat{z}_p = w_1 z_1 + w_2 z_2 + w_3 z_3$$

The error of $\hat{z}_p$ with the true value of z_l is then simply:

$$\varepsilon_p = z_l - \hat{z}_p$$

For n locations the estimation variance σ then is :

$$\sigma_\varepsilon^2 = \frac{1}{n}\sum_{i=1}^{n}(z_{li} - z_{pi})^2$$

The similarity between σ and Y is apparent: the former is equal to twice the latter. For a kriged estimation of $\hat{z}_p$ based on three measurements the solution needs to be found for the following equations:

$$w_1\gamma(h_{11}) + w_2\gamma(h_{12}) + w_3\gamma(h_{13}) + \lambda = \gamma(h_{1p})$$

$$w_1\gamma(h_{21}) + w_2\gamma(h_{22}) + w_3\gamma(h_{23}) + \lambda = \gamma(h_{2p})$$

$$w_1\gamma(h_{31}) + w_2\gamma(h_{32}) + w_3\gamma(h_{33}) + \lambda = \gamma(h_{3p})$$

Where $\gamma(h_{ij})$ is the semivariance between points I and j, obtained from the variogram, and λ is the Lagrange multiplier, used to minimalize the error. For a unique result we need the fourth equation:

$$w_1 + w_2 + w_3 = 1$$

Finding the solution is trivial and will not be explained here.

The method described here is only applicable when z is stationary. If this is not the case for instance *universal kriging* (Goovaerts 1997) needs to be applied, a more general set of equations where a trend or *drift* is added. The drift can be quite complex for locally varying trends. However, the solution is similar to punctual kriging described above. Some other variations on punctual kriging are:

- Co-kriging: Multiple variables with separate variograms are combined to obtain cross-variograms (e.g. Harvey and Gorelick (1995), Kitanidis (1995))
- Disjunctive kriging (Matheron 1976): a nonlinear generalization of kriging.

- Local Anisotropy Kriging (te Stroet and Snepvangers 2005): Uses local anisotropy, requires high data density (e.g. Rhine-Meuse Delta)

2.2.2 Discontinuous facies models

After the success of the first object-based models (see *stochastic shales* below) by Haldorsen and Chang (1986), pixel-based techniques were developed which also allowed discontinuous facies to be modeled. As a first technique Disjunctive Kriging was introduced as early as the 1970s (Matheron 1973), but it was not until the 1980s that discontinuous facies modeling was popularized with the Indicator Kriging method (Journel 1983). In the same year Matheron proposed the Gaussian Threshold model (Matheron et al. 1983) where a facies is assigned based on where the value of a site falls within used-defined threshold values.

For many types of reservoir these Gaussian methods are very well suited, for instance where heterogeneities are defined by differences in cementation or ore abundance. However, more complex facies relationships cannot be modeled as well as complex geometries such as curvilinear structures, such as found in fluvial and submarine channel systems.

2.2.3 Sequential Gaussian Simulation (SGS)

The most common approach in stochastic simulation is the Sequential Gaussian Simulation (Deutsch 2002). It is based on removing an undesired effect of kriging, where the variance is too small in kriged realizations. The workflow consists of visiting each location sequentially, and treating previously visited locations as data. For each new location a kriging estimate is made, and the missing variance is added. Different realizations can be generated by visiting the model locations in a different order.

2.2.4 Truncated Gaussian Simulation (TGS) (Deutsch 2002)

Truncated Gaussian simulation is initially identical to SGS (see above). However, the SGS generated realization is then modified to produce a realization in which distinct facies are present (**Fig. 2.2**). Simulated values falling between certain

thresholds are assigned a facies type, where each facies can subsequently be assigned appropriate properties.

2.2.5 Markov Chains

Realizing the limitations in Gaussian methods with respect to modeling facies transitions and interrelationships, Markov chains were developed (Carle and Fogg 1996). In one dimension this technique is based on quantifying the transition probability from a facies k to j as:

$t_{jk}(\mathbf{h})$ = Probability that k occurs at $\mathbf{x}$

+$\mathbf{h}$ given that j occurs at $\mathbf{x}$

Where $\mathbf{x}$ is a point in space and $\mathbf{h}$ a lag vector. Because the technique starts with a certain facies, matching to well data is straight forward. The probability of k occurring at $\mathbf{x}+\mathbf{h}$ is only dependant on the location $\mathbf{x}$. Ideally the property of a certain point is dependent on all surrounding points. Despite this simplification, Markov chain models are considered to better account for geological features such facies juxtapositions and fining upward sequences than indicator geostatistics (De Marsily et al. 2005).

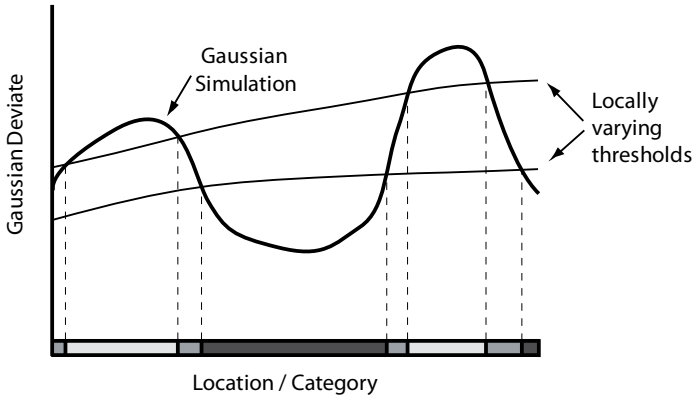

Figure 2.2. Illustration of how a continuous simulation (Gaussian Simulations) can be discretized into distinct facies / catagories. Here location is on the horizontal axis, with the value of the Gaussian simulation on the vertical. The category is found based on where the Gaussian variable falls with respect to (locally varying) threshold values.

2.2.6 Multi-point statistics

Snesim

As discussed above, many pixel-based techniques are not able to accurately model complex geology. Also, object-based techniques (described below) have two drawbacks: (1) They require describing geological bodies as a set of geometries, which is not always possible (2) Conditioning to well data can be difficult, especially when well density is high with regard to the size of the objects. Therefore the *snesim* algorithm was developed by Strebelle (2002) using an approach based on multiple-point statistics originally proposed by Guardiano et al. (1993). The main feature of this technique is that it derives probabilities based on multiple surrounding data points. The algorithm follows several distinct steps, these are illustrated by the attempt to reproduce the model shown in **Fig. 2.3a**, based on a set of measurements (**Fig. 2.3b**):

1. Generate a training image

   The training image (TI) (**Fig. 2.3c,2.3d**) is a representative rendition of the geological structures required for the model realizations. The TI can be derived from a number of sources: it can be obtained from outcrop data, from a realization from a process-based model, from expert knowledge or from seismic information. The TI needs to adhere to several requirements:

- It must be stationary over the entire image, even if the required model realization is not stationary
- It must be large enough that all required features are present
- It must be large enough to capture all the required features completely

2. Scan the training image and place the data in the search tree
   Before scanning the TI it is necessary to determine the required size of a template, which will determine the size of the area around the point of interest to be examined for the data. For this example a template size of 7x7 is used. At each location on the TI we will place the template and, determined by the value of each cell in the template, a place in the search tree (Roberts 1998) will be assigned. The benefit of using a search tree over simply storing the data directly is that only data that is actually present needs to be stored, which is equal to or less than the number of cells in the TI (about 10^4-10^8).

Storing it directly would require $2^{48}=2.8x10^{15}$ values to be stored in computing memory.

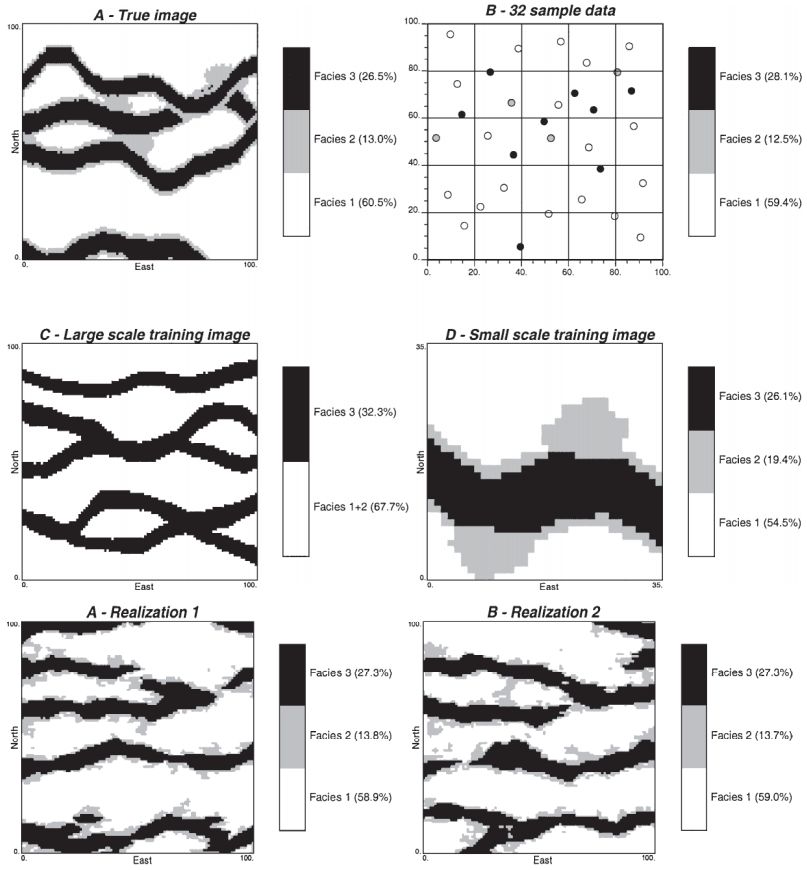

Figure 2.3. Multi point statistics using the *snesim* algorithm. Steps a-f are clarified in text.

3. Generate model realizations (**Fig. 2.3e, 2.3f**)

A model realization is generated by placing the template on a random location on the grid where the model realization will be generated. From the training image all locations will be found containing the same conditioning data. The probability of the location on the model is determined by the ratio of the facies found in the TI. A random value is drawn, and combined with the calculated probability the facies value for that point is determined. The template is then moved and the process is repeated with the new points used

as conditioning data until the model is filled. A different model realization is made by varying the random numbers and/or the order in which all the locations are visited.

Several adaptations to this initial workflow have been added in later stages to model the desired geology more accurately.

- Sequential modeling at different scales
  This adaptation was made because the initial technique often created discontinuous bodies ("dangles") where this was not desired (Stien, Abrahamsen et al. 2007). The workflow consists of first modeling at a large scale, but only filling a fraction of all cells. Thereby generating the large scale structure of the field. The next step operates at a smaller scale and fill in some of the remaining cells, while finally at the cell scale all remaining cells are filled.
- Modeling non-stationary geology
  In many cases the geological features are not stationary over the entire model, such as smaller channels and migrating facies on a delta plain. To allow for rotating and relative scaling it was proposed to allow the template to be rotated and stretched when modeling, but keeping it stationary on the TI. Using this technique it is possible to use maps dictating size and orientation as soft conditioning data (**Fig. 2.4, Fig. 2.5**) (Caers and Zhang 2002). Tetzlaff et al. (2005) Used these techniques to generate a submarine fan using MPS (**Fig. 2.6**)
- Using seismic conditioning data
  Seismic data can provide information on the likelihood of a certain facies being present at a certain location. As the data from the TI also gives a probability, these can easily be incorportated to form a combined probability.

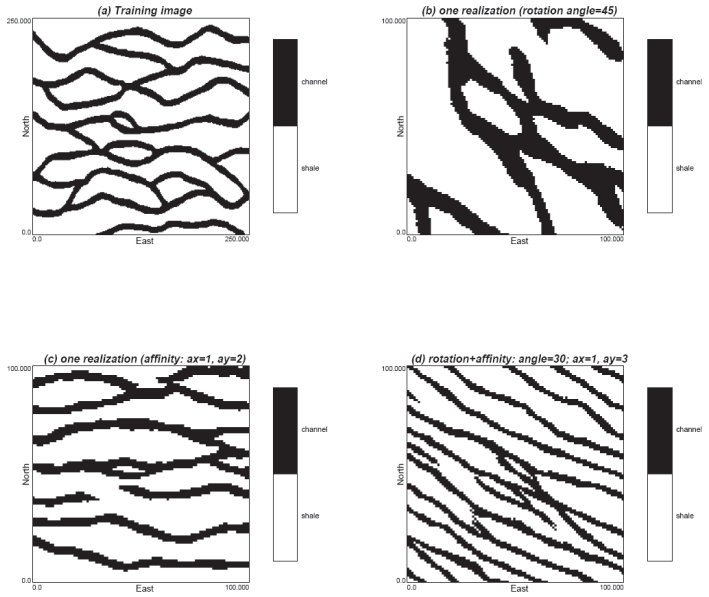

Figure 2.4. Adaptations of the standard procedure (a) to produce rotated (b), shortened in one direction (c) and combined (d) channel models.

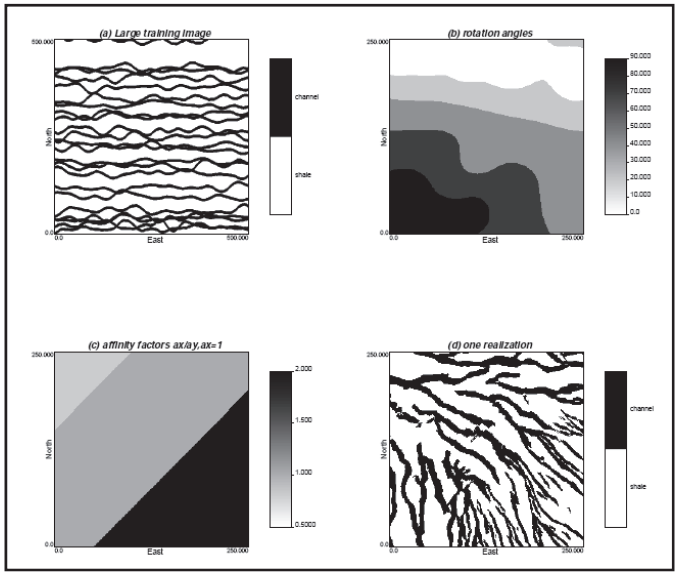

Figure 2.5. Modification of the snesim algorithm to handle non stationary orientation and dimensions. Using a TI (a), map of required orientation (b) and required dimensions (c) to create a representation of a bifurcating channel system (d).

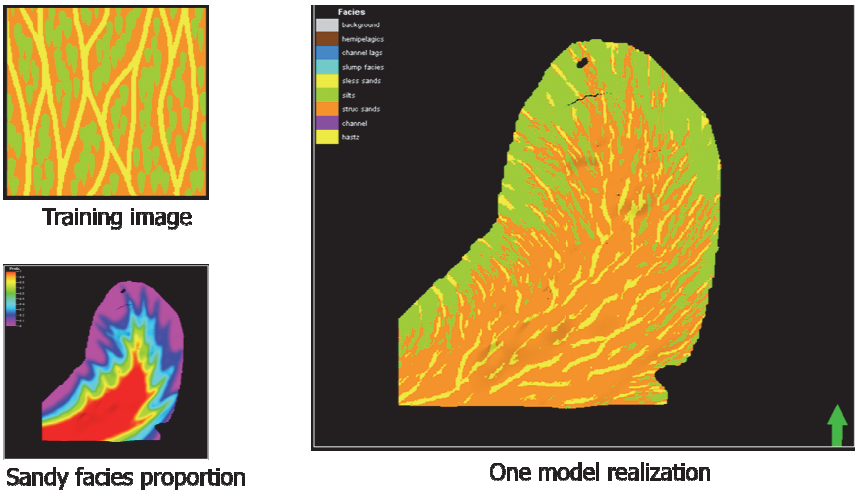

Figure 2.6. Reproduction of a submarine fan using MPS.

2.2.7 filtersim

Multi-point statistical techniques attempt to capture local patterns of variability from a training image and anchor them to the image or numerical model to be built. Snesim requires an exact match of the conditioning data event by the training pattern; if no such match is found, the conditioning data event is reduced by dropping the farthest datum value resulting in a loss of conditioning information.

Filtersim (Zhang et al. 2006) trades the exact data event reproduction for an approximate reproduction. This is done by finding a segment (or puzzle piece) of a training image which best, but not necessarily perfectly, matches the local conditioning data. The algorithm consists of two parts: first classifying the patterns found in the training image (TI), and secondly building a model realization.

The classification of the TI is performed by moving a window across the TI and for each segment calculating a score based on a set of filters, shown in **Fig. 2.7**. In 2D six filters are required, in 3D nine. Each segment is given a score for each filter, so it can be seen as a point in six- or nine-dimensional space. Each axis is discretized into five parts, therefore in 2D 6^5=7776 bins are present. When the classification is finished a set of puzzle pieces have been gathered, each placed in a bin based on its filter properties.

The simulation is performed by randomly visiting each location in the model area and collecting all data present within a certain area (**Fig. 2.8**). This data can include measured well data as well as previously simulated locations. Next the optimal bin containing the TI segments is found, and a puzzle piece is randomly drawn from this bin. This piece is placed in the model with the centre part staying fixed, and the outer parts to be used as soft conditioning data in future steps, thereby improving continuity of the structures. As with the *snesim* approach, multiple scales are used, where first the large scale structures are modeled and subsequently details filled in at higher resolutions. A new realization can be created by visiting the locations of the model in a different sequential order.

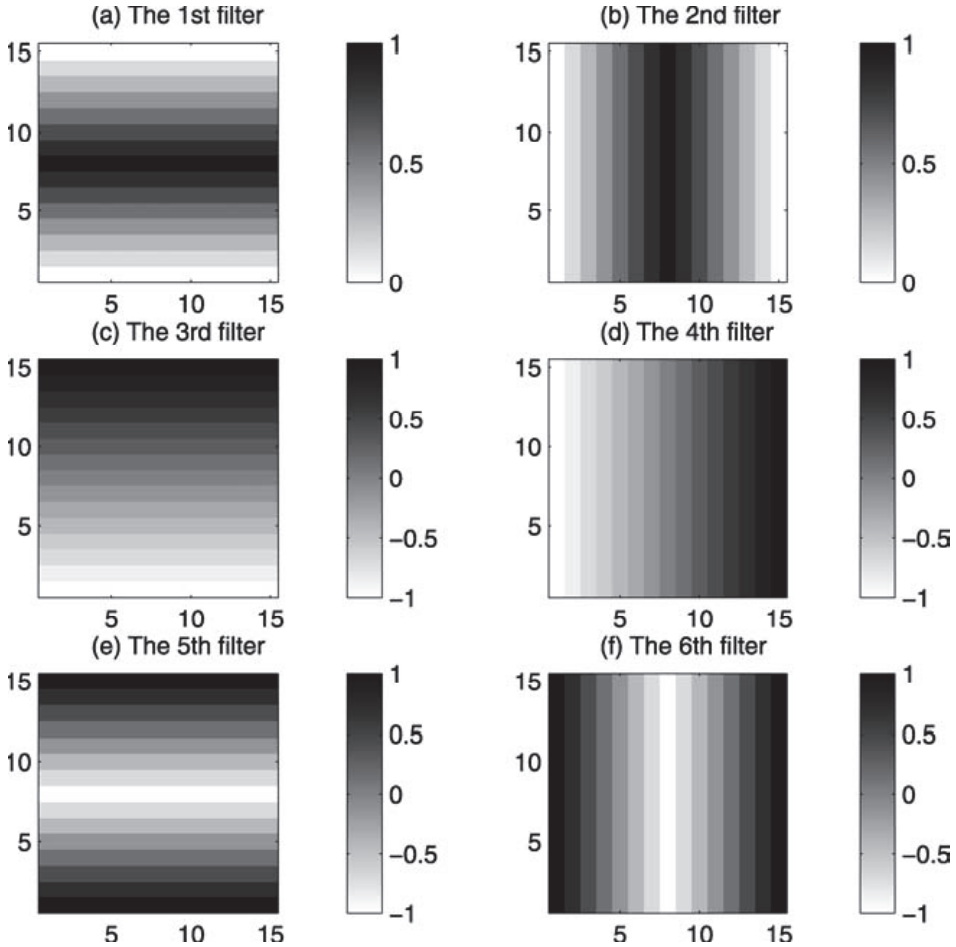

Figure 2.7. Graphic representations of the filters used in the *filtersim* algorithm.

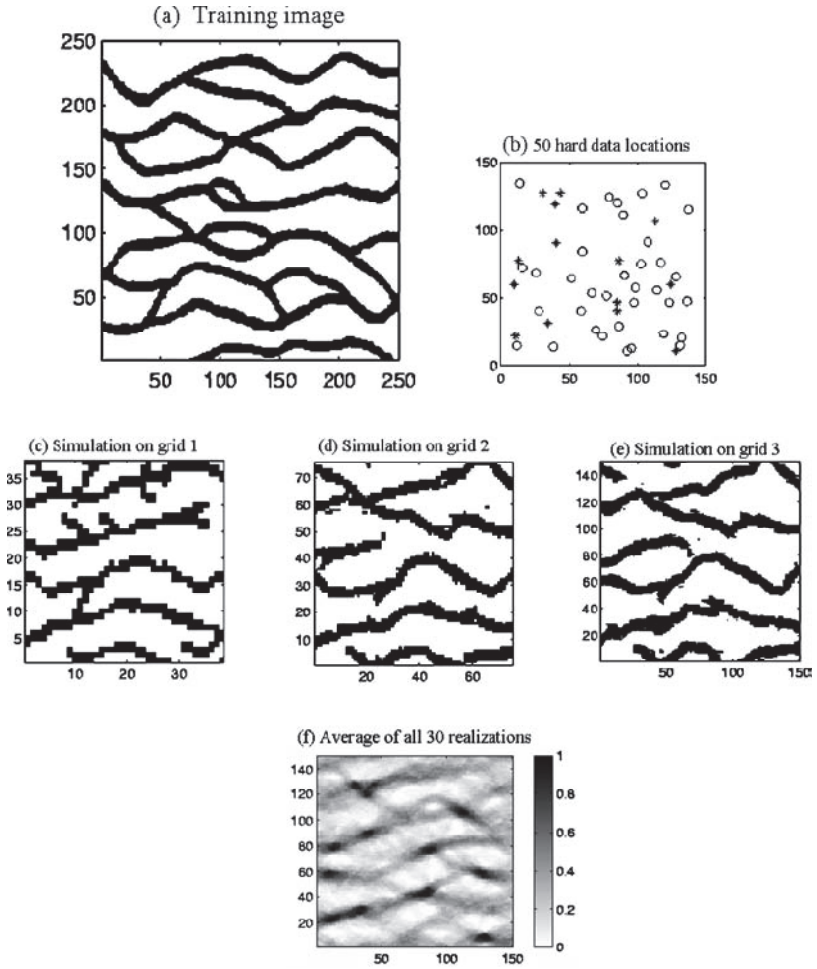

Figure 2.8. (a) Channel training image; (b) hard data locations; (c)–(e) Conditional simulation progressing over the three nested grids; (f) average of 30 conditional realizations.

2.3 **Object-based modeling**

With classical geostatistics using the variogram it is possible to make a model realization of a continuous variable, but is much less suited for a reservoir with a different and more complex distribution. Especially fluvial reservoirs, as one of the most heterogeneous reservoir types, are not suited for such an approach. For these types of reservoirs it is necessary to use another technique, generally either object-based modeling or process-based modeling. For object based models the method is generally based on placing high-porosity and -permeability objects representing

channels or channel belts in a matrix of low porosity and permeability floodplain deposits. The method of describing these bodies geometrically, placement strategy and conditioning criteria are what distinguishes this technique from others. A selection of object-based models will be described below to illustrate the diversity in techniques.

2.3.1 Stochastic shales

In the 1980s Haldorsen and Chang (1986), working in the oil industry, developed the stochastic shales technique, a technique where the objects are discontinuous and embedded in an otherwise homogeneous background or matrix. In this case (**Fig. 2.9**) the bodies represent sand lenses within a clay matrix, but any type of geometry and set of petrophysical properties can be assigned. This technique was a fundamental step towards recreating more complex and realistic models of the subsurface, and it "empirically popularized the underlying concept of connectivity" (De Marsily et al. 2005).

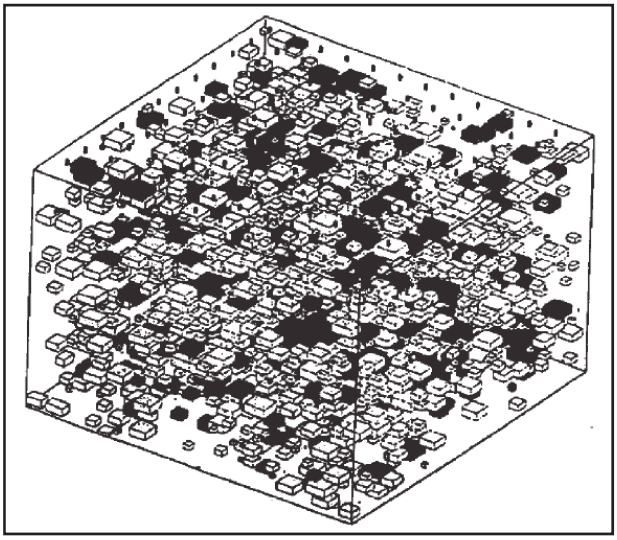

Figure 2.9. A model realization generated by the stochastic shales approach, one of the first object-based models.

2.3.2 Avulsion-based modeling

A method which aimed at forming stratigraphy based on genetic history is the avulsion-based technique developed by Viseur (1999). This technique recognizes the distinct stratigraphic sequences formed by different avulsion scenarios (Allen 1965). Avulsion surfaces are defined in three ways:

- Geometrically: as the top of channel belts
- Genetically: the relief of the environment just before the avulsion event
- Temporally: the period when the channel predominantly changes direction

In this technique avulsion surfaces are used as a framework in which the channel bodies are placed (see **Fig. 2.10**). The surfaces are generally defined by well data. Once the surfaces have been correlated between the different wells, the large scale structure of the field is established and is subsequently be populated with the channel belts, which is done in two steps:

(1) A probability field is generated based on well data and orientated in the paleocurrent direction

(2) Channels are placed stochastically within the reservoir.

2.3.3 Fluvsim

In order to create an open-source and adaptable object-based reservoir modeling tool for both education as well as research the FLUVSIM algorithm was developed (Deutsch and Tran 2002). It creates model realizations of fluvial reservoirs with four facies types: channel fills, levees, crevasse splays and floodplain deposits. Each of the facies is modeled by separate objects or bodies, of which the geometrical properties are defined by triangular distribution curves

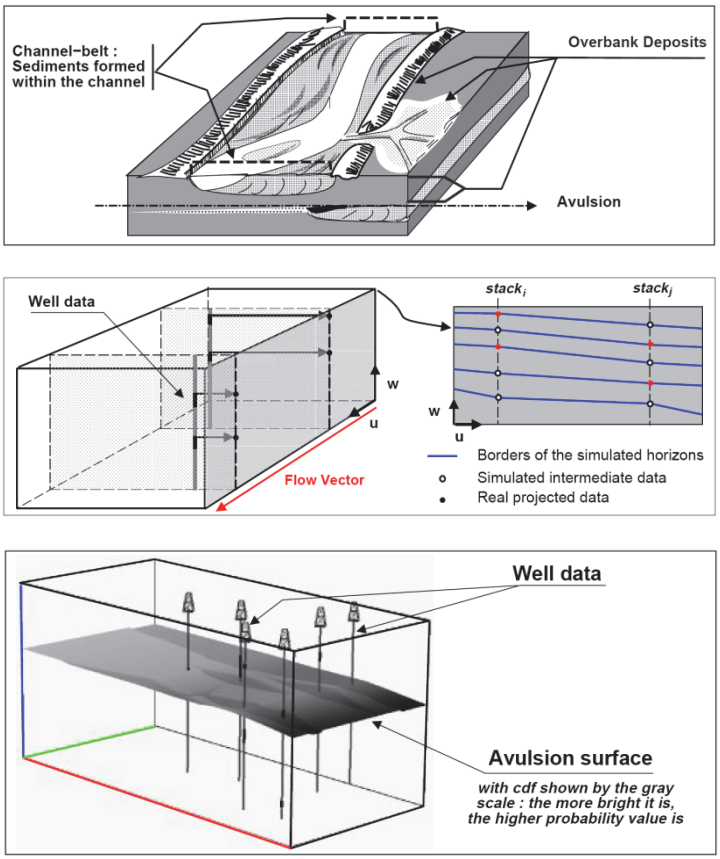

Figure 2.10. (a) Conceptual model for method developed by Viseur (1999); (b) Creating a framework of avulsion surfaces; (c) one avulsion surface showing probability of a channel occurring at a location

The conceptual geological model is shown in **Fig. 2.11a**, with three facies which are placed in a matrix of floodplain sediments. The channel sediments are deposited along a spline (**Fig. 2.11b**) with the geometry in cross-section determined by three parameters (**Fig. 2.11c**). The levee deposits are adjacent to the channel deposits, with user defined geometries as shown in **Fig. 2.12a** and **2.12b**. The crevasse splay geometries are not dictated by the user, but are formed using a random walk procedure. Location of the levee breakthrough is chosen with a probability directly proportionate to the channel curvature, i.e. it is most likely in channel bends. Examples of model realizations are shown in **Fig. 2.12c**.

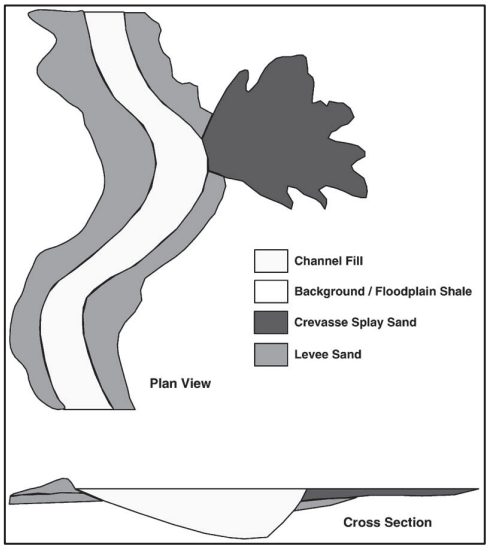

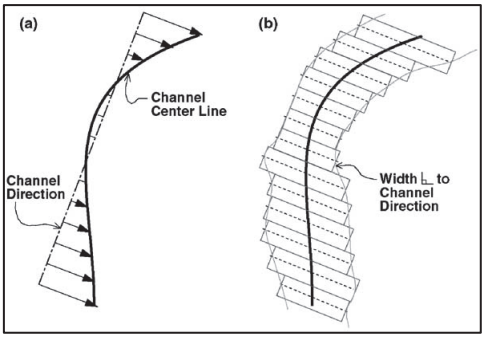

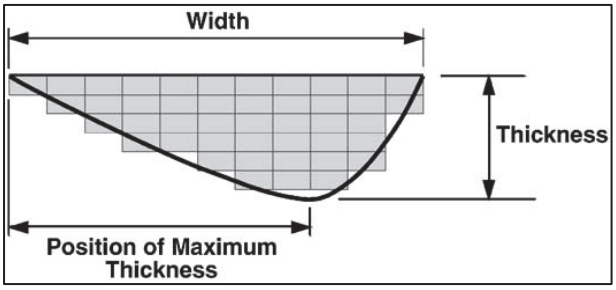

Figure 2.11. (a) Conceptual model used in the FLUVSIM technique; (b) channel placement along spline; (c) cross-section of channel body

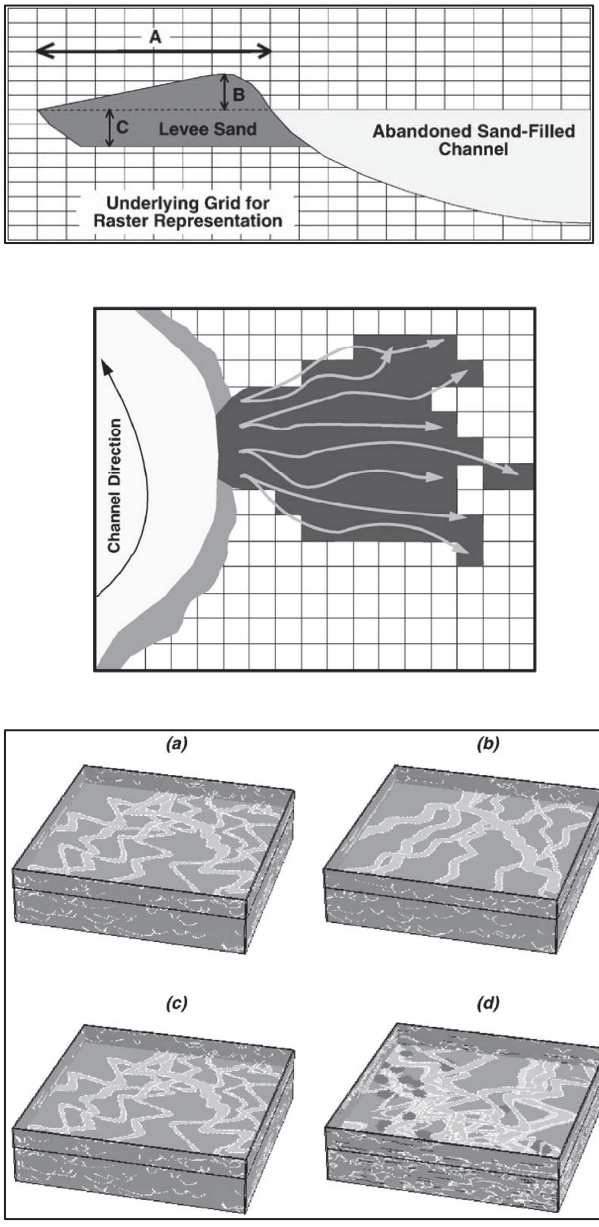

Figure 2.12. (a) Cross section of crevasse splay body; (b) crevasse splay formation using random walkers; (c) FLUVSIM model realizations

This modeling technique is an adaptation of the hierarchical approach (Deutsch and Wang 1996). Placement of the bodies is performed by a simulated annealing technique. Initially the model is filled with channels and associated facies to match the global proportions of the facies. Next the choice is made out of four possible actions: (1) replace a channel object (2) add a channel object (3) remove a channel object (4) correct a particular well interval. After the chosen action is performed the change is tested by the following objective function:

$$O = \omega_1 \sum_{k=1}^{K} \left[P_g^k - P_g^{k*} \right]^2 + \omega_2 \sum_{k=1}^{K} \sum_{z=1}^{N_z} \left[P_v^k(z) - P_v^{k*}(z) \right]^2$$
$$+\omega_3 \sum_{k=1}^{K} \sum_{x=1}^{Nx} \sum_{y=1}^{N_y} \left[P_a^k(x,y) - P_a^{k*}(x,y) \right]^2 + \omega_4 \sum_{i=1}^{n} \sum_{k=1}^{K} \left[i(u_i;k) - i^*(u_i;k) \right]^2$$

Here the asterisk (*) identifies quantities from the stochastic realization and the absence of an asterisk identifies reference or target quantities. Parameter *k* is the facies number, P_g^k is the global proportion, P_a^k is the areal proportion, P_v^k is the vertical proportion, and ω_i are weighting factors. The fourth section of *O* checks for well conditioning data, where the well data is transformed to indicator data:

$$i(u;k) = \begin{cases} 1 & \text{if u is within facies k} \\ 0 & \text{otherwise} \end{cases}$$

If this operation reduces *O* the change is accepted. Modeling is complete when *O* reaches a suitably low value. It is worth noting that combining the well conditioning with the facies proportions in the same objective function can, and quite often does, result in a model realization that has a very good facies proportion convergence but has errors in the well conditioning. Separating these two conditioning aspects into two objective functions would overcome this problem.

2.3.4 Point bars

Most object-based modeling techniques are based on a conceptual geological model of homogeneous high permeable ribbon-like channels within a low permeable matrix, sometimes complemented with levees and/or crevasse splays. The geological foundation for such a situation is limited at best. Generally a channel belt is internally

quite heterogeneous, containing braid bars, point bars, mud plugs, crevasse splays and overbank deposits among others.

Here an object-based model is presented to recreate sinuous channels with point-bar deposits, based on a parameterization technique on point bar deposits in Suriname (Rivera-Rabelo et al. 2007). The workflow for generating one channel and point bar system is shown in **Fig. 2.13**. The following steps are taken:

1. Decide on ratio of r1:r2, larger is less sinuous, here r1=0.9*r2
2. Decide on absolute values of r2 and channel width
3. Find starting point S
4. Place circles with r2 & r3 centred on S
5. Find direction of location of erosive circle, perpendicular to average flow direction
6. Centre point E is at point dictated by rule decided upon in step 1
7. Place circle and erode
8. Decide on next pointbar dimensions r2
9. Find point P at which E and "thalweg" meet. The thalweg is defined as a circle with radius = r2+0.5*(r3-r2)
10. Perpendicular to thalweg at P draw line to S' with distance r2'+0.5*(r3'-r2').
11. Place circles with radii r2' & r3'
12. Find point E' which is the point where two circles with radii r1' meet, centred on S' and centred on P
13. Place new erosive circle and erode where necessary
14. Next pointbar: P', perpendicular to thalweg with distance r2''+0.5*(r3''-r2'')

This process is repeated over the entire model area to create one sequence. In order to create a model realization this sequence is used as an object, similarly to the FLUVSIM technique described above.

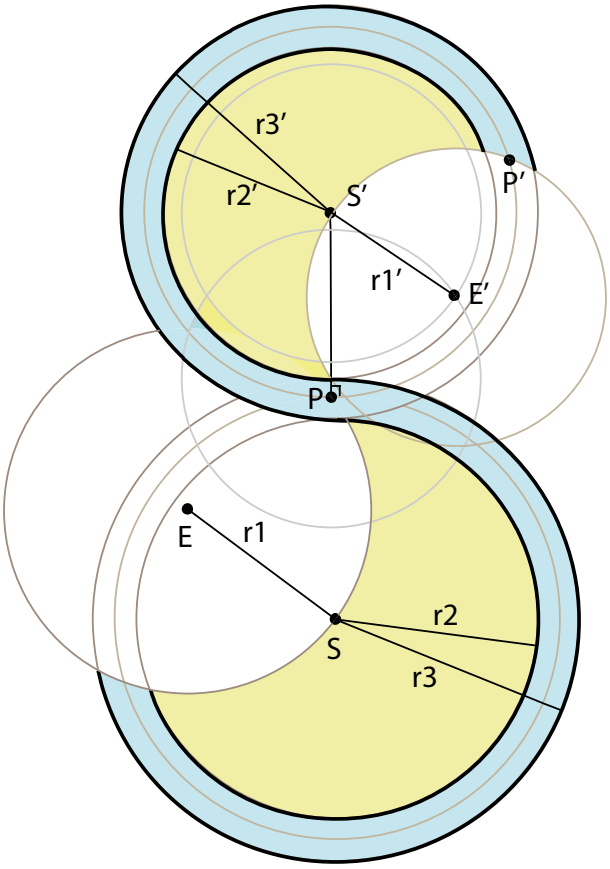

Figure 2.13. Illustration of point bar model creation, see text for explanation.

2.3.5 Combinations

Although mostly only one type of model is used to generate a model realization, it is also possible to combine various modeling techniques. The validity of using combinations of both object-based and pixel-based models was tested (Seifert and Jensen 2000). Here a braided fluvial reservoir from the UK Continental Shelf was modeled in this study using either a pixel-based technique (Sequential Indicator Simulation - SIS), an object-based technique (Boolean Simulation - BS), or a combination of the two. The resulting realizations were assessed by visual inspection and by evaluation of the values and ranges of the single-phase effective permeability tensors, obtained through upscaling. It was concluded that the SIS model recreated

the sheetflood deposits better, but the BS models were better at generating confined channels. The combination of the two (**Fig. 2.14**) is shown to combine the favorable characteristics of both modeling techniques.

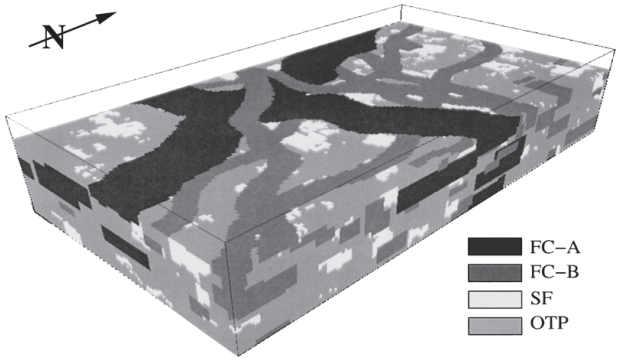

Figure 2.14. Model realization generated by the combined pixel- and object-based approach by Seifert & Jensen (2000).

2.4 Process based / imitating models

Whereas pixel-based and object-based modeling techniques use statistical techniques, process-based models create realizations by simulating some of the important sedimentary processes in creation of the present deposits. Several techniques will be explained, and their benefits and drawbacks discussed.

2.4.1 *J. Allen (1978)*

The first successful attempt to recreate channelized deposits was developed by J. Allen (1978). This model was initially developed to quantitatively compare model realizations with outcrops, which will not be discussed here. It consists of two sedimentary types: channel and overbank deposits. The conceptual model is one of a coastal plain with a number of channels present at each time (**Fig 2.15a**). The model assumes constant subsidence (R), constant avulsion frequency (P) and a fixed area in which each channel can migrate (W). The channel cross-section in **Fig. 2.15b**, shows initial incision after avulsion (h_o) and h_t the thickness added during the time the

channel is present at that location. After each avulsion the channel location is chosen within W, but avoiding the previous channels due to increased elevation at these sites.

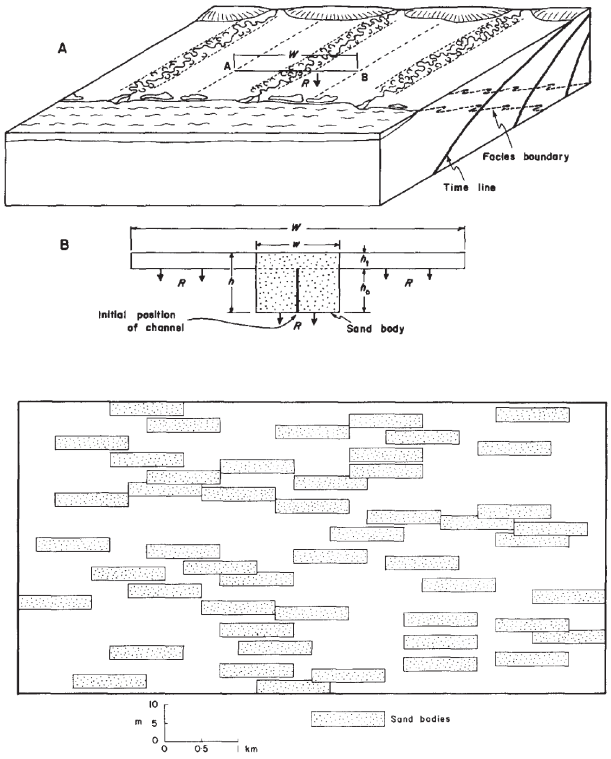

Figure 2.15. (a) Conceptual process-based model used by Allen (1978); (b) cross-section showing the separate channel bodies in an overbank matrix. In this case mainly unconnected channel bodies are present due to high amount of overbank deposits (low N/G).

2.4.2 Bridge & Leeder (1979)

Bridge and Leeder (1979), developed a more realistic process-based model, similar to the model developed a year earlier by Allen (1978). The conceptual model (**Fig. 2.16a**) is similar, with added faults at both edges of the model area. Also laterally variable aggradation and compaction of fine sediment was added. An example of a cross section is shown in Fig. 16b, where the compaction effects are clearly visible,

whereby the need for an artificial avoidance part in the algorithm for new channels is no longer required. For this realization faulting was skewed between the two boundaries, with a larger displacement along the left fault. This causes the channels to preferentially migrate towards the left edge.

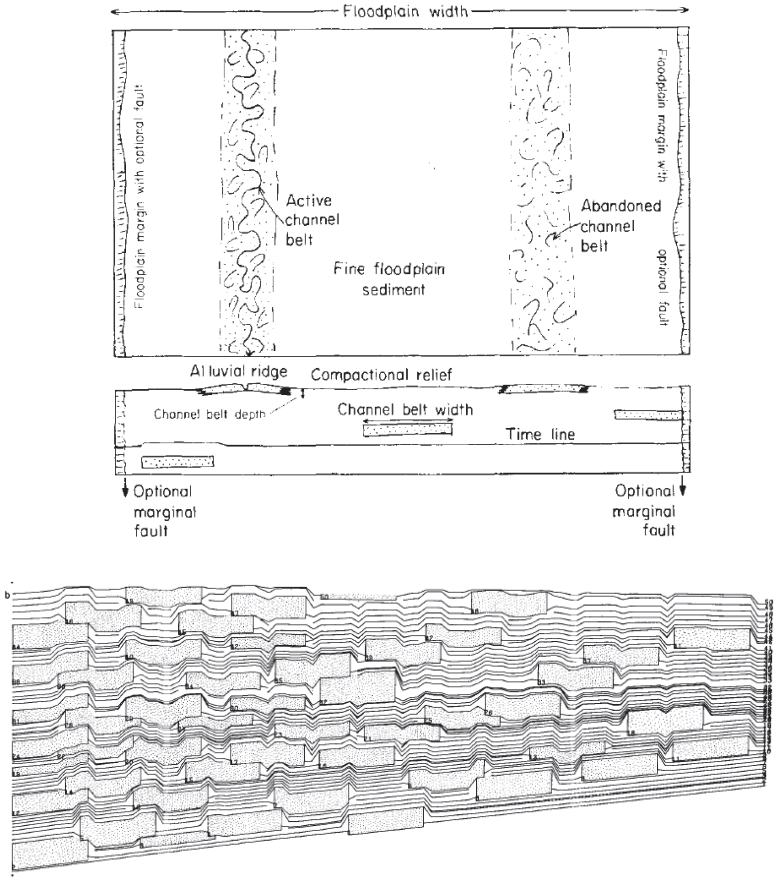

Figure 2.16. (a) Conceptual model used by Bridge & Leeder (1979) process-based model; (b) cross-section showing the separate channel bodies in an overbank matrix as well as sediment compaction.

2.4.3 Koltermann & Gorelick (1992)

Whereas earlier process-based models used the general relationships between geological bodies, Koltermann & Gorelick (1992) tried to recreate observed features at a single location: 600.000 years of deposits on an alluvial fan in California. This location was chosen due to the interesting controls present: river flooding, sedimentation, subsidence, land movement that resulted from faulting, and sea level changes (see **Fig. 2.17**). This produced deposits of alternating coarse and fine material. To make a detailed reconstruction a supercomputer was required, with in total 1450 hours of CPU time. This consisted of a first phase where model parameters were established based on simulation of the first 150,000 years. Once the proper parameters were found, the remaining 450,000 years were simulated.

In **Fig. 2.18** the observations and model results are shown, with the most prominent feature the six wedges of coarse material that are the result of deposition during glacial periods. The right lateral movement of the Hayward fault results in wedges that are horizontally offset to each other.

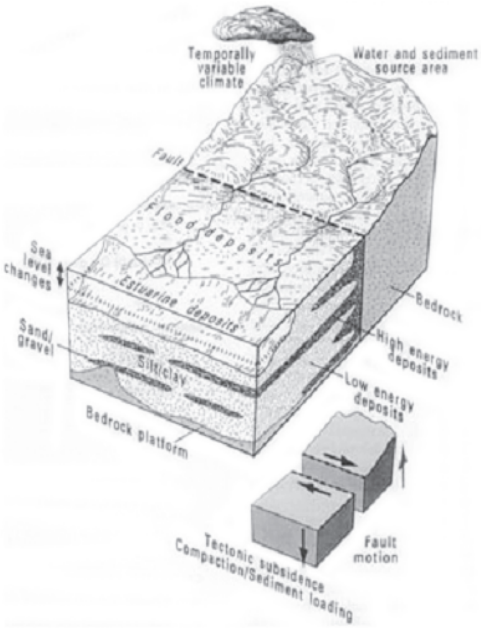

Figure 2.17. Conceptual model of the Koltermann and Gorelick (1992) approach.

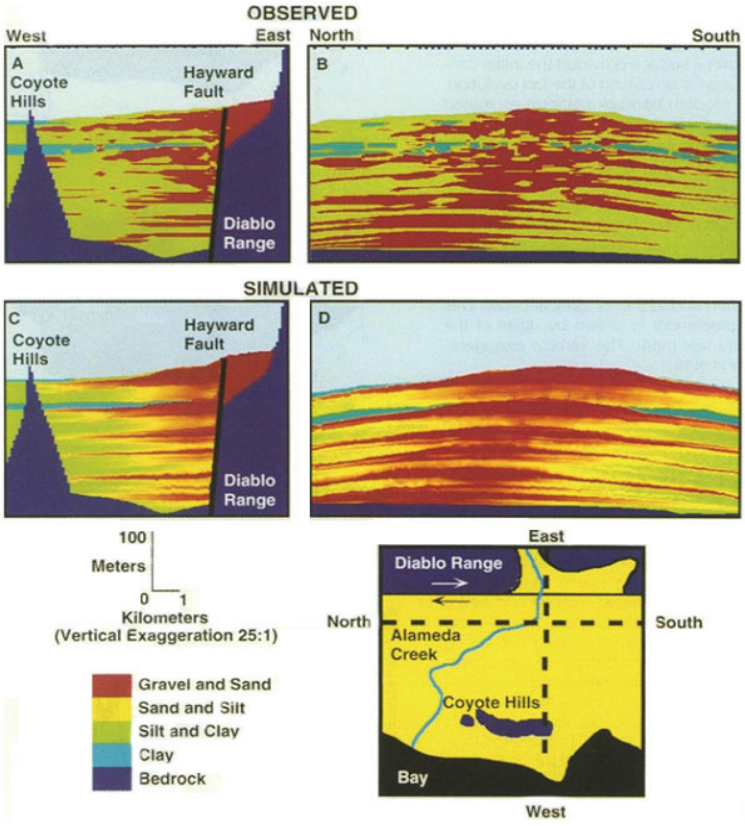

Figure 2.18. Observed and simulated cross-sections showing a high degree of similarity (Koltermann and Gorelick 1992)

2.4.4 Paola (1992)

Where Koltermann and Gorelick (1992) added scale and realism to the field of process-based modeling, the twin articles published in 1992 (Heller and Paola 1992; Paola et al. 1992) formed the basis for later work with regards to the physics of sedimentary systems. The first paper contains a comprehensive set of physical equations, a full review of which is beyond the scope of this paper. This set of equations was derived from fundamental physical formulas instead of the general empirical approach.

The second paper discusses implications for syntectonic conglomerate deposits. A model is used to examine three Neogene basins in order to examine which forcing parameters are dominant in the formation of the conglomerate deposits. Conglomerate deposits were chosen as these are often well studied, and are interpreted as having been influenced by tectonic activity in the hinterland, as well as being under the influence of other forcing parameters. Analysis of numerical reproduction of the three basins showed that generally the techniques are applicable. Furthermore, using numerical simulation the primary driving mechanisms can be established.

2.4.5 Teles et al. (2001)

The main advantage of process-based models is to analyze and compare trends in the sedimentary record with respect to control parameters, as described above. It would be very useful if a model realization can be matched to a specific setting and match the specific locations of geological deposits, as described by Teles et al. (2001).

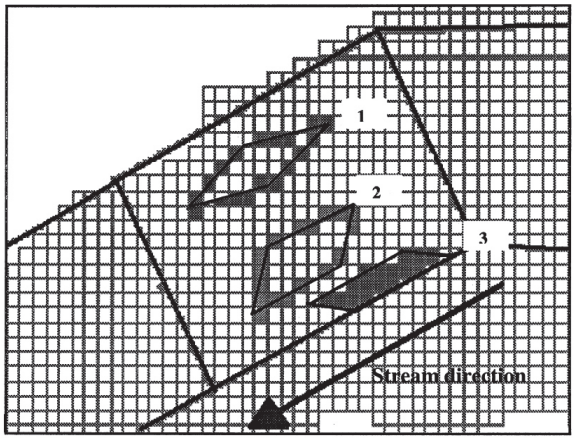

Figure 2.19. The three types of bar shapes in a mesh of the active zone representing the active braided belt within the alluvial plain: 1, longitudinal bar, in the stream direction; 2, transverse bar that grows across the stream direction; 3, lateral bars attached to the banks. In cases 1 and 2, during an erosion period, the meshes of the plain (in grey) around the bar shape are the location where `entities' are taken away from the plain. In case 3, during a deposition period, the meshes of the plain (in grey) below the bar shape are the location where sedimentary entities are deposited.

This paper is based on applying a multi element method, where these elements are water-sediment packages that can either be placed (sedimentation) or that remove previous elements (erosion) (**Fig. 2.19)**. The dynamics are determined by means of local information about the virtual environment and take into account interactions between different types of entities. In the approach presented here, the hydrodynamics of the river are not computed directly. Instead, the main results of deposition and erosion are modeled by simple empirical rules applied to the behavior of so-called `sedimentary entities' at a century to millennia time scales.

2.4.6 Karssenberg et al. (2001)

Although process-based models have the potential to generate more realistic model realizations than stochastic techniques, they have rarely been used to generate subsurface models for flow prediction. The main issue is the apparent difficulty in conditioning to wells.

A technique has been developed by Karsenberg et al. (2001) to generate conditioned realizations of a fluvial channelized system using a Monte-Carlo technique. The process-based model is an adaptation of an earlier alluvial architecture model by Mackey and Bridge (1995), in which a single channel with associated floodplain deposits generates stratigraphy with numerous avulsions. In this model for each timestep the sediment thicknesses are calculated (channel-belt and overbank) as well as the avulsion location and the new channel location (**Fig. 2.20**).

The technique to generate conditioned realizations is essentially a brute-force or trial-and-error approach. Conditioning data in the form of wells is placed in the modeling space. For each of the five wells the mismatch to the conditioning data is checked at each timestep. If a sufficiently large error in the welldata occurs the run is stopped and a new one started. In **Fig. 2.21** an example of well data of a conditioned realization is shown. This method allowed the generation of 50 conditioned model realizations out of 5000 runs using five days of CPU time.

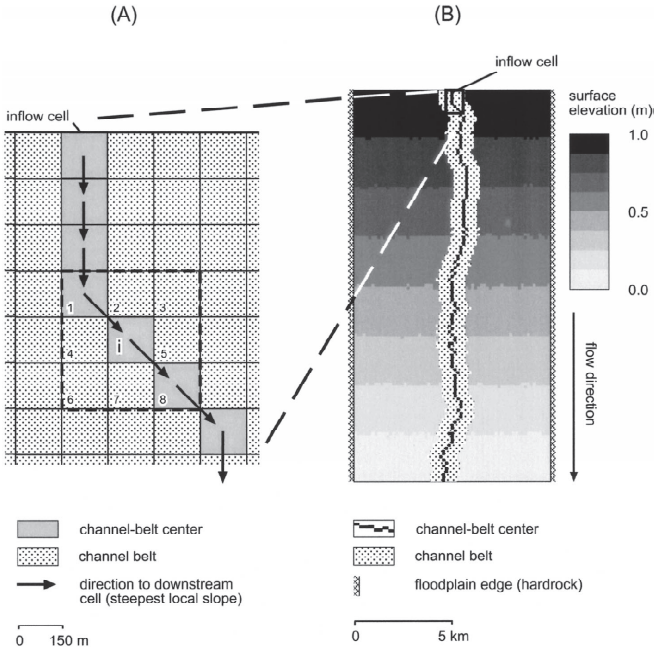

Figure 2.20. (a) Calculation of the channel-belt centerline (b) plane view of initial surface elevation, initial channel-belt centerline and initial channel belt.

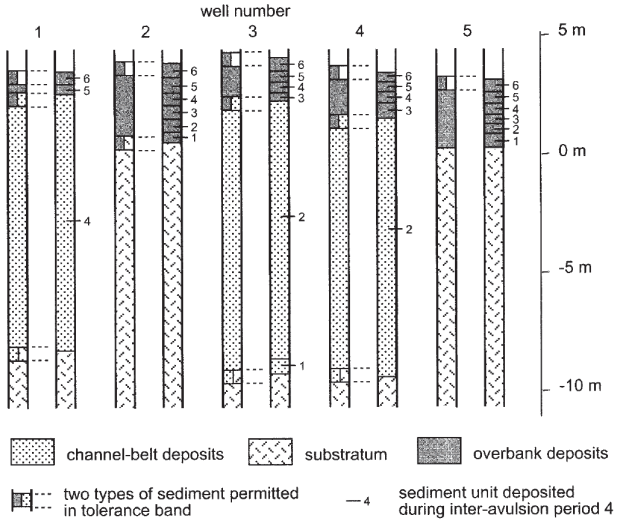

Figure 2.21. Conditioning to well data. For each well number the left column represents the well log with tolerance bands; the right column represents the model output. Numbers to the right of the wells refer to interavulsion periods.

2.5 Conclusions

A large variety of modeling techniques is available, ranging from simple and efficient two-point statistical techniques to complex but realistic process-based models. The appropriate use of these techniques requires a good choice to be made, based on:

- The type of geology to be modeled
- The available data
- The computing power available

3 The effect of two-point statistical modeling parameters on fluid flow behavior of sub-surface reservoirs

3.1 Introduction

The property that most often influences the flow behavior is the distribution of permeability. Its spatial variability depends on a complex interplay of various geological processes, but often the permeability distribution in the model(s) is generated using a geostatistical method (e.g. variogram-based method or object-based modeling). A major difficulty in updating pixel-based permeability fields with dynamic data is that often the geological knowledge of the prior estimate is not preserved in the posterior permeability distribution, due to imperfect updating techniques. A possible circumvention of this problem would be to update a reduced-order parameter set that is used as input in geological or geostatistical modeling methods, as is done in the probability perturbation (Caers and Zhang 2002) and gradual deformation method (Hu 2002).

In closed-loop reservoir management (Jansen et al. 2005) measurements are used to estimate a set of model parameters and the updated or history-matched models are subsequently used to calculate optimal controls that optimize an objective function, such as net present value (NPV). Because the parameter estimation problem in reservoir engineering is ill-posed (Tavassoli et al. 2004), the solution of the parameter estimation problem is non-unique. To regularize the problem and make the solution unique, it would be also useful to use a reduced-order parameter set which can result in the correct control action maximizing the objective function.

Here we examine the sensitivity of geostatistical modeling parameters to reservoir flow behavior, characterized by NPV and water breakthrough time (WBTT). This can be regarded as a first step to examine the possibility of finding a reduced parameter set with geological meaning that can be used to calculate the correct control action maximizing an objective function in closed-loop reservoir management. We expect to find which geostatistical input parameters have a negligible effect on the objective function and which are control-relevant, and thereby to find a mapping function between the geostatistical input parameters and the objective function.

3.2 Methods

3.2.1 Geostatistical method

For the prediction of oil and/or water flow rates in reservoirs, a reservoir simulation model is required that is fit for prediction and control, and at the same time honors available static and dynamic data. The permeability distribution in the model can be generated by many different geostatistical techniques with varying amounts of geological realism. The number of input parameters required for these methods varies from 5 for variogram-based methods to 50 for process-based models, where one input parameter set can be used to generate different permeability fields due to the stochastic nature of the methods. The values or range of values of the input parameters can be based on geological knowledge, seismic data, static and dynamic well measurements. Here we use a variogram-based method (Matheron 1967) with a spherical model, where a filter implementation is used (pers. comm. S. Douma 2007). The six input parameters that define the variogram are the sill, range 1 in the principal direction, range 2 in a direction orthogonal to the principal direction, the nugget, the angle of the principal direction and the mean permeability. All parameters are assumed to be independent of each other.

3.2.2 Parameter choice and experimental design

To find the flow response of models formed by all parameter combinations many models would need to be generated and flow simulations performed on each, because an infinite number of parameter combinations, and thus models, exist. If each parameter is limited to 10 discrete values, $6^{10}=6.0\text{x}10^{7}$ models would need to be simulated to form a full picture of all model responses, an impossible task given limited computer resources. However, it might be possible to limit the number of models required to generate a picture of flow responses to the various parameters, depending on the smoothness of the change in flow behavior when only one parameter is changed. Assuming that the change in flow behavior is gradual, far fewer models need to be used. In the simplest case, where the change in flow behavior to the change in one parameter is zero, only one model needs to be used. For a linear response two models are sufficient, while for a quadratic function three are needed, and so forth. Here a quadratic function was found sufficient to describe the model response. This means that each parameter need only be represented by three values, chosen to be its lowest, mean and high values.

The range is chosen to be the maximum of possible ranges for the reservoir model; and these values can be found in **Table 3.1**. The values chosen are such that even at extreme parameter combination still a realistic model is generated. For example, the combination of range1 and range2 of 120 and 10 respectively was determined to be at

the extreme end of an elongated body, whereas values of 40 and 40 generate an isotropic model.

	Range1	Range2	Angle	Sill	Nugget	Av. Perm (mD)
min. (-1)	40	10	45	0.1	0.1	200
mean (0)	80	25	90	0.4	0.2	300
max. (+1)	120	40	135	0.7	0.3	400

Table 3.1. Geostatistical input parameters and their ranges as used in the experiment setup.

For each input parameter a range of variation is specified by a maximum (+1), mean (0) and minimum value (-1). This means that for 6 parameters and 3 values per parameter $3^6 = 729$ parameter sets can be generated. For each parameter set 30 realizations are generated, leading to in total 729*30=21870 permeability fields. To limit this number experimental design is applied (Atkinson and Donev 1992). Using D-optimal design the number of parameter sets is limited to 300, leading to in total 9000 permeability fields, which are all conditioned on static well data. Examples of permeability fields generated by varying the parameters are shown in **Fig. 3.1**.

3.2.3 Simulation

The reservoir simulation model is a single-layer, horizontal reservoir consisting of 2601 grid blocks whose production is simulated for a duration of 250 days. The other reservoir and fluid parameters are given in **Table 3.2**. The wells are configured as a quarter five-spot; an injector is placed in the NW corner and a producer in the SE corner. The wells are temporarily shut in when the bottom-hole pressure in injector and producer differ by more than 10^7 Pa from the initial reservoir pressure. To limit grid orientation effects multi-point fluxes are applied, which is a technique to correct for the effect that in a simulator fluids preferentially flow parallel to the main axes.

Reservoir parameters		
Parameter	*Value*	*Unit*
Grid block number in x,y,z	51,51,1	-
Grid block size in x,y,z	5,5,1	m
Porosity φ	0.2	-
Compressibility c	1.0^{-09}	Pa
Viscosity μ	1.0^{-03}	Pa*s
Density ρ	1000	kg/m^3
Initial pressure $p(0)$	3.0^{07}	Pa
NPV calculation parameters		
Oil price r_o	100	$\$/m^3$
Water prod. cost r_{wp}	-5	$\$/m^3$
Water inj. costs r_{wi}	-10	$\$/m^3$
Discount factor b	0.10	-

Table 3.2. Reservoir parameters and NPV calculation parameters

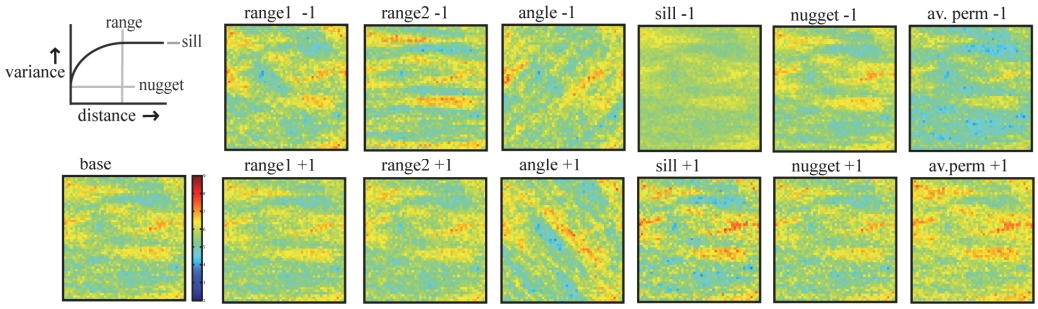

Figure 3.1. The graph in the upper left shows an example of a variogram, and the one at the lower left the permeability field with all input parameters at the mean value (0). The remaining graphs in the upper row show the permeability fields when one input parameter is changed to the minimum value (-1), and the lower row when one input parameter is changed to the maximum value (+1).

3.2.4 Flow data analysis

Analysis of the data from the flow simulations is not straightforward, as the simulation results are in the form of production rates at a limited number of points in time, as shown in **Fig. 3.2**. In order to compare these two data sets a metric or a set of metrics needs to be found which can accurately describe a large portion of the responses of the various models. Two metrics were chosen: the Net Present Value (NPV) and the Water Breakthrough Time (WBTT).

The NPV is defined as:

$$NPV = \max \sum_{k=1}^{N} \frac{q_o(k)r_o + q_{wi}(k)r_{wi} + q_{wp}(k)r_{wp}}{(1+b)^{\tau(k)}} \Delta t(k),$$

where k is the time step, q the surface volume rate, r the cost or revenue, b the discount factor, Δt the time step size and τ the elapsed time in years. The subscript o denotes oil, wi water injection and wp water production. The values we used are given in Table 1, and the change in NPV over time is plotted in **Fig. 3.2**. WBTT is defined as the time in days when a production well first produced water.

Results

3.2.5 Raw data

After flow simulation of the models and reduction of the data to NPV and WBTT, the data that is available in the form of the model parameters and the corresponding flow metrics. As such they cannot be used directly to analyze the flow behavior changes as a response to the input parameters.

The data can be understood in terms of a seven-dimensional space. The six input parameters are located on one axis each, and a metric on the seventh axis. Every model is then represented as a point within this space. The goal then is to find trends of the data within this seven-dimensional space, which is impossible to do visually. Therefore we will be examining the data in terms of projections and cross-sections, both are illustrated for a simple case in **Fig. 3.3**. Two input parameters p1 and p2 and one metric m are shown, with data points in the three-dimensional space. The data is represented by a surface for clarity. To find the effect of p1 on m, one could examine the *projection* of all data points along the p2 axis on one area formed by the p1 and m axes. Also, it is possible to examine the effect of p1 for a single value for p2 by taking a *cross-section* of the data on a face parallel to the p1 and m axes. Both methods of visually examining the data are valuable. When examining a cross-section the average effect of one parameter is found when no knowledge of the other parameters is available. However, when the value of one parameter is known, of p2 in this case, it is advisable to examine cross-sections. To be able to examine cross-sections however, many more data points are required, increasing exponentially for each input parameter.

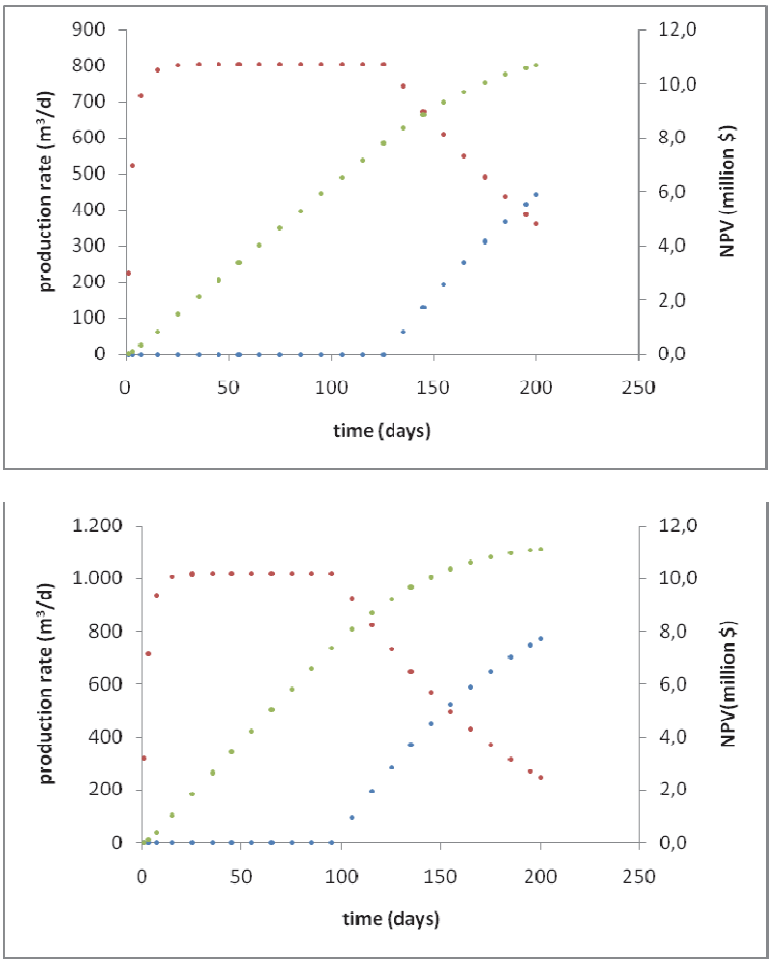

Figure 3.2. Data for two model realizations as obtained after simulation. Water and oil production are shown in blue and red respectively (left axis) and NPV change in green (right axis).

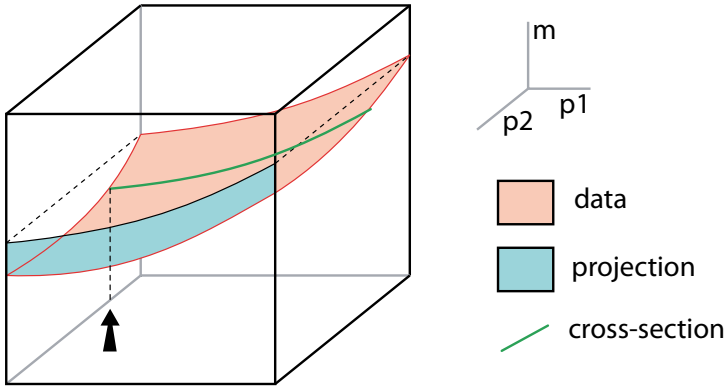

Figure 3.3. Sketch of how parameter interactions can be visualized. The box is defined by three axes representing two input parameters p1 and p2, and one response metric m. Each measurement is a point determined by the three values of p1, p2 and m, here represented by the red surface. The data can examined as a whole by projecting all the data along an axis (blue surface) or by only examining the data on the cross-section for one p value (green line).

Both projections and cross-sections for the data are shown in **Fig. 3.4** for WBTT and **Fig. 3.5** for NPV. The cross-sections are chosen with the all parameters set at their mean (0) values. The generation of these averaged cross-sections is discussed below under *Response surfaces*. When examining the projections of responses for WBTT, it is found that only the angle and permeability have a relatively clear effect on WBTT. The effect of a change in angle can be explained by the fact that the WBTT time becomes smaller, i.e. earlier water breakthrough occurs, when the structures are oriented parallel to the flow from injector to producer. Permeability affects WBTT very strongly; a high average permeability allows earlier water breakthrough to occur.

The results for NPV (**Fig. 3.5**) show that the strongest effects are found for angle and sill. For the angle it is evident that intermediate values are associated with the highest NPV values, caused by early water breakthrough for high values or poor connectivity between injector and producer for low values of angle. An increase in sill is found to reduce NPV, and importantly also to increase uncertainty. The reduction is caused by the fact that an increase in sill causes an increase in permeability difference between high and low within a model, thereby increasing the differences between individual models.

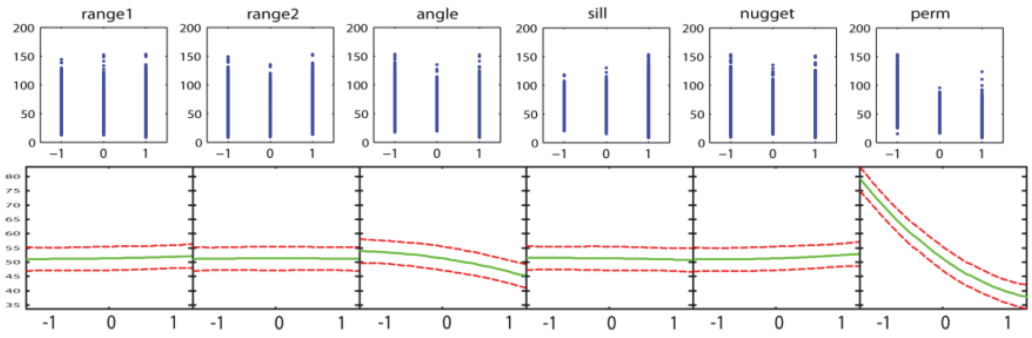

Figure 3.4. The top row shows the spread of the WBTT for the minimum (-1), mean (0) and maximum (+1) value of each parameter. The bottom row shows the response surfaces for each normalized parameter for WBTT. The horizontal axes show the range of the parameter, from (-1) to (+1). The vertical axes show the values of the WBTT in days. The red lines indicate the 95% certainty interval.

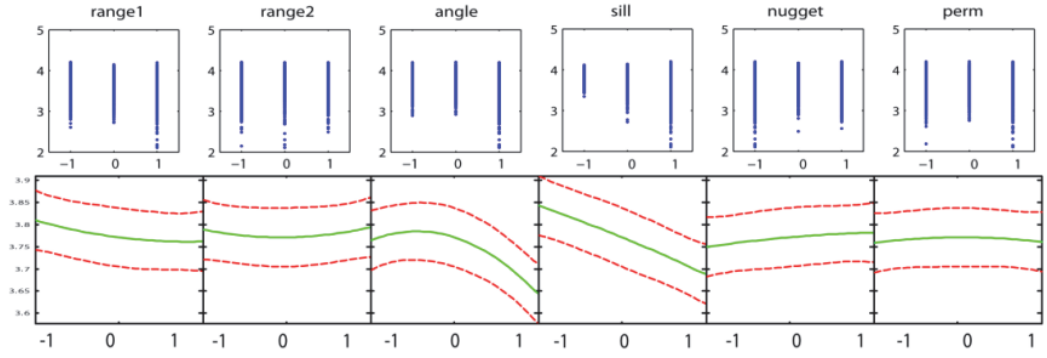

Figure 3.5. The top row shows the spread of the NPV for the minimum (-1), mean (0) and maximum (+1) value of each parameter. The bottom row shows the response surfaces for each normalized parameter for NPV, with on the horizontal axes the range of the parameters and on the vertical axes the values of the NPV in million $.

3.2.6 ANOVA

The second part is the Analysis of Variance (ANOVA), which analyzes the statistical significance of the sensitivity of each parameter. An ANOVA generates a p-value, which is the probability that the null-hypothesis is true. The null-hypothesis states that the parameter of interest does not have an influence on the objective functions. Thus, a low p-value indicates a low probability of the null-hypothesis being true and the alternative hypothesis is accepted, stating that the parameter *does* have an influence. The results are shown in **Table 3.3** where on the diagonal the p-values of the single input parameter are shown and on the off-diagonals the interactions between parameters. The dark yellow colors indicate that a parameter or the interaction between parameters has no influence. For instance, the mean permeability is not influencing the effect of other parameters on NPV.

WBTT	range1	range2	angle	sill	nugget	perm
range1	0.04	0.05	0.44	0	0	0.49
range2	0.05	0.86	0	0.76	0.37	0.83
angle	0.44	0	0	0	0.82	0
sill	0	0.76	0	0.76	0	0.07
nugget	0	0.37	0.82	0	0.01	0
perm	0.49	0.83	0	0.07	0	0

NPV	range1	range2	angle	sill	nugget	perm
range1	0.02	0.33	0	0	0	0.8
range2	0.33	0	0	0	0.33	0.78
angle	0	0	0	0.03	0.1	0.14
sill	0	0	0.03	0	0.45	0.48
nugget	0	0.33	0.1	0.45	0	0.85
perm	0.8	0.78	0.14	0.48	0.85	0.02

Table 3.3 Results of ANOVA analysis, top for WBTT and bottom for NPV. High influence ($p>0.1$) shaded in grey.

3.2.7 Response surfaces

At this point we know which parameters and which combinations of parameters are significant, but the magnitude of this influence is still unknown. To establish the magnitudes, response surfaces (RS) are calculated. A RS is a multi-dimensional linear or quadratic function describing the value of the objective function as a function of the input parameters (Myers and Montgomery 1995). Cross-sections of the RS for each parameter are plotted at the bottom row of **Fig. 3.4** and 3.**5**. In the figures the RS cross-sections are shown for the case when the input parameters are at the mean value. When the value of one parameter is changed, the value of the objective function and RS cross-sections of other parameters may change. The RS cross-sections indicate that the objective functions are most sensitive with respect to average permeability and sill (the variability of permeability values), and significantly less with respect to the other input parameters. The nugget only slightly influences the objective function. In the case of long, thin structures with a high variance and low average permeability (range1=+1, range2=-1, sill=+1, pm=-1) the nugget influences the WBTT the most: from 75.8±4.1 days for a minimum nugget and 78.7±4.1 days for a maximum nugget. The WBTT is therefore for most cases not sensitive with respect to the nugget, and the value of the nugget is set to 0 in the further analysis. The same holds for NPV.

To analyze the influence of parameter combinations the permeability fields are grouped into isotropic heterogeneous, isotropic homogeneous, anisotropic heterogeneous and isotropic homogeneous, as illustrated in **Fig. 3.6**. The isotropy is specified by the relation between range 1 and range 2: if the ranges are equal to each other, then the field is isotropic, otherwise it is anisotropic. The heterogeneity is specified by the sill: if the sill is high, then the field is heterogeneous, otherwise it is homogeneous. Regarding the WBTT, increasing the mean permeability from 100 to 300 mD decreases the WBTT by approximately 45 days. However, this effect is negligible for NPV, which decreases with increasing cost of water production. If the range of mean permeability is increased, a more obvious effect might become clear. Another effect is the large influence of the angle. A minimum value for the angle corresponds to structures in NE-SW direction, and a maximum value to structures in NW-SE direction. In the case of anisotropic, heterogeneous reservoirs (long, thin structures with high variance), the WBTT and NPV decrease when the angle is increased. This effect is negligible for homogeneous isotropic reservoirs (round-shaped structures with low variance), as expected, because for an angle of +1, the injected water can travel through the long, thin structures with high variance fast to the producer, while for an angle of-1, the water needs more time to break through and

resulting in a higher NPV. Furthermore, homogeneous reservoirs have a higher NPV, due to a more efficient displacement of the oil by the injected water. The total computing time of these calculations is approximately 3.1 days on a desktop computer with two 3.2 GHz processors and 1 Gb of RAM memory.

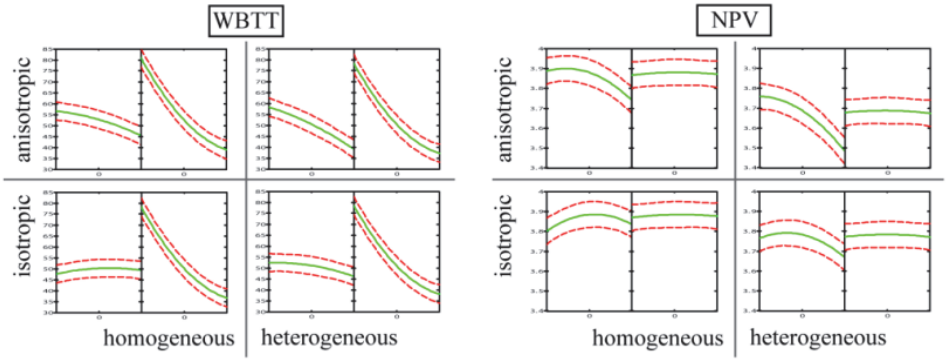

Figure 3.6. For WBTT (right) and NPV (left) the cross-sections of the response surface for the angle (left) and mean permeability (right) are shown. The value for range 1, range 2 and sill determine if the permeability field is characterized as anisotropic, isotropic, homogeneous or heterogeneous.

3.3 Conclusions

The numerical experiment described above shows to what extent the flow behavior, characterized by the two metrics NPV and WBTT, is sensitive to input parameters of the variogram-based method. Of the six parameters only the nugget has a negligible influence. The WBTT is mainly sensitive to the angle, the sill and the mean permeability, while the NPV mostly depends on the angle and the sill. The sensitivity of the interaction between parameters, which affect isotropy and heterogeneity, is also quantified. It has been shown that the approach used here, using experimental design and response surface methodologies, is effective. In further work other geostatistical techniques will be examined in a similar manner.

4. An evaluation of relevant geological parameters for predicting the flow behaviour of channelized reservoirs

This chapter is previously published in Petroleum Geoscience: Gerben de Jager, Jorn F.M. Van Doren, Jan Dirk Jansen, Stefan M. Luthi (2009, Vol. 15, pp. 354-354).

Abstract

We evaluated the relationship between geological parameters and the flow behaviour of channelized reservoirs with the aid of an experimental design approach. The geological parameters included geometrical properties such as channel dimensions and sinuosity, petrophysical parameters such as permeability and net-to-gross ratio, and a derived property: connectivity. The reservoir flow behaviour was characterized with various metrics based on simulated production data generated with the aid of reservoir flow simulations. In the first part of our study, we found a weak correlation between the geometrical parameters and the reservoir flow behaviour, whereas we found a strong correlation between connectivity and the flow behaviour. In the second part we demonstrate how to use the strong correlation between connectivity and flow behaviour to make a selection of models with similar production response from a large ensemble of reservoir model realizations.

4.1 Introduction

Prediction of the amounts and rates of production from a hydrocarbon reservoir has always been a difficult task, mainly because the geological properties that govern the flow response of the reservoir are generally poorly known. Determining these geological properties, and the associated parameters of numerical reservoir simulation models, from static (geological, petrophysical) data and dynamic (production) data is an ill-posed inverse problem. In other words, there are always many more model parameters than can be uniquely determined from the available data. But although different reservoir models may correspond to similar historical production data, the future flow response of these models can be considerably different. The prediction of the amounts and rates of production from a hydrocarbon reservoir should therefore preferably be based on an ensemble of reservoir models that offers the widest possible range of credible geological variety, while honoring all historic data available (e.g.

Oliver et al., 2008). Generation of large ensembles of reservoir models, conditioned to historic static data, can nowadays be performed at relatively low computational costs using e.g. geostatistical or object-based simulation tools (see e.g. Journel et al., 1998; Deutsch et al., 2002). However, conditioning the ensemble members (i.e. reservoir models) to historic dynamic data is a time-consuming process because it involves one or more predictions of the flow response of each ensemble member using numerical reservoir simulation. Another problem of this 'history matching' process is how to adapt the reservoir model parameters without losing the prior geological information, such as sedimentary characteristics, reservoir architecture, permeability relationships, or body dimensions. This is especially the case for highly heterogeneous reservoirs, such as fractured and channelized reservoirs. Examples of channelized reservoirs are the deltaic deposits of the Brent group (e.g. Hohl et al., 2006), turbidite channels in West Africa (e.g. Labourdette et al., 2006), and the North Rankin field in offshore Australia with a high net-to-gross ratio (e.g. Martin, 1993). Specific history matching techniques that limit the loss of geological realism are the gradual deformation method (Rogero and Hu, 1998; le Ravalec-Dupin & Nœtinger, 2000), and the probability perturbation method (Caers, 2003), but these are limited to geostatistically generated reservoir models. Another way to minimize the loss of prior geological information is to restrict the need for large model parameter changes by simply selecting only those ensemble members that already reasonably match the historic dynamic data. Unfortunately this implies that the flow response of an even larger number of ensemble members needs to be simulated because typically most ensemble members will have a flow response that does not reproduce the historic production data. If it would be possible to correlate the historic flow response to a certain (combination of) diagnostic reservoir parameters, one could restrict the computational efforts as follows: 1) simulate the response of a limited number of ensemble members, 2) select those simulated members whose response reasonably matches the historic dynamic data, 3) compute the values of the diagnostic reservoir parameters for the selected members, and 4) search for all other ensemble members with similar diagnostic parameter values. The underlying assumption is that computing the diagnostic parameter values takes significantly less computational effort than performing full flow response simulations. This proposed model screening approach is closely related to various methods for ranking ensembles of geostatistical realizations. For example the ranking method described by Deutsch (1998) uses a connectivity measure as the diagnostic parameter. Streamline-based ranking methods have been described by, for example, Idrobo et al. (2000), Brandsaeter et al. (2001), Wang and Kovscek et al. (2002) and Friedman et al. (2003). A more recent model screening approach has been described in Suzuki and Caers (2006) and Scheidt and

Caers (2007), where the diagnostic reservoir parameter was taken to be a geometric, pixel-based, metric known as the Hausdorff distance.

In this study we examine the influence of various model parameters on reservoir flow behaviour with the goal of 1) obtaining a better understanding of the relationship between reservoir properties and flow response in channelized reservoirs, and 2) finding a parameter or combination of parameters that can serve as an effective diagnostic parameter (see also De Jager et al., 2008 for some early results). Firstly we will examine the relationship between model parameters and flow response using an experimental design approach. Secondly we will demonstrate how using connectivity as a diagnostic reservoir parameter allows rapid selection of model realizations.

4.2 Methodology

To investigate how important the various parameters of a channelized reservoir model are with respect to the flow behaviour, the following steps were taken. First we used an experimental design method to efficiently choose parameter values for each member of an ensemble of reservoir models. The parameters consist of input and derived parameters. Input parameters are used as input in the geostatistical modelling process (**Fig. 4.1**). Examples are channel dimensions, sinuosity, net-to-gross ratio and permeability. Derived parameters characterize the spatial properties of the different reservoir models (Hovadik & Larue, 2007). In particular, we considered connectivity, defined as the number of connected high-permeable cells between all injector-producer combinations. The flow behaviour was characterized by three different flow metrics, as described in detail below. Each realization was simulated to generate synthetic production data, and from the results we calculated empirical relationships between the input and derived parameters on the one hand and the flow metrics on the other. We used the approach as described by Van Doren et al. (2007), where the relationship between flow behaviour and input parameters of a variogram model was investigated in a similar manner.

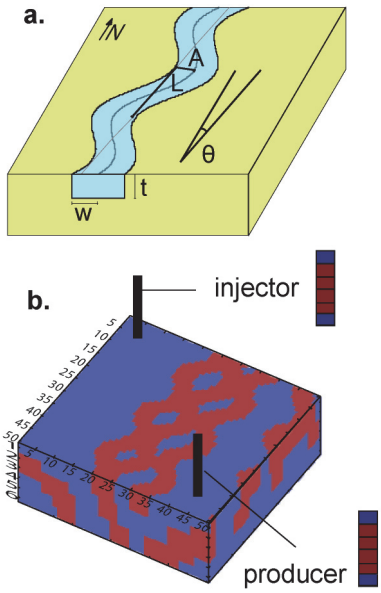

Figure 4.1. (a) Illustration of geometrical input parameters and (b) a realization of the reservoir model with locations of the wells. Channel facies in red and floodplain facies in blue. See Table 4.1 for an explanation of the symbols.

4.2.1 Design of experiments

We used parameter values listed in **Table 4.1**. The values were chosen to span a substantial part of the possible range whilst minimizing parameter combinations that are unrealistic. For instance, channels with a combination of very high sinuosity amplitude and a very short period are seen as unrealistic and should not be included. Apart from single parameter responses we are also interested in interactions between parameters, and the experimental design methodology provides an effective way to examine such interactions. An example of an interaction we are interested in is whether a change in sinuosity will have a bigger effect on flow response for high channel permeability than for a low permeability. After selecting parameters and parameter ranges we used the Design of Experiments approach (Atkinson & Donev, 1992) to select the set of parameter values for the simulations. In this approach, first the range of each input parameter is discretized into a low, medium, and high value,

designated by -1, 0 and 1, respectively (**Fig. 4.2 and 4.3**). This gives a choice of 3 input values for each parameter, or 3^n possible parameter combinations for n parameters (a full factorial set). This set can be reduced using an efficient design, the D-optimal design matrix of the parameter values, which allows a more efficient sampling of the parameter space than the full factorial set or random parameter combinations.

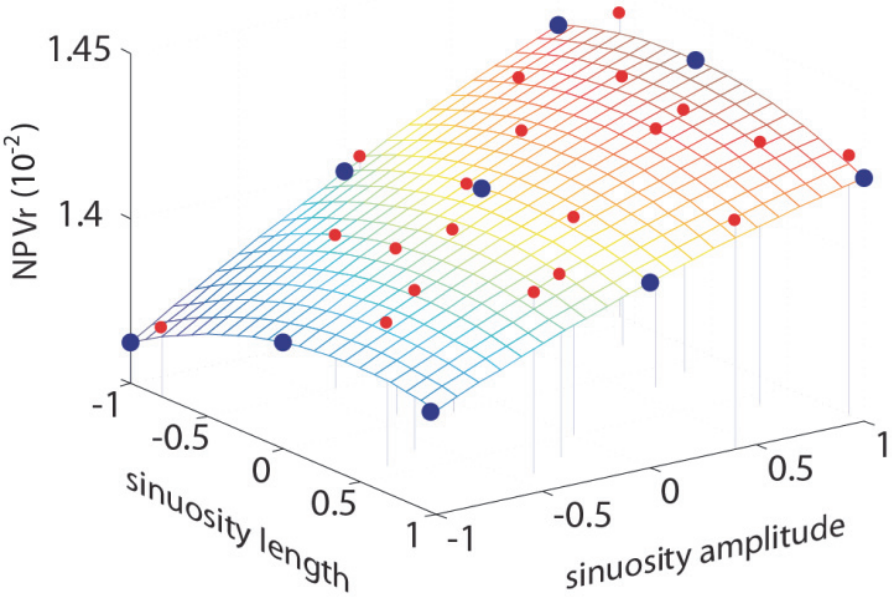

Figure 4.2. Response surface of NPV_r as a function of channel sinuosity length L and amplitude A. Red dots show experiments with random input values, blue dots show the more efficient design of experiment results.

Parameter	Symbol	-1	0	1	Units
Angle	θ	-45	0	45	degrees
Width	w	2	4	6	cells
Thickness	t	1	2	3	cells
Sinuosity – length	L	1	2.5	4	cells
Sinuosity – amplitude	A	0	2	4	cells
Net-to-gross ratio	f_v	0.25	0.50	0.75	-
Floodplain permeability	k_1	10	30	50	mD
Channel permeability	k_2	200	500	800	mD
Connectivity	c	0	5625	11250	cells

Table 4.1. List of input parameters and derived parameter.

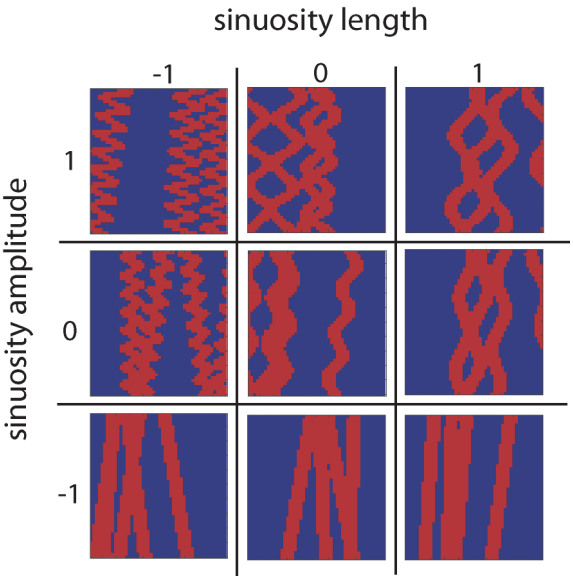

Figure 4.3. Illustration of the nine parameter combinations used in design of experiments shown in Fig. 4.2 with channel facies in red and floodplain facies in blue. Parameters are scaled from -1 to 1.

4.2.2 Geological modelling

In the next step the model realizations need to be created, based on the parameter combinations determined by the design matrix. We decided on an object-based technique that creates models with two facies, user-defined geometries, and that are conditioned to static well bore data. Object-based models have been found to be superior to variogram-based models as well as multi-point statistics for describing complex geological reservoirs, resulting in more accurate flow predictions (Journel et al., 1998; Falivene et al., 2006). Although various techniques for creating models of fluvial systems are available, these were found to be unsuitable for our purposes, mainly because of excessive complexity or imperfect well conditioning. Therefore, it was decided to develop a new code to efficiently generate a large number of simple realizations of a fluvial system (**Fig. 4.1a**). Dimensions of the reservoir model were chosen so as to allow sufficient expression of detail in the relevant parameters. Thus, a rectangular reservoir consisting of six layers and 50 x 50 cells in the horizontal directions (in total 15,000 cells) was generated. Dimensions of each cell are 50 m x 50 m horizontally and 5 m vertically.

The generation of the model realizations is similar to the FLUVSIM algorithm (Deutsch et al., 2002) in that a simulated annealing approach is used. The first part of the algorithm generates the channels such that well-conditioning is achieved. These channels remain fixed for the second part of the simulation, which consists of either adding or removing a channel body from the reservoir, based on the minimizing the error in net-to-gross ratios (N/G) per layer. To add a new channel first a location is chosen. Randomly choosing a point in the reservoir would cause an uneven distribution of channels (i.e. higher density in the centre part). To ensure an even distribution the channel location is found by first placing a line perpendicular to the channel orientation in the reservoir, and then randomly placing a point on this line on which the channel is placed.

Placing the channel is done by choosing a small deviation from the general flow direction, randomly chosen between -10^{o} and $+10^{o}$. This small angle change is included to ensure that between two neighboring channels with identical periods more realistic connectivities will result. If this angle deviation is not used two channels will connect at every period or will always be out of phase and therefore never connect. Every addition or removal is then analyzed by checking if the objective function has decreased, where the objective function is defined as:

$$J_m = \sqrt{\frac{1}{n_L}\sum_{i=1}^{n_L}\left(f_v^i - \bar{f}_v^i\right)^2},$$

where f_v^i is the net-to gross ratio in layer *i*, $\bar{f}_v^i$ is the desired net-to-gross ratio in layer *i* and n_L is the total number of layers. The net-to gross ratio of layer *i* is defined as $f_v^i = n_{gb,ch}^i / n_{gb}^i$, where n_{gb}^i is the total number of grid blocks in layer *i* and $n_{gb,ch}^i$ is the number of grid blocks associated with channel facies in that layer. In order to condition the realizations to well data, the objective function is extended to consist of the sum of the root mean square error of net-to-gross ratios and the mismatch with the well conditioning data. A cut-off value for the objective function of 0.05 or lower was found to result in acceptable models.

4.2.3 Simulation

We simulated each realization using a proprietary black oil simulator using a multi-point flux finite difference discretization (Aavatsmark et al., 1996). An injector – producer pair was placed in the 15,000 cell model as shown in **Fig. 4.1b.** Production and injection rates were kept constant, except when pressure constraints were exceeded. The values of the pressure constraints were set to $200*10^5$ Pa and $400*10^5$ Pa. For the relative permeabilities the Corey model was used, with exponents $n_w = n_o = 2$ and end-point saturations $S_{wc} = S_{ro} = 0.1$. The initial water saturation was chosen as 0.2 and the initial pressure as $300*10^5$ Pa in every grid block. The fields were simulated for approximately 25 years, with approximately 90 timesteps of at most 100 days each. Grid block size and length of time steps were chosen by decreasing the size and length until the simulation results converged. Simulation continued until the water-oil ratio reached 90%. This resulted in simulation times of approximately five minutes per realization on a 1.86 GHz laptop.

4.2.4 Characterization of flow response

In order to compare the simulation results a metric needs to be defined to characterize the production data. It is not possible to use the production data directly for comparison mainly due to varying simulation times and volumes of oil initially in place (OIIP). The metric needs to contain information on the:

1 production behaviour in time;
2 behaviour over the entire simulation time;
3 behaviour over the entire model area.

In other studies flow behaviour has been characterized by the recovery factor (RF), which is valid for (b) and (c) but does not say anything about (a). The water breakthrough time (WBTT) in the production well could also be used: this satisfies (a) but does not contain information on the production over the entire simulation or of the full model area. Based on the results of several pilot experiments we decided to use WBTT and three additional metrics that do satisfy the above mentioned conditions. These are firstly J_1, which represents net present value (NPV), secondly J_2, which represents the relative NPV (NPV_r), i.e. the NPV corrected for OIIP (OIIP varies per realization because the net-to-gross ratio changes), and thirdly the root mean square error of the production rates ($RMSE_p$) relative to an arbitrarily chosen base case. The metrics are defined as:

$$\text{NPV:}\quad J_1 = \sum_{k=1}^{N} \frac{q_o(k)r_o + q_{wi}(k)r_{wi} + q_{wp}(k)r_{wp}}{(1+b)^{\tau(k)}} \Delta t(k),$$

$$\text{NPV}_r\text{:}\ J_2 = \frac{J_1}{N_o},$$

$$\text{RMSE}_p\text{:}\ J_3 = \sqrt{\frac{1}{N}\sum_{k=1}^{N}\left[q_o(k) - \bar{q}_o(k)\right]^2},$$

where k is the time step, N is the total number of time steps, q is the surface volume rate, r is the cost or revenue (water production: -\$50/m^3, water injection: -\$50/m^3, oil production: \$500/m^3), b is the discount factor (0.08), Δt is the time step size and τ is the time in years. The subscript o denotes oil, wi injected water and wp produced water, and the variable N_o represents the OIIP.

4.2.5 Response surface modelling

In order to evaluate the relationship between geological parameters and flow behaviour, we use a finite number of combinations of the input variables. Under the assumption that the response for intermediate input parameter combinations can be obtained through interpolation of the simulated output (i.e. the flow metrics), we can generate a surface (or, in multiple dimensions, a hypersurface) of the response of the simulator to the input parameters. After the seminal article of Box and Wilson (1951) several different techniques have been developed to find such a response surface, from the initial linear response surface method to more complex techniques such as

Multiple Response Modelling (Miró-Quesada et al., 2004) and Hierarchical Nonlinear Approximation (Busby et al., 2007). To decide on the appropriate method a detailed examination of the response to two parameters (net-to-gross ratio and channel orientation) was performed (**Fig. 4**) where the flow response was characterized by WBTT, NPV_r and connectivity (described below). For all tests the flow behaviour can be represented acceptably as a linear or quadratic response. The chosen quadratic response surface E describing the response for n parameters is given by:

$$E = \beta_0 + \sum_{i=1}^{n} \beta_i x_i + \sum_{i=1}^{n-1} \sum_{j=i+1}^{n} \beta_{ij} x_i x_j + \sum_{i=1}^{n} \beta_{ii} x_i^2 ,$$

where x_i denotes the i-th input parameter, and where the linear, interaction and quadratic terms are quantified by a scaling factor β (e.g. for 8 parameters 45 scaling factors are needed). Using the response surface it is now possible to predict the flow response based on various input parameter combinations without having to simulate every experiment.

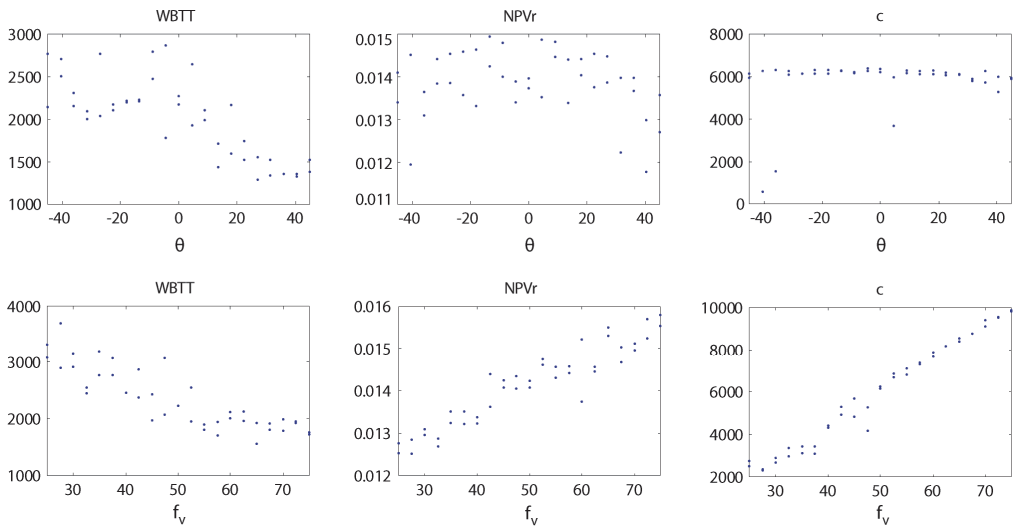

Figure 4.4. Plots showing the effect of changing angle θ and net-to-gross ratio f_v (horizontal axis) on water breakthrough time (WBTT), relative NPV (NPV_r, in \$/m^3) and connectivity (c).

4.3 Results

4.3.1 Correlation between input parameters, derived parameters and flow metrics

Results were analyzed for two groups of metrics; (a) the geometric and non-geometric input parameters and (b) the derived parameter, connectivity. The experiment is designed for 400 parameter combinations, and with 4 realizations for each parameter combination, this results in a total of 1600 model realizations. Simulations were performed on all realizations and for each run the production data were recorded and used to generate quadratic responses surfaces.

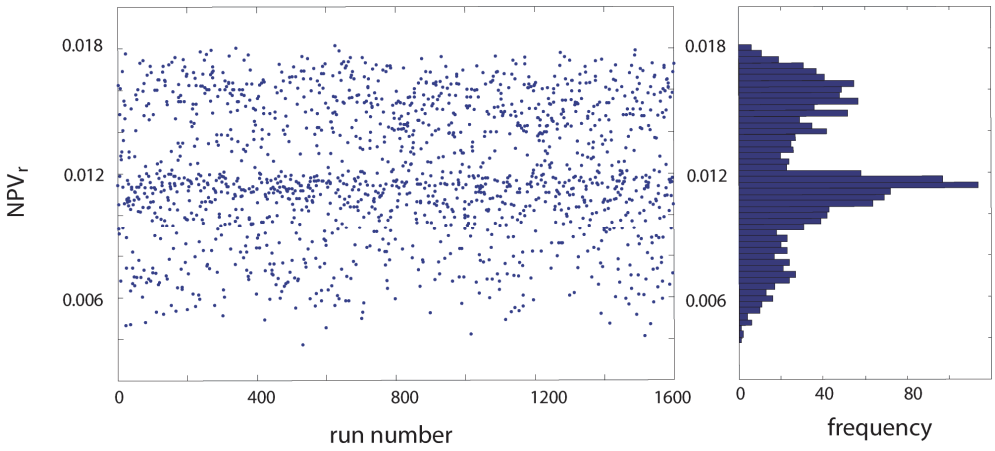

Figure 4.5. The NPV_r for all 1600 simulations (left) and a histogram of the NPV_r distribution (right).

4.3.2 Input parameters

A first visual examination of the data consists of inspecting the unsorted NPV_r values for all 1600 runs (**Fig. 4.5** left). From this figure two horizontal belts are clearly present with higher concentrations of measurements. A histogram of the data (**Fig. 4.5** right) shows the distribution in more detail, with two modes and a smaller third data peak. These modes are mainly caused, from left to right, by the low floodplain permeability cases (10 mD), the low channel permeability cases (200 mD) and the high channel permeability cases (800 mD). Note that the clustering in the histogram is

due to the choice of input value combinations, and does not necessarily imply a multi-modal probability density function.

4.3.3 Response surface

The response surface resulting from the 1600 realizations shows how the 8 different input parameters influence flow as characterized by NPV, NPV_r and $RMSE_p$ **(Fig. 4.6)**. This figure shows how the metrics change when each input parameter varies from its low (-1) to high (+1) value, while maintaining the other input parameters at their intermediate (0) value. These plots of the response surfaces can be interpreted as sets of two-dimensional cross-sections through the 9-dimensional space describing the model response (8 dimensions for the input parameters and a ninth for the flow response). The influences most apparent on NPV_r are the last three parameters: net-to-gross ratio (f_v), floodplain permeability (k_1), and channel permeability (k_2). This is not entirely unexpected; it has long been known that net-to-gross ratio and permeability affect reservoir behaviour to a large extent (e.g. Hewett, 1986; Corre et al., 2000). The approach often used to model channelized reservoirs is to first model the channels within the reservoir, and then to assign permeability values to the different facies (e.g. Zhang et al., 2006). However, this does not highlight the relative importance of the two types of information. The geometric parameters (i.e. the parameters describing the shape of the channels) show an indistinct and non-linear influence on NPV_r. For example, the value for θ causing the highest NPV_r value is at its intermediate value (0). The low value of the angle (-1) causes channels to be oriented along the average fluid flow from injector to producer, which causes early water breakthrough and reduces NPV_r. The high value (1) causes the orientation to be perpendicular to the general flow direction, which causes poor connectivity between injector and producer, also lowering NPV_r. The intermediate value where the channels are oriented obliquely to flow mitigates both negative effects and results in the highest average NPV_r. The response of sinuosity amplitude (A) shows that for increasing values of A the NPV_r also increases. This is presumably caused by the fact that increasing A increases the chance of channels connecting, thereby increasing connectivity.

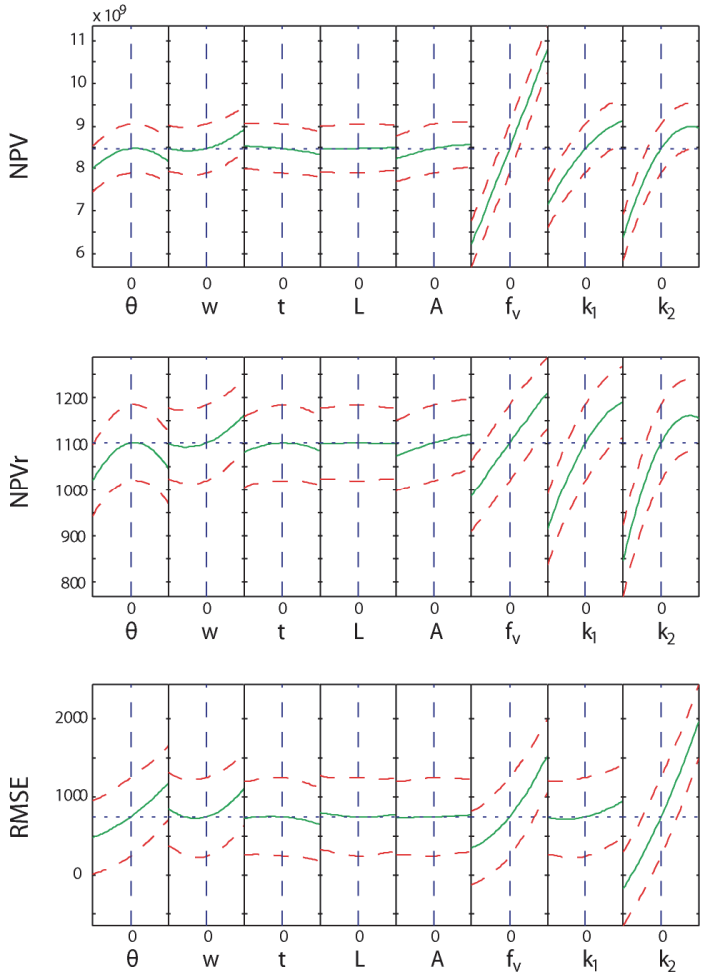

Figure 4.6. Cross sections through the response surfaces of NPV, NPV_r and $RMSE_p$ as a function of the input parameters listed in Table 1.

4.3.4 ANOVA

Analysis of variance (ANOVA) (Hogg & Ledolter, 1987) is a collection of statistical methods for hypothesis testing involving multiple groups of observations. Performing an ANOVA analysis on the results of the simulations can give insight into the statistical relationships between (combinations of) input parameters and the flow response. One value that can be obtained from an ANOVA analysis is the p-value (**Table 4.2**), which can be interpreted as the probability that we find a difference in

flow response even though the null-hypothesis is correct. Here, the null-hypothesis states that a certain (combination of) input parameter(s) is not of influence, or, more precisely, that the mean of the flow response is not significantly influenced by the (combination of) parameter(s). A low p-value allows rejecting the null-hypothesis and accepting the alternative hypothesis, i.e. that the (combination of) parameter(s) does have an influence. Often a value between 0.01 and 0.10 is used as cut-off. In Table 2 we see on the diagonal the single-parameter effects are all equal to zero (within the numerical accuracy) except for one value. The exception is the sinuosity length L, which still has a very low p-value (0.02), indicating a high degree of certainty that the individual parameters have an effect on NPV_r. The symmetrical off-diagonals show whether the interaction between two parameters is significant. The off-diagonal parameter combinations generally show low p-values, except for the combinations of sinuosity length L with most of the other parameters, and the combination of channel width w with channel permeability k_2. This implies that the combined change of these parameters has no significant effect. Another, more informative, result from an ANOVA analysis is the F-value, which can be interpreted as a measure of the relative statistical influence. While the p-value corresponds to whether a parameter or parameter combination is significant, the F-value is a measure of the size of this influence. **Fig. 4.7** shows a Pareto chart for the 9 largest of all 36 F-values. The first three parameters (f_v and permeability values k_1 and k_2) are already sufficient to describe 85% of the model response, while 9 parameter value (combinations) describe 95% of the response.

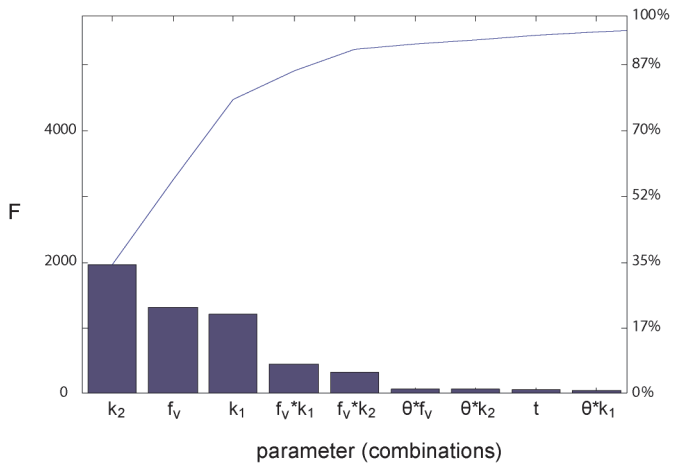

Figure 4.7. Pareto chart showing the highest F-values, or relative importance, of the 9 most important parameters and parameter combinations. For the symbols see Table 1

	θ	w	t	L	A	f_v	k_1	k_2
θ	0.00	0.00	0.00	0.25	0.00	0.00	0.00	0.00
w	0.00	0.00	0.10	0.08	0.02	0.00	0.00	0.32
t	0.00	0.10	0.00	0.01	0.00	0.00	0.00	0.00
L	0.25	0.08	0.01	0.02	1.00	0.11	0.22	0.20
A	0.00	0.02	0.00	1.00	0.00	0.00	0.00	0.00
f_v	0.00	0.00	0.00	0.11	0.00	0.00	0.00	0.00
k_1	0.00	0.00	0.00	0.22	0.00	0.00	0.00	0.01
k_2	0.00	0.32	0.00	0.20	0.00	0.00	0.01	0.00

Table 4.2. ANOVA-derived p-values of parameters and their combinations. A low value indicates a large probability that the parameter (combination) has a significant influence on the NPV_r. Single parameter values (which all happen to be significant) are in blue, parameter combinations of possible significance ($0 < p \leq 0.10$) are in yellow, and combinations with no significant effect ($p > 0.10$) are in orange. In white all values of $p<0.01$, i.e. high significance. The values of 0.00 are all smaller than 10^{-6}. For the symbols see Table 1.

4.4 Connectivity: a derived parameter

The results presented so far show that geometrical parameters only have a weak relationship with flow behaviour of a reservoir, and thus that the possibilities of using this relationship for model selection within a history-matching context are limited. The reason for the indistinct response of the reservoir models is caused by the large difference in flow response between realizations with identical input parameters. Apparently the locations of and relationships between the bodies are more important than their exact dimensions. A derived parameter quantifying features of the realizations themselves, rather than of their input parameters, might produce better results. Several derived parameters have been suggested (Soleng et al, 2006; Suzuki & Caers, 2006). A useful derived parameter should display a clear and continuous trend with respect to reservoir flow behaviour. Connectivity has been shown to have a strong influence on reservoir response (Larue & Hovadik, 2006), and therefore shows

some promise as a parameter for model selection purposes. Connectivity (c) is determined by the location of geological bodies, and is here calculated by counting the number of channel cells connected to either well. Connected cells are defined as cells connected by common faces, omitting those connected by ribs or vertices, in a method similar to the CONNEC3D software (Pardo-Igúzquiza et al, 2003). To examine how the reservoir flow response is related to connectivity, 50 realizations were used to generate a response surface of the flow metrics NPV and $RMSE_p$ as a function of connectivity, *c* (**Fig. 4.8**). The figure shows a clear relationship between connectivity and both flow metrics. The third flow metric, NPV_r was not used, because in reality the OIIP is not known, and therefore NPV_r cannot be used in the workflow described in the following sections.

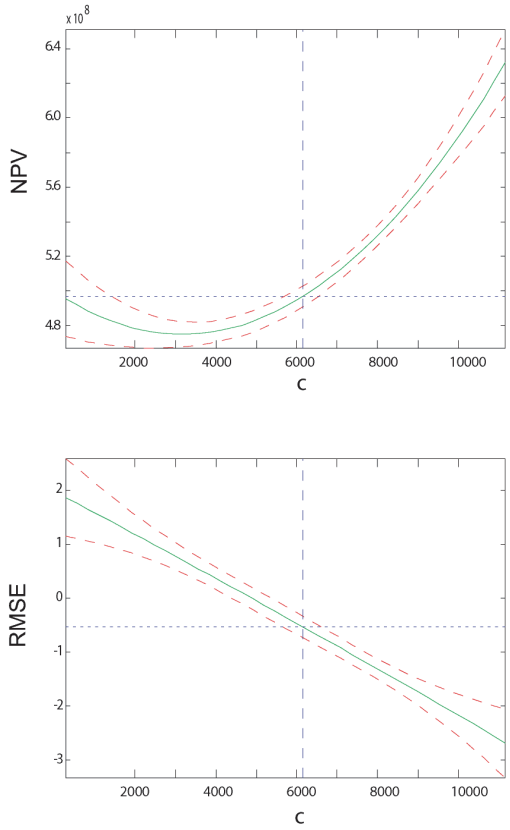

Figure 4.8. Response surfaces of NPV and RMSE as a function of connectivity, c.

4.5 Application to flow-based model selection

4.5.1 Workflow

In this second part of our paper we will use the clear and monotonic relationship between connectivity and NPV (**Fig. 4.8**) to select a reduced set of model realizations from a large ensemble of models. We assume that a response surface can be used to predict connectivity values, and subsequently these connectivity values can be used to select a set of models which will have production profiles similar to the measured data. This only requires calculating the connectivity for each reservoir model, which is computationally much less demanding than performing a flow simulation. This leads to the workflow for history matching purposes depicted in **Fig. 4.9** and consisting of the following steps:

- Generate R realizations, simulate them over the period of interest and create response surfaces of predicted NPV and/or RMSE, as a function of the connectivity parameter, c.

5. Compute the true NPV and/or RMSE from production data.
6. Use the empirical relationship between connectivity and production data from the response surfaces to make an estimate of the connectivity of the true reservoir.
7. Generate new random model realizations, and maintain only those with a similar connectivity as the true reservoir (within a certain tolerance), until the total desired number of realizations R_{target} has been achieved.

The benefit of this method is that it is only necessary to simulate the initial R realizations to generate the response surface. Thereafter we can select R_{target} realizations from an ensemble of size N realizations, where $N >> R_{target}$, by only calculating the connectivity values, which is computationally more than two orders of magnitude quicker than a flow simulation. The underlying assumptions are that there exists a clear relationship between connectivity and NPV and/or RMSE, and that models selected based on historic production data also have predictive value.

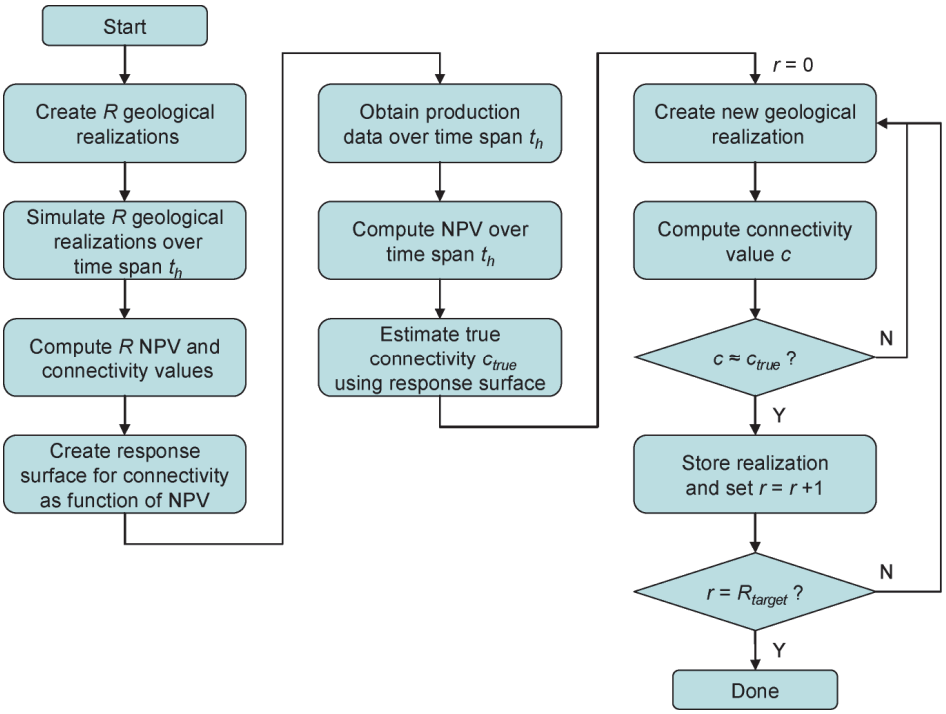

Figure 4.9. Flowchart of the proposed realization selection workflow subdivided into three parts: Left: generation of the empirical relationship between connectivity and NPV. Centre: estimation of true connectivity based on measured production data. Right: selection procedure based on connectivity.

4.5.2 *Validation*

To test the validity of the workflow described above we performed a numerical experiment where the 'true' data were generated using a synthetic 'true' reservoir model which was simulated over the 'historic' time period t_h. A set of R models were also simulated to t_h to find the relationship between connectivity and production data. Subsequently, we selected a history matched set (R_{target}) from an unsimulated ensemble, N. We then simulated both the truth and the R_{target} selected realizations over a 'forecast' time period ending at t_f to compare the quality of the predictions with the 'true' reservoir behaviour. In **Fig. 4.10** the results of this selection procedure are shown for one truth case. In this example we have chosen $R = 50$ and $R_{target} = 10$, and $t_h = 15$ years. The variable t_f varied for each realization and was between 20 and 30

years, depending on when the watercut reached a value of 0.9. For this case N was 270.

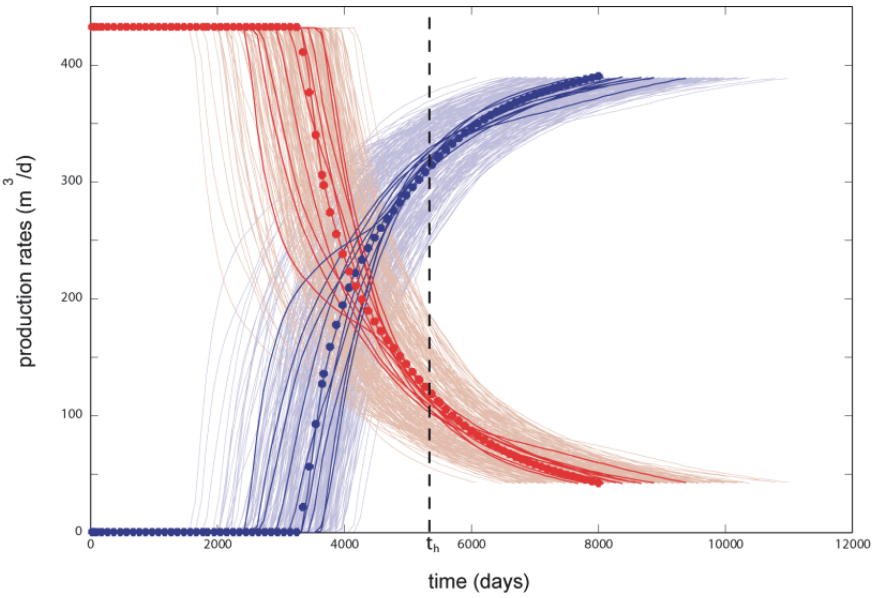

Figure 4.10: Oil- and water production plots of 'truth' (red and blue dotted lines), selected realizations (red and dark blue lines), and discarded unsimulated realizations (light red and light blue lines). The vertical dashed line indicates the end of the history matching time period and the start of the forecast time period. The selection has reduced the root mean square error with respect to the truth case by 53% at time of selection, and by 31% at shut-in.

The quality of the selection can be quantified by the root mean square error of NPV for the entire ensemble and the selection both at t_f and after shut-in at t_h. The workflow was implemented for 10 different truth cases. On average a reduction in RMSE of 58% at t_h was found. After shut-in a reduction of RMSE of on average 31% remained. These reductions are measures of the effectiveness of the methodology. This shows that we clearly reduce the uncertainty using this methodology, both in matching to measured production data as well as predicting future values. The selected models still show a reasonable amount of uncertainty, but show promise to be used as input models for other history matching techniques. It should be noted that the parameters of the realizations are not updated during the procedure and thus have

a high amount of geological realism, thereby increasing predictive power (e.g. Teles et al., 2004). Because the modelling procedure is independent of the workflow for selecting the matched realizations any type of model realizations can be used, including process-based models.

4.5.3 Predicting connectivity based on input parameters

Having examined the relationship between connectivity and flow response, the question arises how geometrical parameters influence connectivity. A response surface using the original 1600 simulated model realizations was generated to examine this effect (**Fig. 4.11**). For all parameters apart from net-to-gross ratio an indistinct relationship to connectivity is found. Increasing the net-to-gross ratios always increases connectivity, as this will cause more channel cells to become available in the reservoir with a fixed number of cells. As expected, permeability values do not influence connectivity, and these have only been added for completeness. When comparing this response surface with the response surface with NPV as response (**Fig. 4.6**) some similarities are visible in the shapes of the curves, suggesting a large part of the flow behaviour can be explained by connectivity.

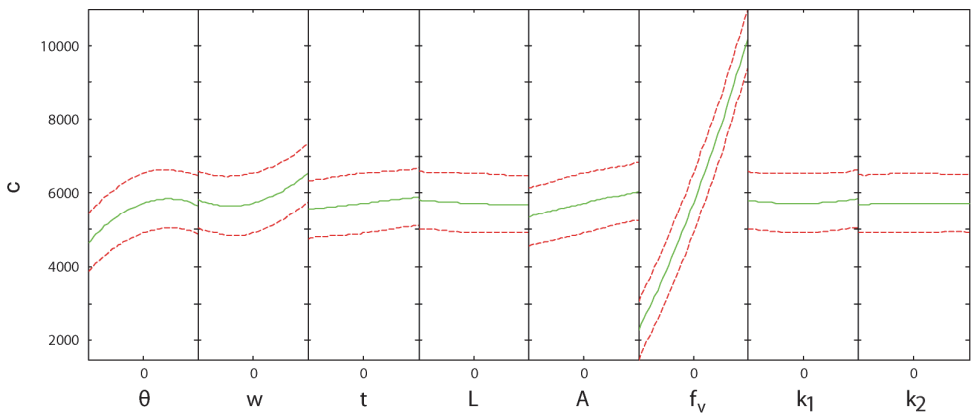

Figure 4.11. Cross-sections through the response surface of input parameters on connectivity. For the symbols see Table 1.

4.5.4 Other static parameters

Using solely connectivity and permeability values to select realizations still causes a significant amount of uncertainty, therefore three techniques were examined that have the potential to improve the quality of the history match. First it was examined whether combining the original parameter set describing the channel geometries with the response surface of connectivity would cause a decrease in uncertainty (combining **Fig. 11** and **Fig. 6**), but this was found not to be the case. From this it can be concluded that the effect should be sought in the location of and relationship between channel bodies; specifically by using a derived parameter similar to connectivity. A second spatial metric examined is the local net-to-gross ratio situated around wells as a conditioning parameter; a technique often employed in the hydrocarbon industry. However, this parameter was found not to influence production directly. A third parameter investigated is the permeability contrast, defined as k/k_2. Response surface modelling showed an influence on the scale slightly less pronounced than the permeability values separately. Future research is needed to examine which parameter or parameter combination can help improve the predictive power of response surfaces.

4.6 Discussion

We have shown that using experimental design for an efficient selection of experiment parameters gives insights into the complex interaction between geological parameters and reservoir flow behaviour. Furthermore, it was found that the geometry of the geological bodies has a relatively weak influence on flow behaviour, but that it is the location of and interaction between the different bodies which was characterized by connectivity that shows a strong influence.

The gradual change of NPV in response to connectivity is different to the sharp one predicted by percolation theory, and shown to be applicable to channelized reservoirs (King, 1990; King et al., 2001). Several authors have indicated causes for behaviour not explained by percolation theory, for instance the limited size of fluvial reservoirs (de Marsily et al. 2005), the absence of an impermeable facies (Knudby & Carrera, 2004) and the non-random body geometries (Hovadik & Larue, 2007). There is also a difference between connectivity as described by percolation theory (a Boolean parameter), whereas here connectivity is a volume connected to the wells. The

combination of these effects can cause a gradual response to net-to-gross to occur, as also found by various other authors (Jackson et al., 2005; Larue & Hovadik, 2006; and for fractured reservoirs by Masihi et al., 2007).

4.6.1 Perspectives for the application to real fields

Since in this approach several assumptions and simplifications are made, the question is as to what extent the observations from this approach are applicable to real reservoirs. Firstly, we assumed that it is possible to reproduce the reservoir in every detail with our modelling technique. For realistic complex geological models this is usually not the case. Secondly, we assumed that the real reservoir model and the model realizations only differed in permeability and porosity values of the grid blocks. For example the fluid properties in each realization were identical to the truth model. On the other hand, no geological information was used that might be available in real cases, e.g. channel dimensions, flow direction, and net-to-gross ratio estimates. Therefore, we found no reason to assume that this technique would not be applicable to real fields, provided the modelling technique can reproduce the spatial characteristics of the real field to a sufficiently high degree of accuracy. The matched ensemble could be used as input for a second history matching technique, such as Ensemble Kalman filtering or the probability perturbation method.

We have demonstrated a fairly high amount of predictability of reservoir flow behaviour without using any geological a priori information apart from the general assumption of a channelized reservoir. Although no knowledge of the magnitude of the geometrical properties was assumed, knowledge of the sedimentary facies present in the reservoir was available. If this knowledge would be incorporated, the uncertainty could be reduced further. The magnitude of the reduction can be estimated by comparing the total number of possible realizations with no knowledge on body shapes with the number of all realizations possible with the object-based technique used in this paper. Assuming a random uncorrelated Boolean model with 15.000 cells would imply 2^{15000} model realizations, or approximately 10^{4500}. However, assuming a sinuous fluvial geometry, the total number of model realizations can be estimated by multiplying the number of channel bodies with all possible geometric parameter possibilities. All parameter possibilities are those which result in a different reservoir model within the discretization of the model. It is in the latter case possible to make fewer than 10^{200} different model realizations. Adding other geological information, such as sequence stratigraphic rules or paleoflow directions, reduces this number even further.

4.7 Conclusions

The applicability of using a methodology combining experimental design and response surface modelling to analyze the sensitivity of reservoir flow behaviour on model parameters has been demonstrated. The influence of the parameters controlling a channelized reservoir was examined by generating a number of realizations using a Boolean object-based modelling tool. A weak relationship between the geometric parameters (channel dimensions, sinuosity, and orientation) and reservoir behaviour was found. However, a strong correlation was found between the parameters describing net-to-gross ratio and the two permeability values with regard to Net Present Value. Using these three parameters it was possible to accurately describe the model response. This led to the conclusion that the remaining portion of the response of a model was determined by the location of the geological bodies, as well as the relationship between them. A parameter which takes this into account has a better predictive power than the geometrical parameters.

This assumption was investigated using connectivity, a derived parameter which has been shown to have a high influence on reservoir flow behaviour. It was found that using connectivity combined with two permeability parameters in a workflow employing a response surface allowed us to make a selection from a large number of model realizations more efficiently than simulating all realizations. In terms of CPU time this is approximately two orders of magnitude faster. One of the advantages of this method is that the modelling process is separate from the workflow. It allows a rapid selection from an ensemble of realizations generated by any technique, whether they are generated by object-based (used here), multi-point statistics-based or process-based methods. This workflow will always generate a selection of models near the measured production data without losing any geological complexity of the original model. The accuracy of these matched realizations with respect to the production data is reasonably high, but connectivity and permeability are not sufficient to fully predict the production data of a hydrocarbon reservoir. The matched ensemble could be used as input for a second history matching technique, such as Ensemble Kalman filtering or the probability perturbation method. Further research is required to test the applicability to other derived parameters.

Acknowledgements

This research was carried out within the context of the ISAPP Knowledge Centre. ISAPP (Integrated Systems Approach to Petroleum Production) is a joint project of the Netherlands Organization for Applied Scientific Research TNO, Shell International Exploration and Production, and Delft University of Technology. We also gratefully acknowledge the use of Shell's reservoir simulator MoReS.

5 Accessibility: a new three-dimensional metric for reservoir characterization and field development planning

This chapter is a manuscript submitted to the SPE Journal by Gerben de Jager and Stefan M. Luthi.

Abstract

A new metric termed accessibility is presented as an alternative to connectivity for describing the degree to which reservoir units are connected with each other. It is borrowed from urban planning and is a measure that describes the ease of reaching a destination from a particular point of origin. In this case the origin is any grid cell in the reservoir model, and the destinations are the production or injection well. An efficient method is developed that finds the optimum paths through the gridded reservoir model from a well to every point in the model. Along these paths accessibility is calculated. After repeating this for every well, the values for each grid cell are summed up to form a 3-D accessibility matrix. From production simulations using a simple channelized reservoir model, statistical parameters such the median accessibility are shown to have a significant correlation with production, expressed as net present value. In another possible application of this metric, accessibility was used to predict water breakthrough, again in a simulated scenario, and showed considerable success. Although accessibility is a strictly static measure, it can thus be used to rapidly evaluate reservoir models when some production history is already available, or to probe well scenarios in early field development planning.

5.1 Introduction

The most critical uncertainties in reservoir models are associated with fluid volume and reservoir connectivity (Meddaugh 2003), affecting hydrocarbon-in-place and recovery respectively. The quality of the predictions of fluid production from a reservoir, therefore, depends strongly on the quality of the numerical description of the subsurface, both in terms of geological heterogeneity as well as fluid flow parameters. Connectivity has often been mentioned as strongly influencing reservoir behavior, and a variety of definitions have been used (King 1990; Hird and Dubrule 1998; Lo and Chu 1998; Pardo-Igúzquiza and Dowd 2003; Knudby and Carrera 2004; Snedden et al. 2007; de Jager et al. 2008; de Jager et al. 2009). While the concept of reservoir connectivity is intuitive and easily grasped by most people, its quantification is far from clear. It is generally accepted that connectivity relates to the degree at

which permeable reservoir units are in touch with each other, such that fluids can move easily from one unit to another. But how much do these reservoir units have to be in touch with each other? How is connectivity calculated if these units differ in permeability? Or how are thin impermeable baffles of limited lateral extent taken into account, since they affect fluid flow in the short term but much less in the long run?

Another intriguing aspect concerning connectivity is the question whether injector and producer wells should be placed such that they are well connected, which improves production rates, or in reservoir units separated by units of lower permeability, which improves recovery. Answers to such questions are usually found through reservoir simulations, by taking into account a company's production strategy. In many cases, however, a reservoir model's connectivity is based on assumptions regarding the spatial properties of the reservoir units, i.e. their lengths, widths, thicknesses, orientations and overall densities. Changing any single one of these parameters can change the reservoir connectivity, regardless of the way in which it is calculated. One can, of course, resort to stochastic modeling whereby these parameters are allowed to fluctuate within a given statistical range (Journel et al. 1998). The outcome, then, is a distribution of connectivity values. After subsequent simulation, the production values will also be in the form of an expected distribution, but which may have, in less favorable cases, such a wide spread as to make it useless for operational decisions. This situation changes, of course, when some production data is already available from the early field development phase. The simulated production over this period can then be compared to the actual production, and all reservoir models that give poor matches can be discarded. In this way a set of reservoir models can be retained that give a better indication of reservoir connectivity and therefore can be more reliably used for simulating future reservoir production (de Jager et al. 2008).

In this paper a new and well-defined metric termed *accessibility* is proposed that captures reservoir connectivity for a given reservoir and well scenario. Its value is calculated for each cell in the reservoir model and is not only dependent on the properties of the reservoir units, but also on well placement, as it takes into account the ease of reach from each cell in the model to the wells in terms of distance as well as permeabilities on the way to the well. In order to demonstrate the viability of this metric, its relationship to production will be shown. The use of accessibility to effectively compare and select model realizations in the case where early production is available will subsequently be discussed. Accessibility can thus be used for a dual purpose, i.e. as a tool for field development planning as well as a tool for reservoir model selection in the early production phase.

5.2 Methodology

5.2.1 Accessibility calculations

To find accessibility as a measure of reservoir connectivity, techniques were borrowed from urban planning. In urban planning accessibility is defined as a measure which describes the ease of reaching destinations from an origin zone (Black 1981). Adapting for reservoir models the origin zones are all cells in the model, and the destination zones are the wells. Thus, the accessibility of a location is a measure of how easily a well can be reached from any point, and is dependent on permeability values and distances to travel. The accessibility differential between two cells is determined by the measure ΔA. This is similar to transmissibility as used in reservoir engineering where it is a measure of the ease of fluid flow between two neighboring cells relating to permeability, cell dimensions and fluid viscosity (Satter 2008). In this study viscosity is assumed constant throughout the reservoir and is not explicitly taken into account.

The accessibility differential (ΔA) between two neighboring cells is defined as:

$$\Delta A = \frac{d}{\ln(\bar{k})}$$

where d is the distance between the centers of the cells and $\bar{k}$ is the harmonic mean of the permeability values. Lower values of ΔA therefore indicate better accessibility, i.e. locations with high values for A are poorly accessible. Using this definition the accessibility of each point in a reservoir model with respect to a well is calculated by summing ΔA along a route from the well to the point of interest. The accessibility of a cell from a distant point can be calculated along many different paths through the reservoir, resulting in a large number of accessibility values. The true retained value for A is the lowest value of this distribution.

The algorithm used to calculate A is an adaptation of Dijkstra's algorithm (Dijkstra 1959), a method developed to find the shortest distance between several nodes with known distances separating them. Here it is used to find the lowest accessibility value from a well to all cells in the reservoir model. The first step of the algorithm starts at the well location and calculates A for all neighboring (M) cells. Next the cell with the lowest accessibility value is found (L); this value of A is called c. From this cell temporary accessibility (A_t) to all neighbors (M) is calculated, and A is updated if a lower value is found than the current A value in M. This is repeated for each next largest value of A. The calculations proceed in a front away from the wells, with in

front of the front only unvisited locations with values unchanged at 0, and behind it locations with accessibility values smaller than *c*. The front itself consists of values larger than c that will be visited when c reaches the value of each of those cells.

A detailed flowchart is shown in **Fig. 5.1**, where the algorithm is seen to consist of three nested loops:

5 Find the current value of c, and check whether the algorithm has finished

6 For all locations L with $A(L)=c$, find all neighbors M, with 18 neighbors per location L.

7 For all M calculate the temporary new accessibility value $A_t(M_n)$. If this is lower than the current value or the current value is 0, $A_t(M_n)$ will become the new value of $A(M_n)$

When the algorithm is finished a matrix A has been created with the accessibility values for each point, calculated from one well. The accessibility of a cell is dependent on how accessible it is to its nearest injector and nearest producer. Therefore, the algorithm described above is performed twice, once for all injectors and a second time for all producers. The final value of accessibility is determined as the sum of the two.

The measure of accessibility as a reservoir characterization tool requires two aspects of mathematical and physical correctness: grid independence and non-dimensionality. The former assures that accessibility values will not change when the grid is downscaled. This can be simply demonstrated when ΔA is calculated without taking the natural logarithm of $\bar{k}$, but is not valid for the calculation used here. The effect of this was tested by calculating A for one model of 100x100x5 cells, and a downscaled version of 300x300x5 cells. After rescaling the two A matrices a root mean square error of only 0.023 was obtained, which is thought to be sufficiently low to justify the use of the natural logarithm. The condition of being dimensionless can be satisfied by dividing all A values by an “average” accessibility value, but this is not performed here as it would unnecessarily complicate the calculations, and would only have the effect of a scaling parameter.

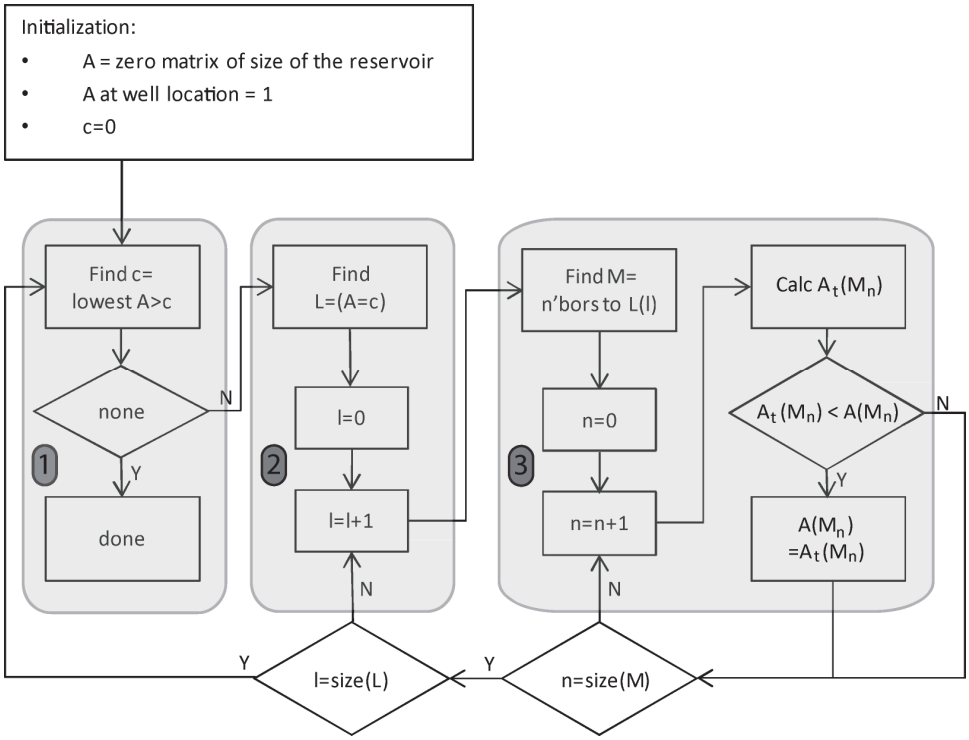

Figure 5.1. Flowchart of the algorithm to calculate the accessibility matrix. The three nested loops are highlighted in grey, see text for explanation.

5.2.2 2D Example of Accessibility

In **Fig. 5.2** a simple two-dimensional example is shown where the permeability field is a two-facies case, with ribbon-like high permeability features (grey) in a low permeability matrix (white). Two wells are present, and for each well *A* has been calculated. For the sake of simplicity neighbors are defined as only those pairs of cells sharing a face. As expected, the well-connected south-western well (Fig. 2b) generates a matrix *A* with lower overall values (i.e. better accessibilities) than the poorly connected well in the north-east (Fig. 2c). When the two matrices are summed, the final matrix of *A* is found (Fig. 2d). Intuitively this figure seems correct: the highly permeable features are prominent as low accessibility elements and the north-west corner has high accessibility values, caused by poor connectivity to either well.

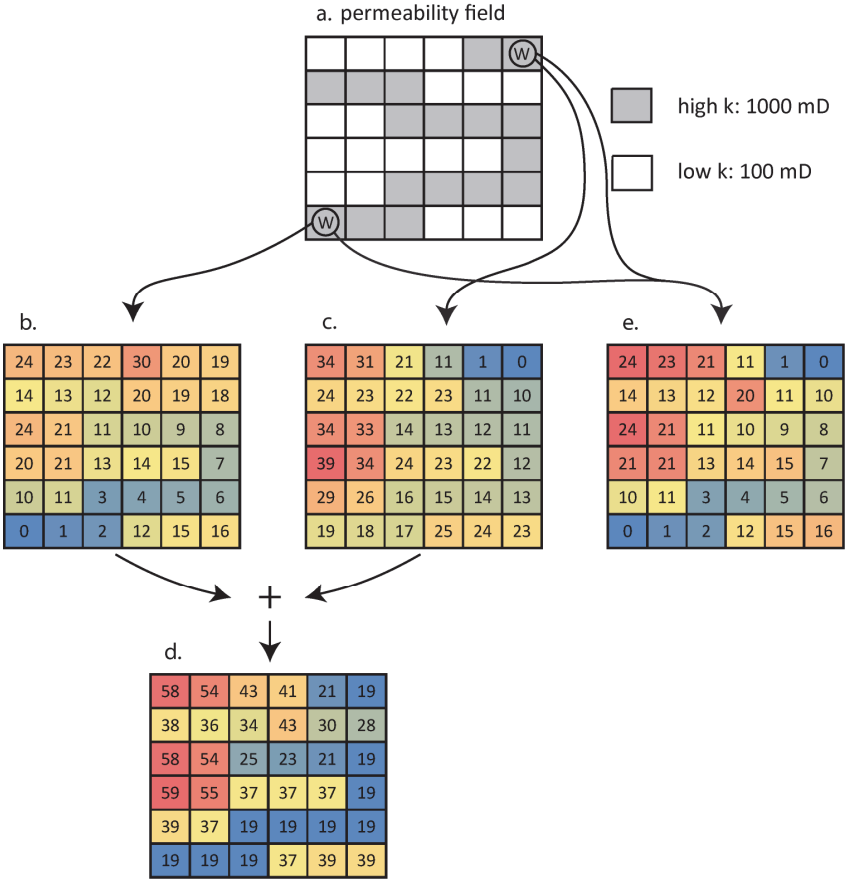

Figure 5.2. Two-dimensional example of a simplified approach of calculating accessibility. Permeability field shown at top, with from left to right accessibility calculated from SW well, from NE well, and from both wells simultaneously. At the bottom the accessibility values for both wells summed.

One adaptation of this algorithm is to calculate A for all wells simultaneously, as this significantly reduces the number of calculations. Computationally this adaptation consists of changing the initialization step to set A at all well locations to 1. The result is shown in Fig. 2e for the 2D example. Comparing this to the summation method reveals that there is the undesired effect that low A values are concentrated near the wells, and have less of a relationship with the heterogeneities of the reservoir, i.e. the channelized feature in the centre of the model. Therefore, the more time-consuming summation method will be used in which A is calculated for each well separately.

5.2.3 *Reservoir modeling*

In this part accessibility as a reservoir characterization tool will be tested on an ensemble of reservoir models. A set of 50 highly heterogeneous channelized model realizations of a channelized reservoir was created using an object-based modeling technique (see de Jager et al. 2008 for a detailed description). The realizations consist of highly permeable channels with associated levees, within a matrix of less permeable floodplain deposits. The input parameters are listed in **Table 5.1**, and one realization and the associated accessibility values are shown in **Fig. 5.3.** The realizations were created by using facies information as conditioning data from three wells, shown in red. Three more wells are placed in the realizations after reservoir modeling was finished (shown in black). The well data was chosen to generate consistency between the model realizations, and should not be interpreted as actual knowledge of the reservoir. Note that the model realizations are identical with respect to most input model parameters, with only the channel locations and orientations varying between the realizations. Geologically this represents a high degree of certainty, but with this approach overprinting of the response of the reservoirs is minimized. Both net-to-gross ratio and permeability have previously been shown to dominate flow response (de Jager et al. 2008).

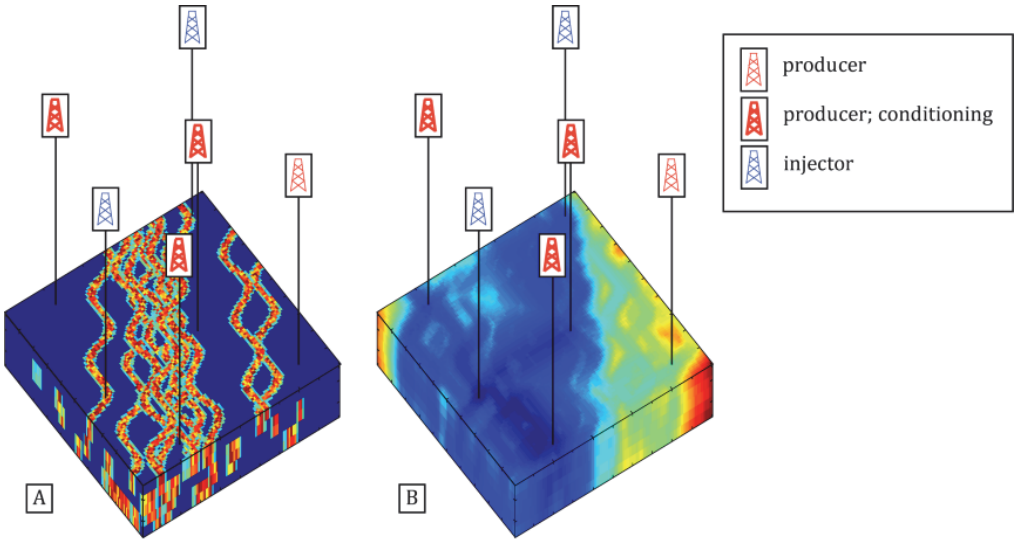

Figure 5.3. A. Reservoir model example showing high permeable channels and 6 wells. B. Accessibility for the same reservoir model. Injectors, producers, and wells from which conditioning data was obtained are also shown.

5.2.4 Flow simulations

Each model realization was simulated using a proprietary black oil simulator. For the relative permeabilities the Corey model (1954) was used, with exponents $n_w=n_o=2$ and end-point saturations of $S_{wc}=W_{ro}=1.0$. The fields were simulated for about 40 years, with approximately 150 timesteps of at most 100 days each. Grid block size and length of time steps were chosen by decreasing the size and length until simulation results did not change with increasing detail. Simulation continued until the water-oil ratio reached 90%. This resulted in simulation times of approximately 10 minutes per realization on a 1.86 GHz laptop.

reservoir model

parameter	**values**	**unit**
reservoir dimensions	5000x5000x50	m
cell dimensions	100x100x5	m
number of cells	50	-
net-to-gross	0,4	-
channel width	200	m
levee width	100	m
channel thickness	10	m
sinuosity length	500	m
sinuosity amplitude	400	m
channel kh	1000	mD
levee kh	500	mD
overbank kh	5	mD
channel kv	1000	mD
levee kv	250	mD
overbank kv	1	mD
channel φ	0,2	-
levee φ	0,15	-
overbank φ	0,1	-
injector 1 location	[12,43]	-
injector 2 location	[90,93]	
producer 1 location	[18,91]	-
producer 2 location	[24,7]	-
producer 3 location	[61,47]	-
producer 4 location	[87,11]	-

production

parameter	values	unit
production rate maximum	12500	m3/d
pressure maximum	4,00E+07	Pa
pressure minimum	2,00E+07	Pa

Table 5.1. Parameters used in modeling and flow simulations.

5.2.5 Relationship of accessibility with production and the use of simple metrics

The first application is the use of accessibility as a metric to characterize a reservoir model, and to assess the difference between models with respect to flow behavior. For this the flow simulation results of the model realizations are compared with accessibility values of these reservoirs. However, comparing production data (a set of time series) with accessibility (a 3D matrix) is not straightforward, and therefore both need to be reduced to a metric.

For the production data a metric is required that takes into account injection, production, and their changes through time. Therefore for each realization net present value (V_p) is calculated as:

$$V_{\mathrm{p}} = \sum_{n=1}^{\mathrm{N}} \frac{q_o(n) r_o + q_{wi}(n) r_{wi} + q_{wp}(n) r_{wp}}{(1+b)^{\tau(n)}} \Delta t(n)$$

where n is the time step, N is the total number of time steps, q is the surface volume rate, r is the cost or revenue (oil production: \$500/m^3, water injection: -\$50/m^3, water production: -\$50/m^3), b is the discount factor (8%), Δt is the time step size and τ is the time in years. The subscript o denotes oil, wi injected water and wp produced water.

Metrics can be derived from A in a number of different ways. The most obvious is the mean of A over the realization. This has a correlation index of 0.5081 with V_p, indicating limited predictive capabilities. For a large part this is caused by locally very high accessibility values with an unproportionally large effect on the mean of A. Therefore several other methods of deriving a metric were investigated:

- The median of A, resulting in a correlation index of 0.6059
- The standard deviation of A, resulting in a correlation index of 0.1176
- The number of cells with $A < 800$, resulting in a correlation index of 0.6369

The scope of using A as a predictor for reservoir flow behavior as characterized by V_p directly is therefore limited.

A second possible approach is to analyze the difference between A for different realizations, and test whether this relates to a difference in flow behavior between the realizations. For A the difference is obtained by calculating the correlation coefficients R between all matrices of A. Sequentially selecting one of the 50 realizations as a base case and correlating it to the other realizations, results in 2500 values of R, which are visualized in a symmetrical 50x50 matrix in **Fig. 5.4**. High values (dark) indicate a high level of similarity and low values (light) a poor similarity between two realizations. In this figure several lines are present with a predominantly light gray, signifying low R values. These are R values for a realization of which A is on average very different to most other realizations.

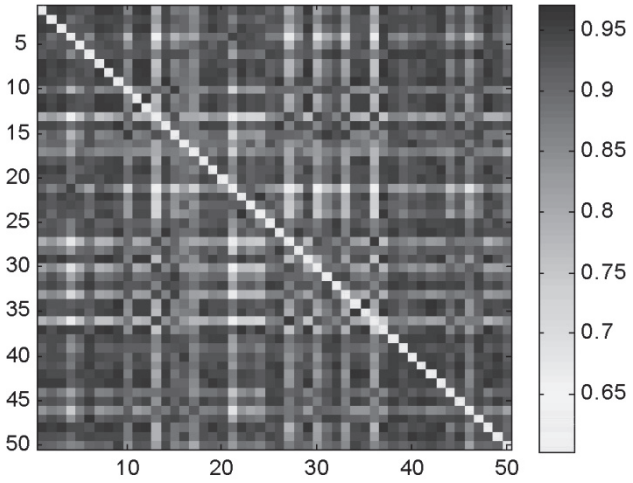

Figure 5.4. R^2 values of 50 accessibility matrices.

5.3 Results

To examine the predictive capabilities of A with respect to production data, in **Fig. 5.5** a crossplot is shown of R of A versus V_p difference using realization number 1 as base case, i.e. the realization with which the comparison is being made. A clear correlation is evident, with a correlation coefficient is -0.8379. A negative correlation is present because realizations which are similar to the base case (high values for R of A) relate to a small difference in production (low values for V_p difference).

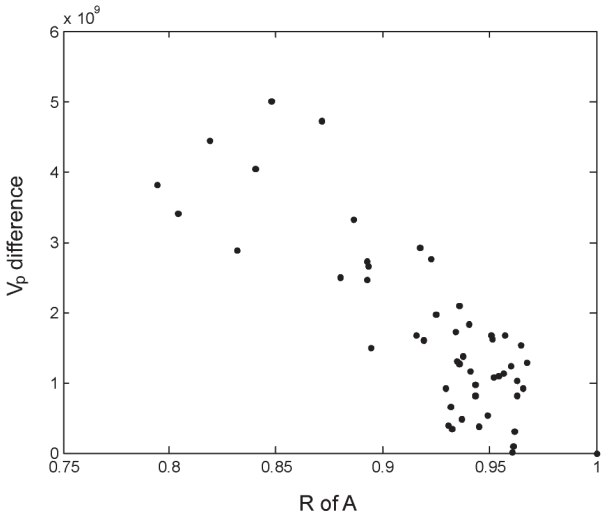

Figure 5.5. Plot illustrating the relationship between correlation of accessibility values (R of A) and production data differences (dcf difference). Correlation coefficient of -0.8379.

Using this data it is possible to show how A can be used to select model realizations from an ensemble. In **Table 5.2** the data on some selections are shown: first the initial ensemble which is the full set of 49 model realizations, secondly the set when the realizations with the largest in difference in A is removed from the set, and lastly the set with the smallest difference in A. Clearly choosing realizations with a smaller value for R of A, i.e. a more similar A matrix, also share production similarities.

	Mean	error of mean (%)	st.dev.
truth	$1.376x10^{10}$		
initial ensemble	$1.207x10^{10}$	12.3	$12.69x10^{8}$
Closest 40	$1.254x10^{10}$	8.9	$7.656x10^{8}$
Closest 10	$1.334x10^{10}$	3.1	`

Table 5.2. NPV data of various selections made based on accessibility similarities.

5.4 Application

The use of accessibility as a selection or comparison tool can enhance various existing inverse modeling techniques. For the ensemble Kalman filter (Evensen 2004) for instance an ensemble of reservoir models is required. The filter can be helped by generating a good starting point by providing it with an ensemble that is near the truth, as well as ensuring enough variability between realizations. Both aspects can be tested using accessibility. For the Probability Perturbation Method (Hoffman and Caers 2003) a series of reservoir models is generated by a multi-point statistical technique. Also here adding variation and correctness can help obtain a match more efficiently. Lastly, in the kernel-based distance measure (Scheidt and Caers 2007) each model is placed in a space based on its similarity to other models, which could also be determined by accessibility.

5.4.1 Well placement analysis

In field development planning a crucial decision is where to locate wells in order to maximize production. For this it is important to be able to establish locations where hydrocarbons might be trapped, i.e. to find poorly accessible locations. To test a certain well configuration with a set of reservoir models using flow simulations is very computer intensive, especially when performed in an iterative fashion and for a large number of reservoir models. Accessibility allows an analysis to be performed of

a well configuration in a fraction of the time of a full flow simulation, and therefore can be used as a useful pre-screening step.

In order to test this, a set of 50 model realizations were constructed based on conditioning data of three wells (**Fig. 5.6**). An additional three wells were added in four different configurations. The modeling process is described above, and an example is shown in Fig. 3. For each of the four well configurations accessibility was calculated for every realization. Next the accessibility matrices were summed vertically for each realization, and these values were summed for all 50 realizations, resulting in a 2D matrix showing averaged accessibility values for each well configuration (**Fig. 5.7**). These images can be used to assess how different well configurations affect flow within the reservoir.

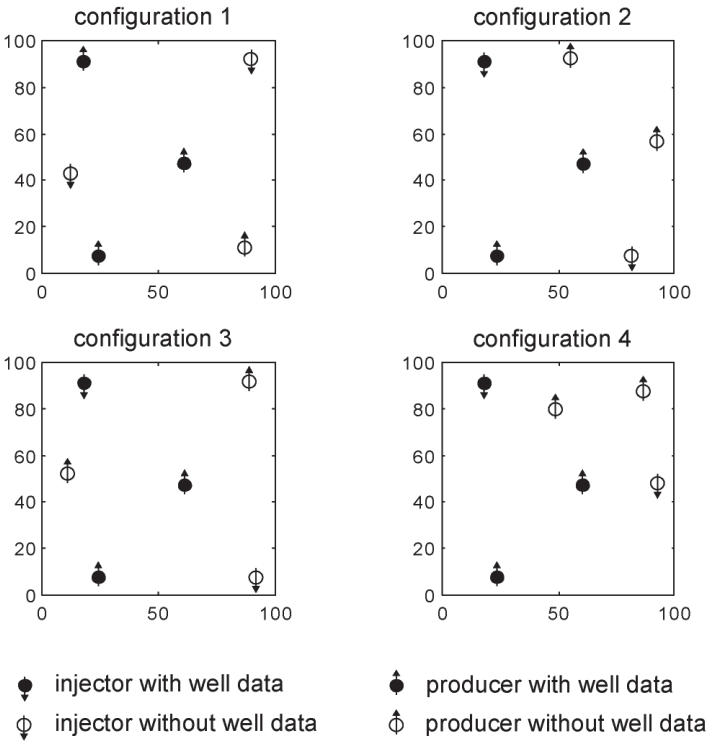

Figure 5.6. Well configurations used to test accessibility. Producers are shown in red, injectors in blue. Filled circles are the three fixed wells with conditioning data, while the three other wells are not used for conditioning.

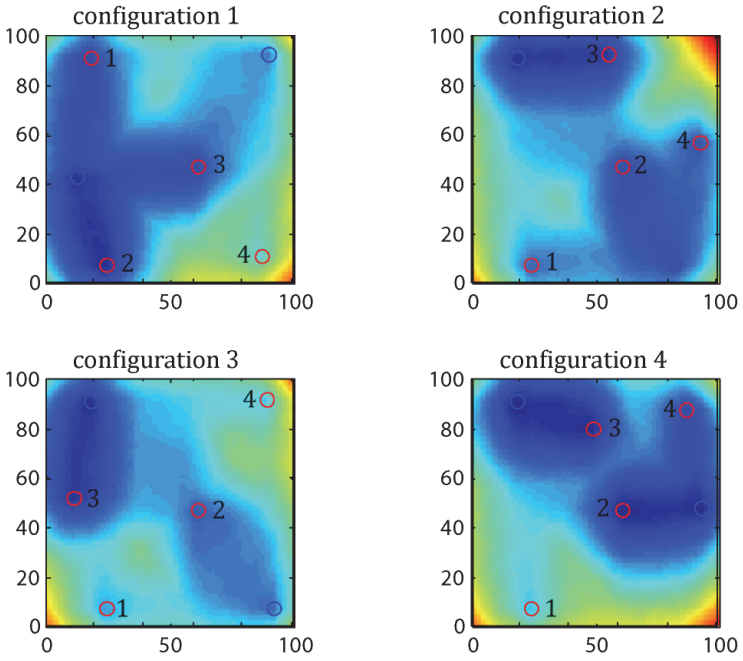

Figure 5.7. Summed accessibility values for all 50 realizations for each well configuration.

The accessibility data can be used in two different ways. Firstly, to use the accessibility matrix for each realization in order to generate a metric that relates to the flow behavior of the reservoir, or secondly by examining the accessibility values at all well locations to form an idea on the production behavior of that well. Both methods will be examined in detail below.

5.4.2 Accessibility and production behavior of wells

From the plots in **Fig. 5.7** it is possible to see that some of the producers might face early water breakthrough, as shown by areas with low accessibility values. Others seem to be isolated from any injector, and therefore might be poor producers. These two types of problems are summarized in **Table 5.3**. To test these predictions the model realizations were flow-simulated, and the well performances were examined.

Poor producers were defined as those with a cumulative discounted oil production of less than 1000 m^3, with a discount factor of 6% being applied. Producers with early water breakthrough were those with water breakthrough within 4 years.

The results are shown in **Table 5.4**, where for each well configuration and each producer the number of realizations is listed where the production of this well falls within the defined cutoffs. Poor producers are not predicted accurately, particularly for well 1, but all six cases of early water breakthrough are predicted correctly using the accessibility plots. The reason that the poor producers were not predicted correctly is that all wells which produced poorly are wells without conditioning data, and therefore have a high probability of encountering few or no channels. This is not visible in the accessibility plots because a small separation between the well and a neighboring channel body only slightly increases accessibility, but has a major influence on production behavior. The relationship between accessibility is examined in more detail in **Fig. 8**, where a plot of water breakthrough time (τ_w) versus local accessibility value at the well show a good correlation between these two parameters, with a correlation coefficient of 0.87.

Configuration	**Poor producer**	**Early water**
1	P4	P2
2		P3, P2?
3	P1, P4	P3
4	P1	P2, P3, P4?

Table 5.3. Predictions of which wells which might be poor producers and wells with early water breakthrough, based on accessibility plots (Fig. 5.7).

Poor producers	**Well 1**	**Well 2**	**Well 3**	**Well 4**
Configuration 1	0	0	0	**8**
Configuration 2	0	0	7	7
Configuration 3	0	0	10	**20**
Configuration 4	0	0	9	13

Early water	**Well 1**	**Well 2**	**Well 3**	**Well 4**
Configuration 1	6	**28**	2	0
Configuration 2	1	**12**	**27**	2
Configuration 3	0	1	**34**	0
Configuration 4	0	**24**	**37**	**11**

Table 5.4. Measured number of poor producers and wells with early water breakthrough. Each number is the number of model realizations which have been found to fall within the criterions discussed in the text for that well and that configuration. Bold indicates proper prediction (Table 3), whereas grey indicate either a not predicted occurrence or a wrong prediction

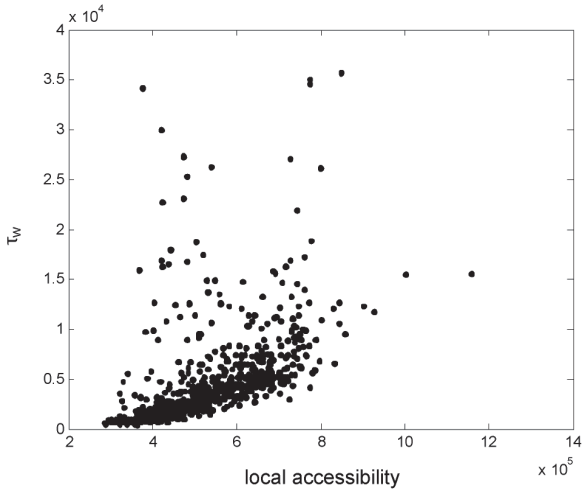

Figure 5.8. Plot of the accessibility values at producer locations versus water breakthrough time (τ_w).

5.5 Discussion & Conclusions

The concept of accessibility is shown to be a useful new tool for reservoir characterization, it relates well with the flow behavior of reservoir models as well as being very efficient to calculate. We have shown two useful applications. Firstly, accessibility can be used as a reservoir characterization tool with a good correlation with flow data. Using accessibility to characterize reservoirs is especially useful to quantify differences between model realizations, as many history matching techniques run more efficiently when a more optimal set of initial realizations is used. Secondly, accessibility can be used as a spatial parameter to assess well positioning. We have shown the capabilities of accessibility to identify well configurations in which early water breakthrough has a high probability, as well as identifying areas which will be poorly drained due to poor accessibility.

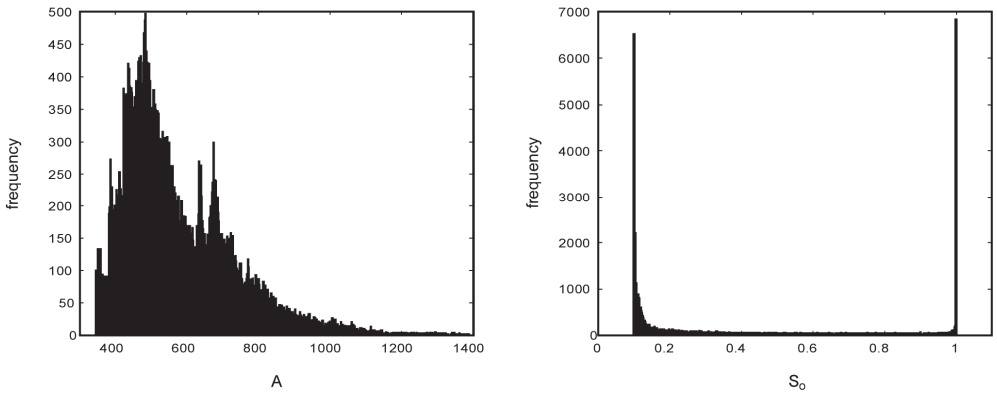

Figure 5.9. Histograms of accessibility (A) and oil saturations at the end of production (S_o), illustrating difficulty in directly comparing the two.

Some problems remain however but the underlying causes are not clear at this time. Two main factors are highlighted here:

- The change in the state of the reservoir during production is mainly dominated by a change in fluid saturations over the reservoir. A comparison of accessibility and saturation, as illustrated in **Fig. 5.9**, shows, however, a different distribution exists in the two properties A and So. With A having a

relatively normal distribution, whereas So has an peaks at 0.1 and 1, or at residual and initial oil saturations respectively. These different distributions alone make a direct comparison difficult.

- The lack of a dynamic part in the algorithm may oversimplify the reservoir behavior. This is on one hand the strength of the technique, as it greatly reduces the computing costs, but the drawback is a lack of information on the change of the reservoir properties over time. Clearly, not all dynamic complexities can be captured with a static parameter such as accessibility.

Nomenclature

b = discount factor, [-]
c = tracking parameter, [-]
d= distance between the centers of cells, [m]
k=permeability, [mD]
$\bar{k}$ = harmonic mean of permeability, [mD]
n=time step, [-]
q_o, q_{wi}, q_{wp} =surface volume rate, [m^3/d]
r_o, r_{wi}, r_{wp} = cost or revenue, [$]
A, A_t = Accessibility, [-]
L=location in reservoir model, [-]
M, M_n=neighboring cell to L, [-]
N =total number of time steps, [-]
T= time, [d]
S_o=oil saturation, [-]
V_p = Net present value, [$]
ΔA= accessibility differential between two neighboring cells, [-]
Δt =time step size, [d]
τ_w = water breakthrough time, [d]
Φ=porosity, [-]

Acknowledgements

This research was carried out within the context of the ISAPP Knowledge Centre. ISAPP (Integrated Systems Approach to Petroleum Production) is a joint project of the Netherlands Organization for Applied Scientific Research TNO, Shell International Exploration and Production, and Delft University of Technology. The authors also gratefully acknowledge the use of Shell's reservoir simulator MoReS.

6 The effect of errors in analogue geological models for fluid flow prediction

6.1 Introduction

Fluvial reservoirs are an important category of hydrocarbon reservoirs worldwide. A significant proportion of the world's hydrocarbon resources is at least partially contained in fluvial reservoirs, including the giant fields at Prudhoe Bay (Alaska), Daqing (China), Messla and Sarir (Libya), Statfjord and many other fields in the northern North Sea, the Athabasca oil sands, Mannville and Belly River fields in Alberta, and hundreds of small fields throughout the world. Due to the heterogeneous architecture of many fluvial reservoirs it is difficult to create accurate model representations of these reservoirs.

When modeling an unknown channelized hydrocarbon reservoir the two main uncertainties are the geometries of the channel bodies and permeability ranges for the various facies. Here we will be focusing on the former. Sometimes information on the size and shape of reservoir bodies can be obtained directly from seismic data, but generally this is not of sufficient quality to image channels as separate bodies. In these cases analogues can be used as a basis to decide on geometrical parameters describing the channels. These analogues can be modern active fluvial systems, outcrops or other well understood subsurface reservoirs. From wherever the data is obtained, it is generally difficult to understand how the choice influences the predicted flow behavior of the reservoir as found by subsequent flow simulations of the models.

To what degree the choice of the analogue effects the prediction of reservoir flow behavior is examined in the following. First a ground truth case was created, after which a number of reservoir models were made based on well data, but using different analogues. These analogues ranged from an exact match to the truth case, to models with increasing errors but still containing channels, and finally to an unrealistic model containing square and circular bodies. For each case the permeability values for the different facies were kept constant, and only the geometries were changed. A flow simulation was subsequently performed on each model realization. The resulting data was analyzed to test to what extent the choice of analogue influences the predictive capabilities of a model set. A more detailed description of the steps taken can be found below.

6.2 Methods

The goal of this study is to examine the effect of using different analogue models in generating model representations of a subsurface reservoir. In total eight analogues were chosen to generate analogue model sets, with 20 realizations for each analogue (**Fig. 6.1**). Of the eight model sets, one was created using identical geometrical data as the truth case, but the location of the bodies in the reservoir was changed. Six model sets are based on data sets derived from literature, and a last set of models was generated using randomly placed geometrical shapes in the model, to test an analogue with a high error with respect to the truth case. The analogues are described in detail below, with data in **Table 6.1**. A flow simulation was subsequently performed on each realization.

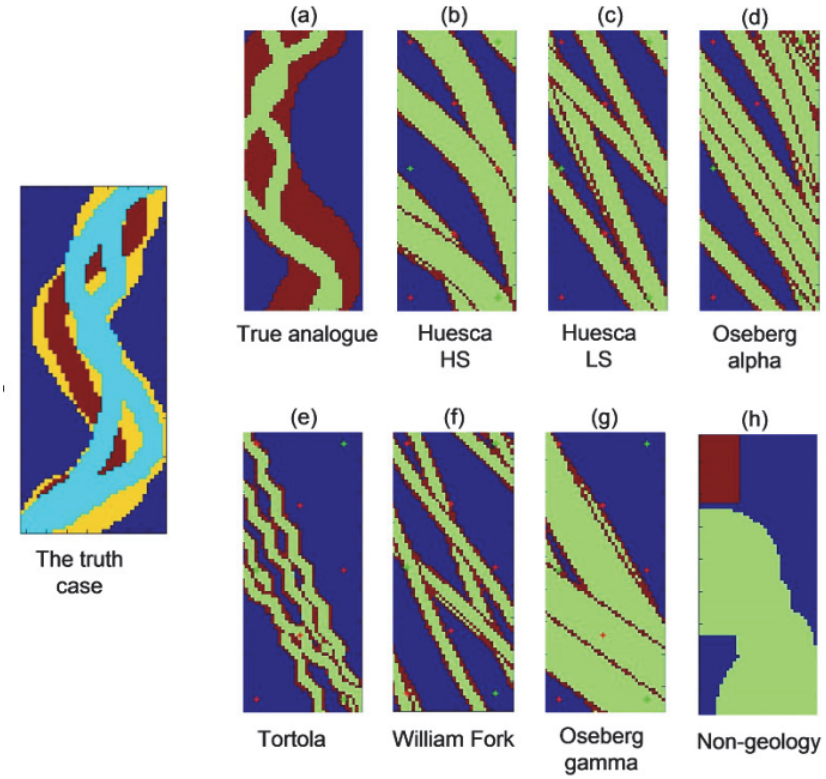

Figure 6.1. Horizontal cross sections of one model from every analogue model set.

	Width [m]	Thickness [m]	Amplitude [m]	Wavelength [m]
Huesca HS	295 (+/-103)	3.7 (+/-1.3)	406 (+/-141)	1488 (+/-463)
Huesca LS	339 (+/-193)	3.6 (+/-1.5)	107 (+/-47)	2745 (+/-853)
Oseberg Gamma	594 (+/-291)	8.8 (+/-2.6)	404 (+/-172)	6266 (+/-1684)
Oseberg Alpha	250-300	5(+/-1)	400(+/- 50)	2375 (+/-75)
Tórtola	35 (+/-23)	4 (+/-2)	43 (+/-31)	444 (+/-210)
William Fork FM	29.6	8	44.4	750

Table 6.1. Geometrical data used for the 6 channelized analogue model sets.

6.2.1 Truth analogue

The truth analogue is based on a well understood fluvial system, the Huesca fluvial fan system (Donselaar and Overeem 2008). This analogue is used to determine the geological properties of the truth case, as well as the set of models representing the truth analogue. This means that the truth analogue model set is a perfect representation of the geology of the truth case, except for the location of these bodies.

The Huesca fluvial fan system is located south of the Pyrenees, in the Huesca province (Spain). The Huesca fan is interpreted to have consisted of relatively large channel belts. The discharge per river was probably quite large and with limited vegetation, resulting in wide, laterally expanding channels. Channel dimensions were obtained from student research projects (Careil 2000; Otten 2000; Thomassen et al. 2004).

The channels are modeled as point bar deposits, in the form of beaded channels. (**Fig. 6.2a**) The conceptual model consists of a channel belt in which several channels are present. These channels consist of point bars connected to each other by the channel fill deposits (Donselaar and Schmidt 2005; Donselaar and Overeem 2008). In the

upper third of the point bar deposits accretion surfaces limit permeability, especially horizontally but to a lesser extent also vertically.

Modeling these deposits was simplified in several ways (**Fig 6.2b**). Geometrically the deposits are constructed by a sinuous channel belt with internal sinuous channels whose extent are constrained by the extent of the channel belt. The channel deposits consist of three layers; the bottom two are a high permeable facies, reflecting the excellent reservoir sands present in the point bar and at the base of the channel fill. The top layer has a reduced horizontal permeability with respect to the underlying layers, and also the vertical permeability is slightly reduced. The stacking pattern of the five channels present in each of the three channelbelts is such that each channel is one layer higher in the stratigraphy than the previous one, resulting in seven layers in each channel belt. The stacking of the channelbelts is such that the top of one is the bottom of the next, making a total of 21 model layers.

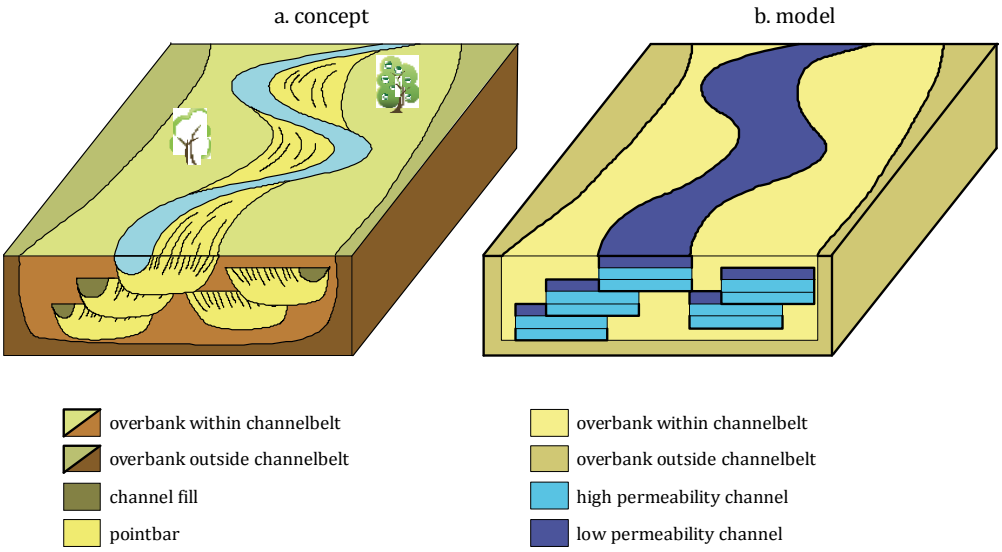

Figure 6.2. Illustration of how the conceptual model is adapted for modeling purposes. a) block diagram of a meandering fluvial system forming pointbars within a channelbelt. b) model representation where the concept has been simplified to three discrete facies, with a further subdivision in the channel facies to correct for permeability modification by accretion surfaces.

6.2.2 Analogues

- *Ness Formation, Oseberg Field*

The data sets for the Oseberg oil field were acquired from Careil (2000) and Liestøl et al. (2005). The Oseberg field is located in an area of the Norwegian North Sea some 140 km north-west of Bergen. It consists of three separate east-northeast tilted fault blocks named Alpha, Alpha North and Gamma. The data used here is from the Alpha North and Gamma Block (a and c hereafter), which are used as separate analogues. The dominant part of the production from this field comes from the Middle Jurassic deltaic deposits of the Brent Group. The Brent Group represents clastic sediments from the wave-dominated Brent Delta and is divided into five formations (Spencer and Larsen 1990).

Four sedimentary facies assemblages are defined: channel fills, crevasse splays, coals and floodplain deposits (Liestøl et al. 2005). The channel facies assemblage represents the reservoir unit in the Ness Formation. The crevasse splay facies assemblage constitutes thin sandstone units (Ryseth 2000). The floodplain consists of interfluvial deposits deposited in standing waters. The width, thickness, amplitude and wavelength values are higher than those of the other analogues examined here. The sandbodies of the Oseberg c are thought to correspond to channel belts with internal stacking of individual cut-and-fill sandbodies. However, the different of W/T ratios and sinuosity index are not much different from other analogues.

- *Huesca fluvial fan, an outcrop analogue*

The data for the Huesca fluvial fan system was obtained from student reports of the TU Delft (Careil 2000; Otten 2000; Thomassen et al. 2004) from which the channel parameters thickness, width, sinuosity wavelength and amplitude have been extracted. This analogue was subsequently modelled in the manner also used in the other analogue models.

- *Tórtola fluvial fan, an outcrop analogue*

The Tórtola fluvial fan is a fluvial deposit of late Oligocene to early Miocene age. It was deposited in the intracratonic Loranca Basin in central Spain. The fluvial bodies have a lenticular geometry and contains several vertically and laterally stacked pointbar units, with each point bar units containing lateral accretion deposits. Several genetic sandstone types are recognized: fluvial channel deposits, sheet deposits (crevasse-channel and crevasse-splay deposit) and deltaic deposits.

The data sets for the Tórtola fluvial fan system were obtained from (Careil 2000). The Tórtola data consists of width, thickness, and wavelength and amplitude values for each sand body. The data shows that sandbody dimensions of Tórtola fluvial fan are very small, in the order of 35 m for width and the average thickness is about 4 m of each single body. The Tórtola fan is interpreted to have been deposited in a period of high accommodation space increase. Sand body growth has mostly taken place in the vertical direction because strong vegetation on riverbanks and the existence of a paleovalley may have blocked lateral migration (Cuevas Gozalo and Martinius 1993). An added explanation about the small width could be that the Tórtola Fan consisted of a large distributary network with many channels, where the discharge of water and sediment per channel was very low, resulting in small sandbody extent. In addition, the amplitude and wavelength parameters show very low values compared to the other analogues, although the sinuosity parameters are in the same range.

- *William Fork Formation, Piceance Basin, an outcrop analogue*

The data sets for the William Fork Formation were obtained from Pranter et al. (2007). The outcrops are located in Coal Canyon near Palisade, Colorado and are approximately 48 km southwest of natural gas fields in the southern Piceance Basin that produce from the same formation. The Piceance Basin was created during Late Cretaceous-early Paleogene.

The William Fork outcrop analogue was used to obtain parameters such as thickness and/or widths of fluvial sandstone or shale bodies. The main point-bar deposits are lens-shaped with a sharp base and an average thickness of 8m. They are overlain by thin mudstones and fine-grained, ripple-laminated sandstones, interpreted as levees or crevasse splays, which have a sheetlike geometry with a sharp planar base, and thicknesses of about 1.5m. Connectivity is greater in the sand-rich intervals, where sand bodies are amalgamated. Six main lithofacies are distinguished based on outcrop measurements: trough cross-bedded sandstone, current-rippled sandstone, nodular siltstone, laminated siltstone, conglomeratic mud-chip sandstone, and coal and bentonite beds. The maximum lateral extent of a point bar sand body or reservoir elements relates to the meander-belt width and meander wavelength, both of which can be estimated from channel size (Collinson 1978). The average value of point-bar thickness is around 8 m, the average horizontal width in the main point bar sand body is 30 m. The point bar deposits reveal a finingupward succession from medium- to finegrained sandstone, and from cross-bedded to ripple-laminated sandstone. The average meander wavelength is estimated from the relationships of (Leeder 1973), which gives 750 m.

- *The non-geological analogue*

To test the extremes of errors in the choice of analogue model, a non-geological analogue model was used. It consists of circles and squares for the two high permeable facies, with the range for circle is 1.8-5.4 cells, and the range of width for the square input is 3.6-10.8 cells. Using this model it will be possible to assess how very large errors in the model data relate to the magnitude of errors in predictions derived from flow simulations.

6.2.3 Modeling Workflow

For each analogue model 20 model realizations were created. Each reservoir model is rectangular with dimensions of 89x36x21, totaling 67,284 cells. Each cell has dimensions of 50x50x2 m. The entire reservoir dimensions are 4450x1800x42 m, or approximately 8 km^3. Each reservoir model has eight wells, configured in a double five-spot as shown in Fig. 1. Well data was extracted from the truth case in the form of facies information, and each model realization was constrained to this. For each facies the porosity and permeability values shown in **Table 6.2** are used.

Facies	**Color**	**Facies number**	**Porosity (%)**	**Permeability (mD)**
Floodplain	Blue	1	14	10
Channel sand	Green	2	24	600
Levee/channel belt	Brown	3	20	200

Table 6.2. Facies properties as used in modeling.

An object-based technique is used that creates models with three facies, with user-defined geometries and conditioned to well data. Object-based models have been found to be superior to variogram-based models as well as multi-point statistics for describing complex geological reservoirs, resulting in more accurate flow predictions (Journel et al. 1998; Falivene et al. 2006). Although various techniques for creating object-based models of fluvial systems are available, these were found to be unsuitable for our purposes, mainly because of excessive complexity or imperfect

well conditioning. Therefore, it was decided to develop a new code to efficiently generate a large number of simple realizations of a fluvial system. The generation of these model realizations is similar to the FLUVSIM algorithm (Deutsch and Tran 2002) in that a simulated annealing approach is used. The first part of the algorithm generates the channels such that well-conditioning is achieved. These channels remain fixed for the second part of the simulation, which consists of either adding or removing a channel body from the reservoir, based on the minimizing the error in net-to-gross ratios (N/G) per layer. To add a new channel first a location is chosen. Randomly choosing a point in the reservoir would cause an uneven distribution of channels (i.e. higher density in the centre part). To ensure an even distribution the channel location is found by first placing a line perpendicular to the channel orientation in the reservoir, and then randomly placing a point on this line on which the channel is placed. Placing the channel is done by choosing a small deviation from the general flow direction, randomly chosen between -10^o and +10^o. This small angle change is included to ensure that between two neighboring channels with identical periods more realistic connectivities can result. If this angle deviation is not used two channels will connect at every period or will always be out of phase and therefore never connect. Every addition or removal of a body is then analyzed by checking if the objective function has decreased, where the objective function is defined as

$$J_m = \sqrt{\frac{1}{n_L}\sum_{i=1}^{n_L}\left(f_v^i - \overline{f}_v^i\right)^2},$$

where f_v^i is the net-to-gross ratio in layer i, f_v^i is the desired net-to-gross ratio in layer i and n_L is the total number of layers. The net-to gross ratio of layer i is defined as $f_v^i = n_{gb,ch}^i / n_{gb}^i$, where n_{gb}^i is the total number of grid blocks in layer i and $n_{gb,ch}^i$ is the number of grid blocks associated with channels in that layer. In order to condition the realizations to well data, the objective function is extended to consist of the sum of the root mean square error of net-to-gross ratios and the mismatch with the well conditioning data. A cut-off value for the objective function of 0.05 or lower was found to result in acceptable models.

6.2.4 *Fluid-flow simulation*

We simulated fluid-flow for each realization using a proprietary black oil simulator using a multi-point flux finite difference discretization (Aavatsmark et al. 1996). Production and injection rates for the wells shown in Fig. 1 were kept constant, except when pressure constraints were exceeded. The values of the pressure constraints were set to $200*10^5$ Pa and $400*10^5$ Pa. For the relative permeabilities the Corey model was used, with exponents and end-point saturations. The initial water saturation was chosen as 0.2 and the initial reservoir pressure as $300*10^5$ Pa. The fields were simulated for approximately 25 years, with approximately 90 timesteps of at most 100 days each. Grid block size and length of time steps were chosen by decreasing the size and length until the simulation results converged. Simulation continued until the water-oil ratio in the production wells reached 90%. This resulted in simulation times of approximately five minutes per realization on a 1.86 GHz laptop.

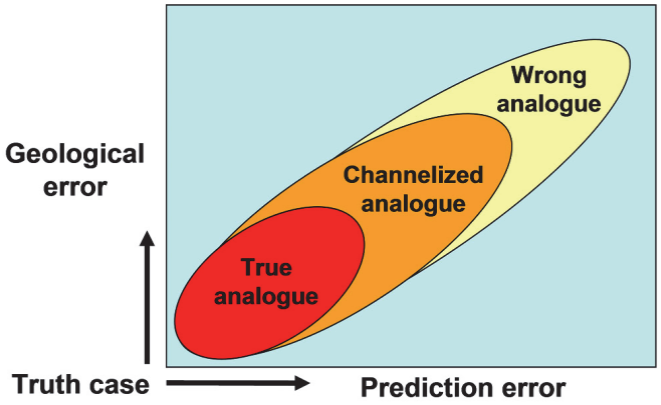

Figure 6.3. Intuitive relationship between error in geological information and production prediction resulting from models created with this information.

6.3 Results

This study has two main goals: firstly, to analyze to what extent an ensemble of model realizations with an incorrect geological input can predict various aspects of the flow behavior, for instance NPV and water breakthrough time. And secondly, to test how errors in the choice of analogue model affect the errors in predicted flow data derived from simulations. The simplest and most intuitive result would be that an increase in the geological error causes an increase in the production prediction error,

as illustrated in **Fig. 6.3**. These two aspects are further elaborated below under *histograms* and *dGdP plots* respectively.

6.3.1 Histograms

As it is difficult to compare production behavior based on production profiles, here we compare the production data by simplifying it to represent a single characteristic aspect. To do this the production data has been reduced to a number of metrics characterizing the production behavior, and subsequently histograms of the data can be analyzed. The metrics used are:

NPV: Net present value
Shut-in time: The time until the reservoir became uneconomical to produce and was shut in.
WBTT: the time until the first water is encountered in any production well

The following parameters were used to calculate these metrics:

Water injected cost	: \$ 40 / m^3
Water produced cost	: \$ 40 / m^3
Oil produced price	: \$ 140 / bbl, hereafter converted into \$ / m^3
Discount factor	: 8%
Initial capital investment	: \$ 4.0×10^7

The resulting histograms are shown in **Fig. 6.4**. For each of the three metrics histograms are shown for every analogue model set, showing the distribution of values for this metric. The value of the truth case is also shown as a red asterisk. For reservoir modeling purposes it is important that a model set has a range of values that captures the true value for this metric. In other words, the true value must lie within the histogram shown in Fig. 3.The histograms for the first metric, NPV, show that not every analogue model set can accurately predict a valid range of NPV values. One of the worst performing model sets are based on the Oseberg C data, which predicts NPV values of 13.2 $x10^6$ to $14x10^6$, where the true value is $12.3x10^6$. Other model sets show varying ranges, with some capturing the true value quite well. For the shut-in time, a different trend emerges. Here all the model sets except for the true analogue show a much too short production time. This shows that the difference in geology between the true analogue and the others in some manner causes the lifetime of the

reservoir to be severely shortened. Which difference is causing this change is as yet unclear.

The last metric, WBTT, shows again that some model have predictions in the right range as to capture the true value, whereas others do not. Surprisingly, the Oseberg c set shows that the predictions are fairly accurate, which is at odds with the large error when predicting NPV. It seems valid for other model sets as well that accurate prediction regarding one metric does not relate to predictive capabilities on other metrics. It is important to note that the true analogue captures the true value for each metric, indicating the methodologies used here are valid.

From these results we can conclude that it is not sufficient to solely have an accurate estimate of reservoir parameters such as permeability values, net-to-gross and a channelized nature. More accurate data is required to be certain that the modeled set of realizations can capture the main reservoir behavior and therefore a solid prediction of its future performance.

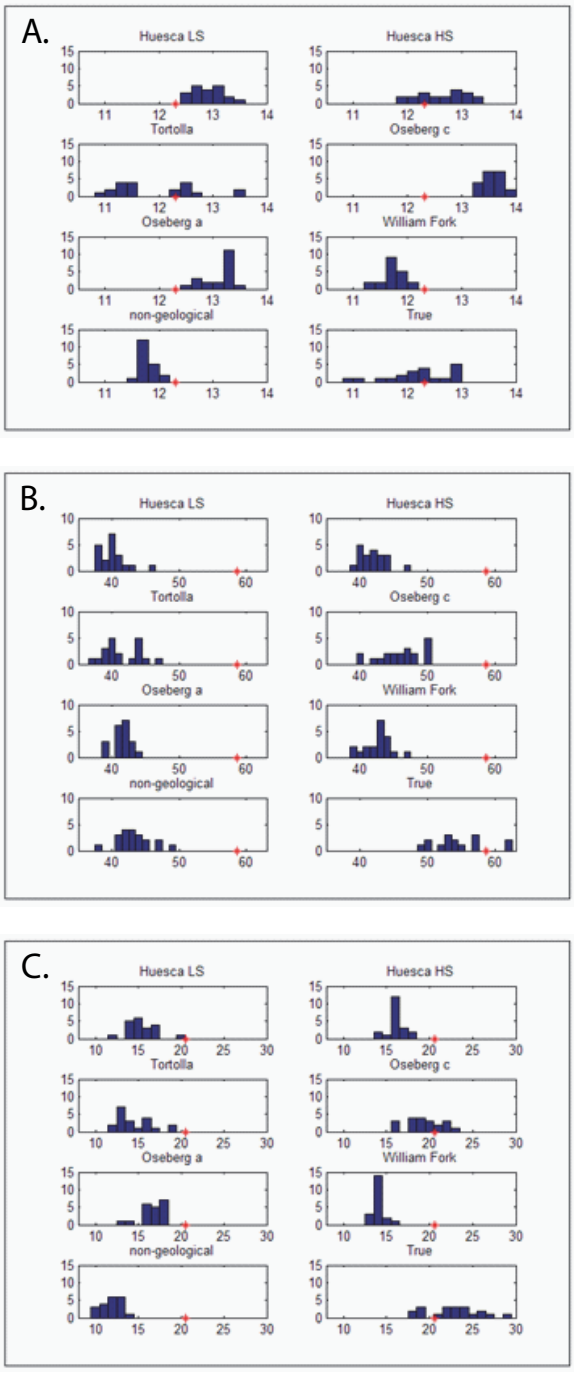

Figure 6.4. Histograms of NPV (a), shut-in time (b) and water breakthrough time (c) for each analogue model set.

6.3.2 *dGdP plots*

After analysis of the variability in the predictive capabilities of the various model sets, it is interesting to test whether a larger error in geological information relates to an increase in error in prediction of production data. One would expect a relationship as shown in **Fig. 6.3**. To test this relationship two metrics need to be constructed: one for the geological error, and one for the production error. For the geological error a combination of connectivity, input parameters and local net-to-gross was used as follows:

$$E_G = \frac{C - C_T}{C_{\max}} + \frac{1}{N}\sum_{n=1}^{N}\frac{P_n - P_{nT}}{P_{nmax}} + \frac{1}{A}\sum_{a=1}^{A}\frac{NG_a - NG_{aT}}{NG_{amax}}$$

With E_G is the geological error, C the connectivity of the realization, P the modeling parameter, N the number of model parameters, NG net to gross, A the number of areas analyzed separately. The subscripts are: T for the true value, max: for the maximum value, n for the parameter number, a for the area number.

For the production error (E_P) simply the root mean square error was taken over the lifetime of the reservoir with respect to the true case.

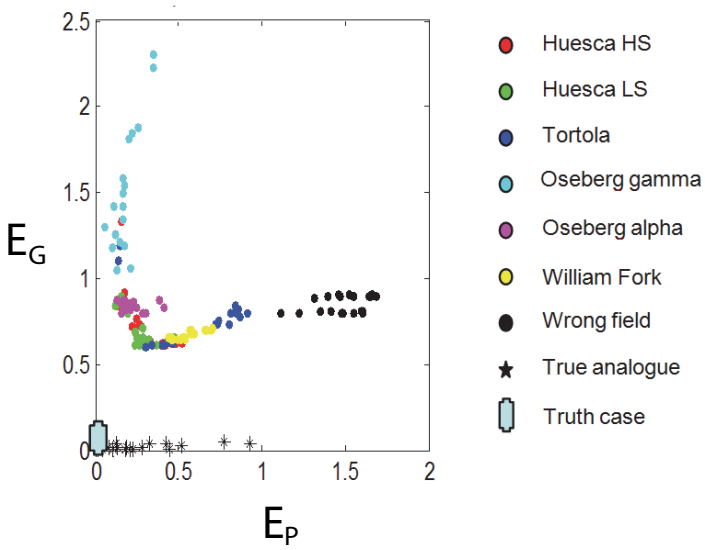

Figure 6.5. Cross-plot of error in geological information versus error in production prediction for each model realization.

The results are shown in a cross-plot of E_G and E_P values for each model in **Fig 6.5**. At first glance it is already evident that the trend from Fig. 4 is not reproduced. However, when examining the data in more detail, general trend can be found to emerge when examining single model sets separately. For instance, the William Fork and Tortola model sets, as well as the Oseberg C set. Using different metrics for geological and production errors gives similar results. We can therefore conclude that the assumed behavior cannot be said to be valid in a general sense.

6.4 Acknowledgements

I would like to thank Tigor Hamonangan for his work on this subject for his Master's thesis.

7 Discussion

7.1 Summary

In this thesis various aspects of the interaction between reservoir modeling and flow prediction are discussed. First the effect of modeling parameters on flow behavior is examined for variogram-based and object-based reservoir modeling techniques. Because the individual geological model parameters are not sufficiently correlated with flow behavior, the metrics connectivity and accessibility are shown to be model properties that better relate to flow behavior. Additionally, an analysis is made on how an error in interpretation of geology relates to flow prediction errors.

The results illustrate the complexity of reservoir modeling, in particular when relating geological properties of a reservoir to how the fluids behave within that reservoir.

7.2 Modeling

One of the most heterogeneous reservoir types are channelized of fluvial origin. Due to the large difference between high permeability channel sands and low permeability overbank deposits, fluid flow in a reservoir of this type is strongly dependent on the exact properties (e.g. geometry, location, interaction) of these bodies. Due to the interesting relationship between geology and fluid flow this thesis focuses on channelized fluvial reservoirs.

Throughout this work an object-based modeling technique was used. This technique was chosen because a large amount of control was required to create model realizations with specific geological properties, such as body dimensions and permeability values. Unfortunately this sacrifices some realism with respect to other techniques, notably process-based techniques, and this limits the applicability of the conclusions from this thesis to other modeling techniques. However, most conclusions here are qualitative in nature and can be applied in a more general, conceptual sense. For instance the applicability of accessibility (chapter 5) or the difficulty in relating geological error to production data (chapter 6) are independent of the modeling technique used.

The use of object-based modeling for an unknown reservoir can be difficult in practice, as it is not certain if the model being used can create a valid reproduction of the actual reservoir. In the cases used in this thesis however this is not a problem, as

the same technique is used to create both the truth case as well as the model realizations.

7.3 Discussion of the individual chapters

In **Chapter 2** a number of modeling techniques is reviewed, highlighting an apparent inverse relationship between geological realism and mathematical simplicity. On one hand geological realism is required to make best use of geological information, such as the properties of various geological bodies or their interrelationships. On the other hand, mathematical simplicity is required for efficient conditioning of the model realizations to data such as well logs or seismic data. How these two contradicting requirements can be handled is the subject of much recent research, but increasing computer power and improved levels of sophistication of the computer models allow ever more complex models to be efficiently handled.

In **Chapter 3** an analysis is performed of how reservoir flow behavior responds to changing parameters of variogram-based models. This chapter has two main aspects which are important for this thesis. On one hand the results show how model parameters affect flow behavior, and on the other hand it is a proof of concept with regards to the techniques used.

The results show that reservoir parameters do not have a clear and simple to predict effect on flow behavior. This is caused by the fact that models with almost identical parameters can exhibit very different flow behavior. This, in turn, can be related to the heterogeneity of the models. For very homogeneous models we find (chapter 3, figure 6) that the dimensions of the bodies do not relate to flow behavior, as all models are fairly similar in their behavior. Conversely, for very heterogeneous models the body dimensions do not relate to specific flow profiles because the locations of the bodies is of much greater importance. These are considered the main results of this study.

The proof of concept aspect of this chapter is shown to be valid. The combination of experimental designs with response surface modeling gives good insights into the model responses. It is worth repeating here that this workflow can only be used when model responses are gradual. For more complex model responses more sophisticated techniques may be required.

Chapter 4 applies the experimental design / response surface methodology tested in chapter 3 on a more complex model. Here the results show a weak correlation between geometric parameters of the fluvial bodies and flow behavior. One goal of this study is to examine to what extent geological parameters can be used as a reduced order parameter set, or, in other words, if geological parameters can be estimated from the flow behavior of a reservoir. This was found not to be the case for the examples used here, and it seems unlikely that a different geological setting or production plan will change this conclusion. The main cause again is the large variation in flow behavior between reservoir models with almost identical parameters. Therefore, the concept of *connectivity* is applied and is found to be promising. One aspect of this parameter is that small changes in the reservoir model can cause connectivity values to drastically change. This is not realistic in terms of the expected actual gradual change in flow behavior in response to a minor change in reservoir properties.

In chapter 5 instead of connectivity as in the previous chapter, a new concept termed *accessibility* is introduced. It shows an improved relationship with flow behavior over connectivity, in particular for more realistic reservoir models with more realistic continuous petrophysical properties. One possible application is as a quick-look method for evaluating well configurations, where it can be used to indicate possible poorly drained areas within the reservoir. Regardless of the applicability of the parameter, the lack of a physical meaning is somewhat disconcerting. In that sense accessibility is purely an empirically derived but potentially useful parameter. In conclusion, having already been shown to be valuable in urban planning, it has been shown to be useful for reservoir modeling applications.

Chapter 6 describes how the data used in generating the reservoir model influences the predicted flow response of a set of reservoir models. The approach tests analogue models with varying degrees of correctness with regards to the truth case, and the errors in flow prediction are analyzed. With regards to the methodology a criticism might be that the modeling techniques are not accurate enough to represent the analogue models used. However, the goal was not to create accurate representations of the analogues but rather to use the model sets as representations of one possible set

of estimates of the truth case. The same reasoning validates the choice of some analogue models which are not representative of the truth case geology.

The results suggest that a large error in the analogue model relates to a large error in flow prediction. However, it was found to be difficult to find this relationship unequivocally for all data combined. In part this is caused by the difficulty in simplifying the complex interaction between geological properties and fluid flow behavior in a two-parameter relationship. The struggle with finding the expected relationship indicates that it is difficult to assume a priori, that if an error in the geological information is small, the error in flow prediction will be small too. Although the trend will show occasionally, the relationship is more complex than simply stating that a poor geological accuracy will result in a poor prediction of flow behavior.

References

Aavatsmark, I., Barkve, T., Boe, O., and Mannseth, T. 1996. A Class of Discretization Methods for Structured and Unstructured Grids in Anisotropic, Inhomogeneous Media. Presented at the 5th European Conference on the Mathematics of Oil Recovery, Leoben, 3-6 September.

Ainsworth, R.B. 2006. Sequence stratigraphic-based analysis of reservoir connectivity: influence of sealing faults – a case study from a marginal depositional setting. Petroleum Geoscience, Vol. 12, 127-141.

Allen, J. R. L. 1965. A review of the origin and characteristics of recent alluvial sediments. Sedimentology 5: 89-101.

Allen, J. R. L. 1978. Studies in fluviatile sedimentation: an exploratory quantitative model for the architecture of avulsion-controlled alluvial suites. Sedimentary Geology 21(2): 129-147.

d'Ambrosio, A., Spataro, W., Iovine, G. 2006. Parallel genetic algorithms for optimizing cellular automata models of natural complex phenomena: An application to debris flows. Computers & Geosciences, 32, 861-875.

Atkinson, A. C.and Donev, A. N. 1992. Optimum Experimental Designs. Oxford University Press.

Black, J. 1981. Urban transport planning: theory and practice. London: Croom Helm.

Box, G. E. P. & Wilson, K.B. 1951. On the experimental attainment of optimum conditions (with discussion). Journal of the Royal Statistical Society Series B 13(1), 1-45.

Brandsæter, I., Wist, H.T. Næss, A., Lia, O., Arntzen, O.J., Ringrose, P.S., Martinius, A.W., Lerdahl, T.R. 2001. Ranking of stochastic realizations of complex tidal reservoirs using streamline simulation criteria. Petroleum Geoscience, Vol. 7, S53-S63.

Bridge, J. S.and Leeder, M. R. 1979. A simulation model of alluvial stratigraphy. Sedimentology 26: 617-644.

Busby, D., Farmer, C.L. & Iske, A. 2007. Hierarchical nonlinear approximation for experimental design and statistical data fitting. SIAM Journal on Scientific Computing, Vol. 29, Issue 1, 49 – 69.

Caers, J.and Zhang, T. 2002. Multiple-point geostatistics: a quantitative vehicle for integrating geologic analogs into multiple reservoir models. in AAPG memoir: Integration of outcrop and modern data in reservoir models,ed. G. M. Grammer.

Caers, J. 2003. History matching under training-image-based geological model constraints. Paper SPE 74716. SPE Journal. Vol. 8, Nr. 3, 218-226.

Careil, F., 2000, Sensitivity analysis of a stochastic reservoir architecture model; Huesca Fluvial Fan, Ebro Basin, Spain., MSc Thesis. Delft University of Technology, Delft, the Nethelands, 76 p.

Carle, S. F.and Fogg, G. E. 1996. Transition probability-based indicator geostatistics. Mathematical Geology 28(4): 453-476.

Collinson, J. D. 1978. Vertical sequence and sandbody shape in alluvial sequences. in Fluvial Sedimentology: Canadian Society of Petroleum Geologists Memoir,ed. A. D. Miall, v. 5, p. 577-586.

Corey, A. T. 1954. The interrelation between gas and oil relative permeabilities. Producers Monthly 19(38).

Corre, B., Thore, P., de Feraudy, V. & Vincent, G. 2000. Integrated uncertainty assessment for project evaluation and risk analysis. Paper SPE 65205, presented at the SPE European Petroleum Conference, 24-25 October 2000, Paris, France.

Cuevas Gozalo, M. C.and Martinius, A. W. 1993. Outcrop data-base for the geological characterization of fluvial reservoirs: an example from distal fluvial fan deposits in the Loranca Basin, Spain. . in Geological Society, London, Special Publications,ed. C. P. North, and D. J. Prosser, v. 73, p. 79-94.

Demyanov, V., Subbey, S., Christie, M. 2004. Uncertainty assessment in PUNQ-S3: neighborhood algorithm framework for geostatistical modeling. Proceedings of ECMOR IX, 2004, Cannes, France.

Deutsch, C. V.and Wang, L. 1996. Hierarchical object-based stochastic modeling of fluvial reservoirs. Mathematical Geology 28(7): 857-880.

Deutsch, C.V., 1998. Fortran programs for calculating connectivity of three-dimensional numerical models and for ranking multiple realizations. Computers & Geosciences, 24, 69-76.

Deutsch, C. V. 2002. Geostatistical Reservoir Modeling. Applied Geostatistics Series: New York, USA: Oxford University Press, 376 p.

Deutsch, C. V.and Tran, T. T. 2002. FLUVSIM: a program for object-based stochastic modeling of fluvial depositional systems. Computers & Geosciences 28: 525-535.

Dijkstra, H. & Parsons, R.L. 1950. The Prediction of Oil Recovery by Water Flood. In: Dykstra, H. & Parsons, R.L. (eds) Secondary Recovery of Oil in the United States, Principles and Practice (2nd edn). American Petroleum Institute, New York, 160–174.

Dijkstra, E. W. 1959. A note on two problems in connexion with graphs. Numerische Mathematik 1: 269-271.

Donselaar, M. E.and Overeem, I. 2008. Connectivity of fluvial point-bar deposits: An example from the Miocene Huesca fluvial fan, Ebro Basin, Spain. AAPG Bulletin 92(9): 1109-1129.

Donselaar, M. E.and Schmidt, J. M. 2005. Integration of outcrop and borehole image logs for high-resolution facies interpretation: example from a fluvial fan in the Ebro Basin, Spain. Sedimentary geology 52: 1023-1042.

Van Doren, J.F.M., Jager, G. de, Jansen, J.D., Luthi, S.M., Douma S.G. 2007. Sensitivity of Geostatistical Modeling Parameters on Reservoir Flow Behavior, In Proc. EAGE Petroleum Geostatistics 2007, Cascais, Portugal, 10-14 September.

Dubuisson, M.P., Jain, A.K. 1994. A modified Hausdorff distance for object matching. 12th International Conference on Pattern recognition, A, 566-568.

EIA, 2010, International Energy Outlook 2010, Technical report, Energy Information Administration.

Van Essen, G.M., Zandvliet, M.J., van den Hof, P.M.J., Bosgra, O.H., Jansen, J.D., 2006. Robust waterflooding optimization of multiple geological scenarios. Paper SPE 102913, presented at the 2006 SPE Annual Technical Conference and Exhibition San Antonio, Texas, U.S.A., 24–27 September 2006.

Evensen, G. 2004. Sampling strategies and square root analysis schemes for the EnKF. Ocean Dynamics 54: 539-560.

Falivene, O., Arbués, P., Gardiner, A., Pickup, G., Muñoz, J. A., and Cabrera, L. 2006. Best practice stochastic facies modeling from a channel-fill turbidite sandstone analog (the Quarry outcrop, Eocene Ainsa basin, northeast Spain). AAPG Bulletin 90(7): 1003-1029.

Friedman, F., Chawathé, A., Larue, D.K. 2003 Assessing uncertainty in channelized reservoirs using experimental design. Paper SPE 85117. SPE Journal, Vol. 6, Nr. 4, 264-274.

Gluyas, J. and R. Swarbrick (2005). Petroleum Geoscience. Oxford, UK, Blackwell Science.

Goovaerts, P. 1997. Geostatistics for natural resources evaluation. London, United Kingdom: Oxford University Press.

Guardiano, F.and Srivastava, R. M. 1993. Multivariate statistics: beyond bivariate moments. in Geostatistics-Troia,ed. A. Soares, p. 133-144. Dordrecht, The Netherlands: Kluwer Academic Press.

Haldorsen, H. H.and Chang, D. M. 1986. Notes on stochastic shales from outcrop to simulation models. in Reservoir characterization,ed. L. W. Lake, and H. B. Carol, p. 152-167. New York, USA: Academic.

Harvey, C. F. and S. M. Gorelick (1995). "Mapping hydraulic conductivity: Sequential conditioning with measurements of solute arrival time, hydraulic head, and local conductivity." Water Resour. Res. 31: 1615-1626.

Heller, P. H.and Paola, C. 1992. The large-scale dynamics of grain-size variation in alluvial basins, 2: Application to syntectonic conglomerate. Basin Research 4: 91-102.

Hewett, T. A. 1986. Fractal distributions of reservoir heterogeneity and their influence on fluid transport. Paper SPE 15386, presented at the SPE Annual Technical Conference and Exhibition, New Orleans, LA, 5–8 October.

Hird, K. B.and Dubrule, O. 1998. Quantification of reservoir connectivity for reservoir description applications SPE Reservoir Evaluation & Engineering 1(1). SPE-30571.

Hoffman, B. T.and Caers, J. 2003. Geostatistical history matching using a regional probability perturbation method. Paper SPE 84409 presented at SPE Annual Technical Conference and Exhibition, Denver, USA, 5-8 October.

Hogg, R. V., and J. Ledolter, 1987. Engineering Statistics, MacMillan, New York.

Hohl, D., Jimenez, E.A., Datta-Gupta, A. 2006. Field experiences with history matching an offshore turbiditic reservoir using inverse modeling. Paper SPE 101983, presented at the 2006 SPE Annual Technical Conference and Exhibition, San Antonio, Texas, U.S.A., 24-27 September 2006.

Hovadik, J.M. & Larue, D.K. 2007. Static characterizations of reservoirs: refining the concepts of connectivity and continuity. Petroleum Geoscience, Vol. 13, 195-211.

Hu, L. Y. 2002. Gradual Deformation and Iterative Calibration of Gaussian-Related Stochastic Models. Mathematical Geology 32(1): 87-108.

Idrobo, E.A., Choudhary, M.K. and Datta-Gupta, A., 2000. Swept volume calculations and ranking of geostatistical models using streamline simulation. Paper SPE62557 presented at the SPE/AAPG Western Regional Meeting, Long Beach, USA, 19-23 June.

Jackson, M.D., Yoshida, S., Muggeridge, A.H., Johnson, H.D. 2005. Three-dimensional reservoir characterization and flow simulation of heterolithic tidal sandstones. AAPG Bulletin, Vol. 89, No. 4, 507-528.

Jager, G. de, Van Doren, J.F.M., Luthi, S.M. 2008. Efficient model selection based on connectivity for geologically complex reservoirs. In Proc. 70th EAGE Conference & Exhibition, Rome, Italy, 9 - 12 June.

de Jager, G., Van Doren, J. F. M., Jansen, J. D., and Luthi, S. M. 2009. An evaluation of relevant geological parameters for predicting the flow behavior of channelized reservoirs. Petroleum Geoscience 15: 345-354.

Jager, G de. and S. M. Luthi (2011). "Accessibility: a new three-dimensional metric for reservoir characterization and field development planning." SPE Journal submitted.

Jansen, J. D., Brouwer, D. R., Nævdal, G., and van Kruijsdijk, C. P. J. W. 2005. Closed-loop reservoir management. First Break 23: 43-58.

Johnson, H. D.and Krol, D. E. 1984. Geological Modeling of a Heterogeneous Sandstone Reservoir: Lower Jurassic Statfjord Formation, Brent Field. Paper SPE 13050 presented at SPE Annual Technical Conference and Exhibition, Houston, Texas, USA, 16-19 September, 1984.

Journel, A. G. 1983. Nonparametric estimation of spatial distribution. Mathematical Geology 15(3): 445-468.

Journel, A. G., Gundeso, R., Gringarten, E., and Yao, T. 1998. Stochastic modeling of a fluvial reservoir: a comparitive review of algorithms. Journal of Petroleum Science and Engineering 21: 95-121

Journel, A. G., Gundeso, R., Gringarten, E., and Yao, T. 1998. Stochastic modeling of a fluvial reservoir: a comparitive review of algorithms. Journal of Petroleum Science and Engineering 21: 95-121.

Karsenberg, D., Törnqvist, T. E., and Bridge, J. S. 2001. Conditioning a process-based model of sedimentary architecture to well data. Journal of sedimentary research 71(6): 868-879.

King, P.R., 1990. The connectivity and conductivity of overlapping sandbodies. In: Buller, A.T., Berg, E., Hjelmeland, O., Kleppe, J., Torsaeter, O. & Aasen, J.O. (eds). North Sea oil and gas reservoirs II: London, United Kingdom, Graham and Trotman, 353-358.

King, P.R., Buldyrev, S.V., Dokholyan, N.V., 2001. Predicting oil recovery using percolation theory. Petroleum Geoscience, 7, 105–107.

Kitanidis, P. K. (1995). "Quasi-linear geostatistical theory for inversing." Water Resour. Res. 31: 2411-2419.

Koltermann, C. E.and Gorelick, S. M. 1992. Paleoclimatic signature in terrestrial flood deposits. Science 256: 1775-1782.

Knudby, C., Carrera, J., 2004. Evaluation of different measures of flow and transport connectivity of geologic media. In: Vila et al. (eds.) geoENV IV – Geostatistics for Environmental Applications, 235-246.

Krige, D. G., 1951, A statistical approach to some mine valuations and allied problems at the Witwatersrand, Master's thesis of the University of Witwatersrand.

Labourdette, R., Poncet, J., Seguin, J., Temple, F., Hegre, J., Irving, A. 2006. Three-dimensional modeling of stacked turbidite channels in West Africa: impact on dynamic reservoir simulations. Petroleum Geoscience, 12, 335-345.

Larue, D.K. & Hovadik, J.M. 2006. Connectivity of channelized reservoirs: a modelling approach. Petroleum Geoscience, Vol. 12, 291-308.

Leeder, M. R. 1973. Fluviatile fining-upward cycles and the magnitude of paleochannels. Geological Magazine 3: 265-276.

Liestøl, F. M., Hodneland, E., Hatland, K., Zachariassen, E., and Andersen, T. 2005. Improved Modelling and Recovery from Fluvial Reservoirs in the North Sea. Paper SPE 10378 presented at International Petroleum Technology Conference Doha, Qatar, 21-23 November 2005.

Lo, T. S.and Chu, J. 1998. A program and method for identifying connectivity of well perforation locations to cells of a reservoir description that meet selected pay criteria. US 5757663.

Mackey, S. D.and Bridge, J. S. 1995. Three-dimensional model of alluvial stratigraphy: theory and application. Journal of Sedimentary Research B65: 7-31.

De Marsily, G., Delay, F., Gonçalvès, J., Renard, P., Teles, V., and Violette, S. 2005. Dealing with spatial heterogeneity. Hydrogeology Journal 13: 161-183.

Martin, J.H., 1993. A review of braided fluvial hydrocarbon reservoirs: the petroleum engineer's perspective. In: Best, J.L., Bristow, C.S. (eds). Braided Rivers: Geological Society (London) Special Publication 75, 333-368.

Masihi, M., King, P.R., Nurafza, P. 2007. Fast estimation of fractured reservoirs using percolation theory. Paper SPE 94186. SPE Journal, Vol. 12, Nr. 2, 167-178.

Matheron, G. 1963. Principles of geostatistics. Economic Geology 58: 1246-1266.

Matheron, G. 1967. Elements pour une théorie des milieux poreux. Paris, France: Masson.

Matheron, G. 1973. Le krigeage disjonctive [Disjunctive kriging]. Note Interne N-360, Centre de Géostatistique, Fontainebleu.

Matheron, G. 1976. A simple substitute for conditional expectation: the dsjunctive kriging. in Advanced Geostatistics in the Mining Industry,ed. M. Guarascio, C. J. Huybrechts, and M. David, p. 221-236. Dordrecht, The Netherlands: Reidel.

Matheron, G., Beucher, H., de Fouquet, C., Galli, A., Guerillot, D., and Ravenne, C. 1983. Conditional simulation of the geometry of fluviodeltaic reservoirs. SPE Journal: 591-599. SPE-16753.

Meddaugh 2003. Assessing reservoir connectivity uncertainty in geostatistical models. Presented at the AAPG annual meeting, Salt Lake City, 11-14 May.

Miró-Quesada, G., del Castillo, E., Peterson, J.E., 2004. A Bayesian Approach for Multiple Response Surface Optimization in the Presence of Noise Variables. Journal of Applied Statistics, Vol. 31, No. 3, 251–270.

Myers, R. H.and Montgomery, D. C. 1995. Response surface methodology. New York: Wiley.

Nielsen, L.K., Subbey, S., Christie, M. & Mannseth, T. 2006. Reservoir description using dynamic parameterisation selection with a combined stochastic and gradient search. Computational Geosciences, 10, 321-342

Oliver, D.S., Reynolds, A.C. and Liu, N., 2008. Inverse theory for petroleum reservoir characterization and history matching, Cambridge University Press, Cambridge.

Otten, F. W. K., 2000, The Huesca Project: Sedimentary architecture modelling of a fluvial sandstone succession, Ebro Basin, Spain., MSc Thesis. Delft University of Technology, Delft, the Nethelands, 40 p.

Paola, C., Heller, P. H., and Angevine, C. L. 1992. The large-scale dynamics of grain-size variation in alluvial basins, 1: Theory. Basin Research 4: 73-90.

Pardo-Igúzquiza, E., Dowd, P.A. 2003. CONNEC3D: a computer program for connectivity analysis of 3D random set models. Computers & Geosciences 29, 775-785.

Pranter, M. J., Ellison, A. I., Cole, D. C., and Patterson, P. E. 2007. Analysis and modelling of intermediate-scale reservoir heterogeneity based on a fluvial point-bar outcrop analogue, William Fork Formation, Piceance Basin, Colorado. AAPG Bulletin 91: 1025-1051.

Le Ravalec-Dupin, M., Nœtinger, B. 2000. Optimization with the gradual deformation method. Mathematical Geology, Vol. 34, No. 2, 125-142.

Rivera-Rabelo, I., Luthi, S. M., and van Vliet, L. J. 2007. Parameterization of meander-belt elements in high-resolution three-dimensional seismic data using the GeoTime cube and modern analogues. in Seismic geomorphology: applications to hydrocarbon exploration and production,ed. R. Davies, H. W.

Posamentier, L. J. Wood, and J. A. Cartwright, v. 277, p. 121-137. London: Geological Society Special Publications.

Roberts, E. S. 1998. Programming abstractions in C: A second course in computer science. Reading, U.K.: Addison-Wesley.

Roggero, F. and Hu, L.Y. 1998. Gradual deformation of continuous geostatistical models for history matching. Paper SPE 49004, presented at the 1998 SPE Annual Technical Conference and Exhibition, New Orleans, USA, 27-30 September.

Ryseth, A. 2000. Differential subsidence in the Ness Formation (Bajocian), Oseberg area, northern North Sea: facies variation, accommodation space development and sequence stratigraphy in a deltaic distributary system. Norsk Geologisk Tidsskrift 80(9).

Satter, A. 2008. Practical Enhanced Reservoir Engineering: Assisted with Simulation Software. Tulsa: PennWell.

Scheidt, C., Caers, J. 2007. Using distances and kernels to parametrize spatial uncertainty for flow applications. Presented at the Petroleum Geostatistics conference, 10-14 September, Cascais, Portugal.

Seifert, D.and Jensen, J. L. 2000. Object and Pixel-Based Reservoir Modeling of a Braided Fluvial Reservoir. Mathematical Geology 32(5): 581-603.

Snedden, J. W., Vrolijk, P. J., Sumpter, L. T., Sweet, M. L., Barnes, K. R., White, E., and Farrell, M. E. 2007. Reservoir Connectivity: Definitions, Examples, and Strategies. Presented at International Petroleum Technology Conference, Dubai, U.A.E., 4-6 December.

Soleng, H.H., Syversveen, A.R., Kolbjørnsen. 2006. Comparing Facies Realizations – Defining Metrices on Realization Space. Presented at the 10th Eropean Conference on the Mathematics of Oil Recovery, Amsterdam, The Netherlands, 4-7 September.

Spencer, A. M.and Larsen, V. B. 1990. Fault traps in the northern North Sea. in Geological Society, London, Special Publications: Tectonic Events

Responsible for Britain's Oil and Gas Reserves,ed. R. F. P. Hardman, and J. Brooks, v. 55, p. 281. London.

Stien, M., P. Abrahamsen, et al. (2007). Modification of the snesim algorithm. Petroleum Geostatistics. Cascais, Portugal.

Strebelle, S. 2002. Conditional simulation of complex geological structures using multiple-point statistics. Mathematical Geology 34(1): 1-21.

te Stroet, C. B. M.and Snepvangers, J. J. J. C. 2005. Mapping curvilinear structures with local anisotropy kriging. Mathematical Geology 37(6): 635-649.

Suzuki, S., Caers, J. .2006. History matching with an uncertain geological scenario. Paper SPE 102154. Presented at the SPE Annual Technical Conference and Exhibition, San Antonio, USA, 24-27 September.

Tavassoli, Z., Carter, J. N., and King, P. R. 2004. Errors in History Matching. SPE Journal 9(3): 352-361. SPE-86883.

Teles, V., Bravard, J. P., de Marsily, G., and Perrier, E. 2001. Modelling of the construction of the Rhone alluvial plane since 15 000 years BP. Sedimentology 48: 1209-1224.

Teles, V., Delay, F. & de Marsily, G. 2004. Comparison of genesis and geostatistical methods for characterizing the heterogeneity of alluvial media: groundwater flow and transport simulations. Journal of Hydrogeology, 294, 103-121.

Tetzlaff, D.M. 2004. Input uncertainty and conditioning in siliciclastic process modeling. In: Curtis, A. & Wood, R. (eds.) Geological Prior of Information: Information Science and Engineering. Geological Society, London, Special Publications, 239, pp. 95-109

Tetzlaff, D. M., Davies, R., McCormick, D., Signer, C., Mirowski, P., and Williams, N. 2005. Application of multipoint geostatistics to honor multiple attribute constraints applied to a deepwater outcrop analog, Tanqua Karoo Basin, South Africa. in Society of Exploration Geophysicists Technical Program Expanded Abstracts,ed., p. 1370–1373.

Thomassen, R., Copes, H., and Vogelaar, A., 2004, Reservoir Geological Fieldwork Huesca, Fieldwork report, MSc Thesis. Delft University of Technology, Delft, the Nethelands, 42 p.

Viseur, S. 1999. Stochastic Boolean simulation of fluvial deposits : a new approach combining accuracy with efficiency. Paper SPE 56688 presented at SPE Annual Technical Conference and Exhibition, Houston, USA, 3-6 October 1999.

Van Wagoner, J.C., Mitchum, R.M., Campion, K.M. & Rahmanian, V.D. 1990. Siliciclastic sequence stratigraphy in well logs, cores, and outcrops. AAPG methods in exploration series, No. 7

Wang, Y. and Kovscek, A.R., 2002. A streamline approach for ranking reservoir models that incorporates production history. Paper SPE 77377 presented at the SPE Annual technical Conference and Exhibition, San Antonio, USA, 29 September-2 October.

Zhang, T., Bombarde, S., Strebelle, S. & Oatney, E. 2006. 3D porosity modeling of a carbonate reservoir using continuous multiple-point statistics simulation. Paper SPE 96308, SPE Journal, Vol. 11, Nr. 3, 375-379.

Zhang, T., Switzer, P., and Journel, A. G. 2006. Filter-based classification of training image patterns for spatial simulation. Mathematical Geology 38(1): 63-80.

Summary

For efficient production of hydrocarbons from subsurface reservoirs it is important to understand the spatial properties of the reservoir. As there is almost always too little information on the reservoir to build a representative model directly, other techniques have been developed for generating reservoir models. Different assumptions about the distribution of, and relationships between these properties are required for each different technique. However, it is poorly understood how these assumptions, and errors thereof, affect the predictive capability of the resulting reservoir models. In this study these relationships are analyzed from several different perspectives.

In **chapter 2** (*Literature review)* a summary is made on the current state of geological modelling, with a focus on reservoir modelling. A large variety of different examples are shown, illustrating the complexity of the reservoir modelling workflow. Each different technique requires several different assumptions to be made. Which assumptions are valid for the case being modelled, as well as the requirements of the resulting model, dictate which technique can be used. Often a trade-off is made between geological accuracy and mathematical simplicity.

As shown in chapter 2, several simplifications and assumptions are required when creating a reservoir model. However, it is poorly understood how these choices influence the accuracy of the finished reservoir model with all its limitations. In **chapter 3** (*The effect of two-point statistical modelling parameters on fluid flow behaviour of sub-surface reservoirs)* a first analysis in made. The modelling technique used is a simple one, using two-point statistics to create model realizations. This technique was chosen due to its mathematical simplicity, which allowed the development of the analysis technique used. The results show the difficulty in directly relating spatial geological properties of a reservoir model with how this reservoir behaves when being produced.

In **chapter 4** (*An evaluation of relevant geological parameters for predicting the flow behaviour of channelized reservoirs)* the type of analysis described in chapter 3 is applied to a more complex reservoir modelling technique. An object-based modelling technique is used, allowing for analysis of more realistic geological parameters. In this case a channelized reservoir is chosen as example, allowing the investigation of sinuosity, size, and number of channels, and permeability. As with the two-point statistics it is difficult to relate different reservoir parameters with flow behaviour of the reservoir when being produced. However, *connectivity,* a derived parameter, is

shown to relate better to flow behaviour. Connectivity is a measure of how well the channel bodies of the reservoir are connected to one another.

An example of a possible application of connectivity is shown, where it is used as a selection parameter. The goal is to rank model realizations by correctness with respect to a truth case. This is done by first taking a limited number of reservoir models and calculating connectivity as well performing a flow simulation on each. This gives a relationship between correctness of each realization as found by the flow simulation and connectivity. Calculating connectivity therefore allows a very quick and efficient ranking of each model realization.

In **chapter 5** (*Accessibility: a new three-dimensional metric for reservoir characterization and field development planning)* another reservoir characterization parameter is presented: *accessibility*. This is a parameter which takes some inspiration from urban planning, where for each location an accessibility value can be calculated based on both spatial distance, as well as ease of travel along each route. This is adapted for reservoir models by also using spatial distance, and combining this with permeability as an "ease-of-travel" parameter. A good correlation with flow behaviour is shown.

Two possible applications are discussed. The first is similar to how connectivity was used: as a ranking parameter for possible model realizations. An improved applicability over connectivity is shown, specifically the capability to analyze more complex and realistic reservoir models. The second application is as a quick-look parameter for well configurations. It is possible to calculate accessibility for different well configurations, and if this results in areas with very poor accessibility, this could indicate bypassed hydrocarbons. Subsequent flow simulations confirm the validity of this technique.

Having sketched a picture of how separate reservoir parameters influence flow behaviour in the previous chapters, in **chapter 6** (*The effect of errors in analogue geological models for fluid flow prediction)* the effect of errors in the complete set of reservoir parameters is investigated. An attempt to reproduce a reservoir is made using analogue models with increasing degrees of errors. The truth case is a channelized system consisting of channel belts with internal channels. The analogue models (with increasing error) consist of (1) one case of identical geological properties, but unknown channel locations, (2) a number of analogues which are also channelized, but with very different dimensions, and (3) a "non-geological" analogue consisting of square and circular bodies representing the subsurface.

Although one might expect an increase in geological error of the model to cause an increasingly large error in the predictions of flow behaviour calculated from those models, it was difficult to support this relationship based on the data collected here. A large part of the cause is the difficulty in finding a numerical approximation for an intuitive concept as geological correctness.

In conclusion this thesis illustrates the complicated relationship between geology and flow behaviour of a reservoir. It is shown that intuitive relationships between geological properties of reservoirs are at best difficult to reproduce, and at worst hardly present. Although this might lead one to conclude that geological information in reservoir modelling is next to useless, this is clearly not the case. In chapter 6 using a very good geological data set generated consistently good reservoir models, and thus good flow predictions.

Samenvatting

Voor de efficient productie van koolwaterstoffen uit ondergrondse reservoirs is het belangrijk om de ruimtelijke eigenschappen van het reservoir te begrijpen. Omdat er meestal te weinig informatie van het reservoir is om direct een model te maken, zijn er andere methodes ontwikkled om een model te creeeren. Verschillende aannames over de verspreiding van en de relaties tussen de verschillende parameters worden gebruikt voor elke method. Men begrijpt echter slecht hoe deze annames, en fouten daarin, het voorspellende vermogen van de resulterende modelen verandert. In dit onderzoek worden deze relaties van verschillende perspectieven geanalyseerd.

In **hoofdstuk 2** is een overzicht gemaakt van de huidige staat van geologisch modeleren, met de aandacht op reservoir modeleren. Een grote verscheidenheid aan voorbeelden wordt getoond, welke de complexiteit van het reservoir modeleren illustreert. Elke techniek vereist date er verschillende annames worden genomen. Welke aanname geldig is voor het scenario welke gemodelleerd wordt, also ok de eisen voor het resulterende model, bepalen welke techniek gebruikt kan worden. Vaak moet een keuze tussen geologische preciezie en mathematische eenvoud gemaakt worden.

Zoals omschreven in hoofdstuk 2 zijn verschillende simplificaties en aannames nodig voor het maken van een reservoir model. Het is echter niet goed begrepen hoe die keuzes de kwaliteit van het uiteindelijke reservoir model beinvloeden. In **hoofdstuk 3** wordt een eerste analyze gemaakt. Hier wordt een simpele modeleer methode gebruikt die slechts data uit variogram gebruikt om realizaties te genereren. De keus voor een simpel model is genomen wegens zijn simpele wiskunde, waardoor de ontwikkeling van de analyse techniek kon worden gemaakt. De resultaten laten de zien hoe moeilijk het is om de relatie te vinden tussen geologische eigenschappen van een reservoir en productie data.

In **hoofdstuk 4** wordt dezelfde analyse techniek die beschreven is in hoofdstuk 3 toegepast op een complexer modeleer techniek. Om realistischere reservoir eigenschappen te generen is voor een modeleer techniek gekozen die direct geologische lichamen in het model kan plaatsen. Hier is gekozen voor een geologisch systeem met ingevulde geulen. Hierdoor is het mogelijk om sinuositeit, aantal en permeabiliteit van de geulen te onderzoeken. Ook hier is het moeilijk om ruimtelijk reservoir eigenschappen te relateren in productie eigenschappen. Het is echter mogelijk om de parameter *connectiviteit* te defienieren die beter de relatie weergeeft.

Connectiviteit is de mate waarin de geul lichamen in het reservoir met elkaar zijn verbonden.

Een mogelijke toepassing van connectiviteit is getoond, waar het gebruikt wordt als selectie parameter. Het doel is om model realisaties te rangschikken naar hoeverre ze overeenkomen met een waarheids model. Dit wordt gedaan door eerst de relatie tussen connectiviteit en productie gedrag te bepalen voor een klein aantal modellen. Door vervolgens connectiviteit te bereken kan van elk model snel een mate van gelijkenis met de waarheid worden bepaald.

In **hoofdstuk 5** wordt een volgend parameter getoond: *toegankelijkheid*. Deze parameter vindt zijn inspiratie in steden planning, waar toegankelijkheid berekend wordt door middel van afstand en reis gemak. Dit is aangepast voor reservoir modellen door reis gemak te vervangen door permeabiliteit. Een goede correlatie met stromings gedrag wordt aangetoond.

Twee mogelijke toepassing worden besproken. De eerste is een zelfde techniek als met connectiviteit: om model realizaties te rangschikken. Een verbeterde correlatie wordt aangetoond wat vooral duidelijk wordt voor complexe en meer realistische modellen. De tweede toepassing is om een snelle eerste inschatting te maken van put configuraties. Als voor een bepaalde configuratie gebieden worden gevonden met slechte toegankelijkheid kan dit leiden tot niet winbare koolwaterstoffen. Dit wordt geverifieerd door middel van vloeistof stromings simulaties.

In hoofdstuk wordt in plaats aparte reservoir parameters te analyseren wordt in **hoofdstuk 6** gekeken naar complete sets parameters welke worden gehaald uit een aantal analoog modellen. Hier wordt gepoogd om een serie reservoir modellen te creeeren met oplopende fouten. De analoog modellen bestaan uit (1) identieke eigenschappe als het waarheids model maar met onbekende locaties van de geulen, (2) een aantal modellen die ook geulen hebben, maar met verschillende afmetingen, en (3) een “niet-geologisch” model bestaand uit vierkanten en cirkels.

Men zou verwachten dat een toename in geologische fout zou leiden tot een fout in voorspelde vloeistof stromen. Het was echter moeilijk om die relatie daadwerkelijk terug te vinden in de resultaten. Een gedeelte van de moeilijkheid kan verklaard worden door de lastige kwantificatie van een intuitief concept als geologische fout.

In conclusie toont deze scriptie de complxe relatie tussen geologie en stromings gedrag van een reservoir. Ook is aangetoond dat de intuitieve relatie tussen geologische fout en productie fout op zijn best moelijk te reproduceren valt, en in het

slechtste geval nauwelijks aanwezig is. Dit zou tot de conclusie kunnen leiden dat geologische informatie voor een reservoir model zo goed als nutteloos is. Dit is echter verre van de waarheid, in hoofdtuk 6 wordt getoond hoe een set modellen met de geologische eigenschappen consistent tot goede productie voorspellingen leiden.

Acknowledgements

First thanks go to my promoter, Stefan Luthi. Our discussions were essential for this thesis. It seems our sprint-pause-sprint appointment scheduling has finally paid off.

Also thanks to Jan Dirk Jansen. Although you were never an official part of my PhD in the sense of a (co)promoter, your help and motivational support were more than I could have expected.

Having spent the last 6 years at the TU Delft, first on my PhD and now as a post-doc, there are many colleagues to thank. Both past (Gijs, Jorn, Ali, Mattia, Mario, Renato, Joris, Rory, Wiebke, Wieske, Adriaan) and present (Andrea, Geertje, Ilja, Pantelis, Nico).

Also thanks to Gert Jan Weltje, we never did get to work together, but you have often steered me in the right direction with a single comment.

Thanks Joep, for helping me to continue my work and allowing me to take my research in a more geological direction.

A special thanks to my committee who have all taken time to be here: Rector Magnificus, Prof. Dr. S.M. Luthi, Prof. Dr. Ir. J.D. Jansen, Prof. Dr.Ir. M.F.P. Bierkens,Prof. Ir. C.P.J.W. van Kruisdijk, Prof. W.R. Rossen, Dr. J.E.A. Storms and Dr. Ir. E. Peters.

Friends that I would like to thank are Thijs, Linda, Pieter, Eefje, Joost, Rory and Christa for many great times, evenings, concerts and especially the yearly guy weekends: a very welcome break!

Maarten and Hedy, my little brother and sister. We might not see each other as much as I'd like to, but it's good to know you two will always be a phone call away.

My parents I can thank for getting me where I am today: from pushing for a VWO instead of HAVO education, the financial support, the motivational phone calls (even when half a world away) and instilling a love of nature in general and geology specifically from a young age.

The last thanks go to my family: Iris, Roan and Timo. Iris, thanks for the support: for moving to Delft when I started my PhD, and accepting that I would be gone regularly for conferences and fieldwork. You three are what make life worth living.

Curriculum Vitae

Gerben de Jager was born in Nijmegen on the 2nd of February 1977. He soon moved to the Hague, after which he spent his childhood living in Gabon, the United States of America, and Australia. In 1990 he moved to Assen, where he would spend his high school years at the Christelijke Scholengemeenschap Assen, later Christelijke Scolengemeenschap Vincent van Gogh.

Gerben started studying geology at Utrecht University in 1996, from which he graduated as doctorandus with a specialization in sedimentology in 2003. After graduation he spent a year travelling throughout Asia. On returning to the Netherlands Gerben started work with Argo Geoconsultants, detached at Wintershall in the Hague.

In 2006 Gerben started his PhD titled “geometric reservoir modelling” with prof. Stefan Luthi as promoter. This research was performed within the ISAPP group (Integrated Systems Approach Petroleum Production), a collaboration between TU Delft, TNO and Shell. Preferring to stay at TU Delft, he started as a post-doc developing a numerical model for fast forward and inverse modelling of fluvial systems in 2010.